INTEGRATION OF THE PASSIVE AIR CONDUCTION SYSTEMS' AERODYNAMIC DESIGN INTO INDUSTRIAL BUILDINGS

A dissertation presented

by

Ádám László KATONA

to

Breuer Marcel Doctoral School of Architecture,

The University of Pecs, Faculty of Engineering and Information Technology

for the degree of

Doctor of Philosophy in the subject of

Architecture engineering

Pécs, Hungary

2022

1. Summary

New studies and reports are published on a daily basis about the dangers of climate change and its main reason, humanity's constantly growing population, built floor space and resource consumption. The built environment is responsible for approx. 40 % of the total energy consumption, and a huge portion of energy consumption in buildings comes from heating, ventilation, and air conditioning. Numerous previous works assessed the potential of natural ventilation compared to mechanical ventilation and proved their justification on the field.
Some of them created databases about the yearly potential of Natural Ventilation (NV) solutions in different meteorological zones, and in some climates NV can be used almost during the whole year, achieving approx. 45% energy conservation.
Others are reviewed the different options and aspects of NV from traditional structures to modern examples, and created a wide base of knowledge for NV design.
During the development of scientific methods, numerous techniques became available for researchers in aerodynamic topics, and ventilation system designers. Beside modern measuring tools, wind and water tunnels, Computational Fluid Dynamics (CFD) simulations are the most widespread device for airflow modeling and analyzing.
Maneuvered by educated and experienced engineers and scholars, it is able to replace the previous options, and save time, energy and financial expenses during the aerodynamic assessments.
Since Bahadori's first publication – in the 1970s – about the vernacular wind catchers in Iran, the vertical wind driven building structures are come to the spotlight of natural ventilation's field. These so-called "baud-geers" caught the wind on their top openings and drove it down to the interior, thus securing the fresh air supply and the cooling of the overheated internal structures. There is more than one method for the natural ventilation with these towers, e.g. wind towers – up-ward air movement, combined wind towers with solar chimneys, multiple towers with differentiated purpose, evaporative cooling effects etc. The difference between these options are often blurred, and for scientific purpose there are no strict definitions for the different operational methods or geometries. From aerodynamic approach the lack of boundaries is not problematic, because the architectural difference between a skylight and a tower can be negligible from the airflow's point of view. On the other hand, from scientific approach it is very difficult to find general answers or optimal solutions if the boundaries are not given nor defined. Therefore, in this study a new nomenclature is suggested, which should emphasize the general investigation of NV techniques in given situations, where the building structures are not identified as architectural shapes, but aerodynamically – purely on the pressure differences of the supposed ventilation system. The suggested name for this kind of collective is: Passive Air Conduction Systems (PACS).
Nevertheless, the available, wide literature, it is a major difficulty to collect enough information from the literature to make decisions between different natural ventilation solutions with a given situation and boundary conditions. If an architect or ventilation engineer attempts to design a new PACS for fresh new buildings with no similarities to any previous studies, it is complicated to find universal suggestions for specific cases, therefore further investigations are necessary to deepen the aerodynamic topology of air conducting building structures' shape properties
Fort the different stages of the Ph.D. dissertation a good base model was necessary. The base model is suitable for set up the questions and methods of the scientific purpose, and because of the specific requirements of CFD simulations it is also acceptable as a basic validation source for later simulations with similar boundaries also.
As a base model, an existing building is presented which was designed with a PACS, where wind and buoyancy effects induce air to be exchanged without external energy needs. The aim

was to show that the design methodology, using numerical simulation to give accurate results, is able to use them in further developments. Due to this design process, the specific building possesses numerous special properties, including airflow accelerating elements, solar-heated "chimneys", and the indoor heat sources coming from the industrial technology. As the building has been constructed and was equipped with around 750 sensors (integrated and manual), it is possible to analyze the ongoing physical phenomenon in a highly detailed way and to collect the experienced dataset for further investigations. The result carried out a complex validation of the design and the used numerical methods to give general design rules for further PACS design and support following investigations, e.g., occupant comfort prediction or latent heat storage calculation. The experiences showed that the developed computational fluid dynamics technique gives a below 99% accuracy in the velocity and the temperature field, and approximately 85% accuracy in the volume flow values, resulting in a good prediction for aerodynamic characterization of buildings, i.e., passive ventilation air exchange rate.

In the next phase different PACS solutions were investigated in a blank project, where no NV source was determined, therefore the tests was about PACS variations in the design phase of a medium-sized new winery's cellar and production hall in Villány, Hungary. A computational fluid dynamics simulation based comparative analysis enabled to determine the differences in updraft (UD) and downdraught (DD) PACS which are two systems with significantly different aerodynamic behavior in similar building structures. During the complex CFD simulations, the latter was found to be more efficient: while the DD PACS performed an air change range of 1.02 h^{-1} to 5.98 h^{-1}, the UD PACS delivered −0.25 h^{-1} to 12.82 h^{-1} air change rate in the industrial hall and the cellar of the building, where the NV techniques were applied. The ventilation performance of the DD version possessed lower amplitudes, but the distribution was more balanced under different wind incident angles, thus this version was chosen for construction. It could be concluded that the DD PACS provides a more general applicability for natural ventilation in moderate climates and in small to medium scale industry hall domains with one in- and one outlet

Based on the experiences a new question was formed. A universal and general application of PACS solution should be developed, such as an applicable tool for new industrial halls with typical heights and internal air quality (IAQ) requirements, but without restrictions not he sizes. The rapid far eastern industrial revolution has huge potential and practice in industrial constrictions, and the constantly growing energy hungers creates an opportunity for the spread of PACSs. Therefore, a co-operation was proposed with the Jiaotong Shanghai University about this topic.

Particular study looked for answers that what is the potential in industrial building sin the sub-tropical far east regions with PACS. The created base model was taken as a CFD validation point, and as an already working and qualified integrated PACS within industrial hall. Since the tested building is implemented and used regularly in operation, complex measurements could be carried out to support the calibration of the CFD model's calculated results in a comparative analysis with measured values. In a second step, the validated CFD model served as initial point for further tests with up- and downdraft ventilation concepts under different climate conditions. During the tests first a simple unit of a freely expandable system was created and simulated, then a 6,050 m^2 4-unit big industrial hall was tested, with multiple wind incident angles. The prototype buildings had great results and the simulations obtained useful experiences for further studies. The performances of the PACS were 7.5 h^{-1} ACH ventilation potential. The prototype can be identified as a generic model for further development of passive ventilation- and cooling systems, because it was generated as a modular, generic and flexibly arrayal system which can adapt to different urban situations.

Another aspect of the PACS design is the micro geometrical topology design, where only some parts are investigated and improved within a chosen system. Hence, in the next phase new simulations were conducted applying different wind catcher geometries in the previously mentioned DD PACS system. This research evaluated whether further improvements in ventilation efficiency are possible due to the aerodynamic shaping of the roof integrated inlet structures. Four different wind catcher geometries were examined to determine the most advantageous dimensional settings in the natural ventilation system's given boundaries. After multiple series of basic and developed calculation runs, diverse shape designs of the passive air conduction inlet (PACI) were examined including wind deflector geometries. The worst version of the wind catcher's air change rate was increased by approx. 30% during the simulations. The results deliver the potential measure of improvements achievable in the aerodynamic shape design of structures under identic conditions of the same building domain. As a consequence, more sophisticated natural ventilation structural solutions will be possible in more operation cost- and performance effective ways.

As a last step a method is suggested based on the collective experience of the previous works, how to start to design any PACS for any purpose. The situation was simplified to achieve an understandable and manageable situation, therefore a series of two dimensional CFD studies were conducted. A wind tower's roof structure was chosen as a basic model, where three parameters were selected, and with those a parametric combination matrix was created with 27 cases. The results were meant to test the sensitivity of the dimensions of a low pressure zone on top of the wind tower. Based on the results the best scenario had a 400% increase in ventilation performance compared to the worst. The results emphasize the potential of the proposed method, and it can be a good recommendation for practical use in the design process of industrial buildings.

However, even with a few parameter and a simplified method, the general approach consumes a huge amount of preprocessing and computational time for CFD simulations. The possible outlook of this dissertation is an opportunity to combine the experiences with the Energy Design Synthesis, which is a parametric graph based mathematical approach to find optimal solutions for architectural problems. The huge opportunity with this co-operation is the developed strategy's great potential to reduce time and organizing requirements by created a perfectly general and effective sorting and ranking mechanism for vast amount of geometrical data.

2. Table of content

1. Summary 2

2. Table of content 5

3. Nomenclature and abbreviations 7

4. Introduction and Literature review 8

5. The complex analysis of the industrial integration of PACS systems' potential 15

5.1. The base model of the study 15

5.1.1. Materials and Methods 15

5.1.2. Prototype Building 15

5.1.3. Instrumentation 18

5.1.4. The CFD Model 23

5.1.5. Boundary Conditions 26

5.2. Results of the validation process 27

5.2.1. Validation of the Reference CFD Model 27

5.2.2. Evaluation of the PACS Efficiency 31

5.2.3. Conclusions of the in situ measurements and validation 34

5.3. System comparisons of different PACS solution with identical boundary conditions 37

5.3.1. Case study building and Site 37

5.3.2. Simulations and Model Set Up 40

5.3.3. Limitations of the method 42

5.4. Results 43

5.4.1. Scenario Site A—Lower Density, Closer Neighbors 43

5.4.2. Scenario Site B—Higher Density, Further Neighbors 47

5.4.3. Conclusion of the comparison of DD and UD PACS 48

5.5. Potential analysis of a spacious building prototype with passive bidirectional ventilation 49

5.5.1. Background 49

5.5.2. Concept of the innovative new and modular PACS for industrial buildings 50

5.5.3. Prototype basic unit model description 52

5.5.4. Prototype basic unit model, modified inlet tower with integrated downdraught cooling 55

5.5.5. Wind and thermal induced performance of the prototype basic unit model 60

5.5.6. Integrated bidirectional PACS into the prototype model with enhanced floor area 61

5.5.7. Simulation results 62

5.5.8. Discussion of the innovative PACS implementation's ventilation performance 69

5.6. The questions of *micro level* geometry optimization of PACS' elements 71
5.6.1. Shape design test variations of the PACS inlet structure 71
5.6.2. Simulations and Model Set Up 75
5.6.3. Results and discussions 78
5.6.4. Effects of deflectors 82
5.6.5. Modified deflector design 84
5.6.6. Conclusions of the micro level geometry optimization 88
5.7. New approach – parametric design-optimization 89
5.7.1. The results of the parametric approach of the micro level modifications 91
6. Outlook 93
6.1.1. The promising unified Energy Design Synthesis theory 94
7. Bibliography 96
Appendix A – CFD meshing validation 103
Appendix B – Graphical data about the results of the complex new PACS geometry development 105
Appendix C – Graphical data for parametric micro level geometry optimization 109

3. Nomenclature and abbreviations

PACS – Passive Air Conduction System
NZEB – Near Zero Energy Building
NV – natural ventilation
MV – mechanical ventilation
CFD – Computational Fluid Dynamics
RANS – Reynold averaged Navier-Stokes
RNG – re-normalized group
SME – small European enterprise
ACH – air change per hour
PV – photo voltaic
IAQ – Internal air quality
IECQ – internal environment comfort quality
BMS – Building management system
MMS – Mobile Monitoring System
PTE- University of Pécs
HVAC – Heating, ventilation air conditioning
AHU – air handling unit
PDEC – passive down draught evaporative cooling
UD – up draft
DD – Down draught
GHG – greenhouse gas
ABL – atmospheric boundary layer
ASHRAE – American Society of Heating, Refrigerating, and Air-Conditioning Engineers
EN15251
TNM 7/2006 V.24
FVM – finite volume method
UDF – user defined function
VFR – volume flow rate
PACI – passive air conduction inlet
PACO – passive air conduction outlet

4. Introduction and Literature review

Low-carbon technologies in sustainable buildings have become more popular in recent years, mainly because of the aim to reduce the greenhouse effect and to save energy and natural resources. The EU is working to achieve the a 20% reduction in greenhouse gas emission by 2030 compared with the emission levels of 1990 [1]. The built environment contributes almost 35% of the total European CO2-emissions and factory buildings are highly represented in this share [2]. On the other hand, newly designed buildings have to meet the requirements of the Near Zero Energy Building (NZEB) standard, where renewable resources must have a share in energy consumption of at least 25%.

The proposed sustainable building design approach in this particular study is substantially based on natural ventilation (NV), which is a passive ventilation method, based on wind- and/or buoyancy-based pressure differences to refresh air from indoor spaces with outdoor air [3]. The main benefits of NV are the lower operation energy cost in contrast to mechanical ventilation and the improved indoor environment air quality [4]. Many parameters should be analyzed carefully to achieve these advantages and the main design of NV has to be approved in the design phase. Unfortunately, NV is still not recognized in the regulations, therefore it cannot be calculated and considered into the 25% rule of renewables. In addition, NV requires an appropriate understanding of building pressurization, façade design [5], wind patterns, and local climate conditions, which only can be achieved by a specific design method, not regulated by the NZEB standard or any other legislations and codes.

Passive ventilation is an increasingly popular method to reduce building energy use by drawing in outdoor air without the aid of mechanical equipment. In buoyancy-driven natural ventilation systems, appropriate air inlets in the building envelope and vertical connection between each floor must be provided, directly connected to an exhaust opening typically located in or on the roof. These design elements are to be defined in the early design stage. There could be various types of architectural solutions to connect spaces vertically [6], e.g., atria commonly provide this solution. Although well-designed atria can help significantly to lower the energy consumption of a building through natural ventilation, poorly designed atria can increase energy use [7]. To ensure a proper design, various simulation tools predict atria performance during the design stage.

In most cases, wind flow influences even stronger building ventilation performance, infiltration rates, and the associated heat losses or gains [8]. Therefore, the building envelope bears great importance in buildings' energy behavior: the façade and roof performance, i.e., form (geometry), structure and openings should be improved according to indoor requirements and the surrounding outdoor environment conditions and neighboring structures, since they modify the local microclimatic flow characteristic and may cause unexpected flow effects. Appropriate aerodynamic building design, in turn, enables one to benefit from given circumstances, creating wind-climate responsive solutions.

The complexity of the aforementioned aspects is the reason why building designers often do not consider NV. The lack of knowledge in this field and the missing expertise for evaluation and implementation may result in poorly designed, constructed and operated naturally ventilated buildings. On the other hand, many methods could be used to predict ventilation in theoretical research studies [9]. Among them, computational fluid dynamics (CFD) has been the most advanced method for predicting NV performance [6,10–13] and among the numerous simulation tools available, CFD models have become one of the most popular in the literature and accounted for 70% of publications on simulating building ventilation recently reviewed by Chen [14]. Although the literature review did not solely focus on either natural ventilation or atria, it concluded that the v2f-dav, RNG k–ε, and k-Ω turbulence models performed best of all

the Reynolds-Average Navier–Stokes (RANS) models [15]. Numerous studies have drawn similar conclusions [16–19]. Other CFD studies have simulated atria: Awbi simulated a 15-m high atrium to evaluate temperature, wind velocity, and CO2-levels within the space [20]. This CFD method can optimize the building solutions by simulation instead of trial-and-error techniques that require much effort, time and resources. Moreover, several studies [21–25] have been developed to assist the CFD model definition. The current research is therefore based on CFD to assist architects in the optimization of NV behavior in buildings.

Based on the above, only few concepts with NV can reach the executing stage, therefore there are rare opportunities for the evaluation and validation of these kinds of buildings, their aerodynamic performance and the simulation modelling technology. Only a marginal part of the publications reports experimental measurements, whereby such studies were rarely carried out in aerodynamically complex, voluminous buildings. Implemented building examples with innovative natural ventilation systems are rarity, and their publications usually have no scientific data [11,26–30]. As a result, knowledge of passive ventilation systems is poor due to system complexity and lack of measurements.

This case study analyzes the effect of a combination of distinct façade inlet openings with roof-integrated exhaust openings on the indoor airflow distribution to improve the NV behavior. An air sweeping effect is achieved by a special wind deflector, installed above the outflow. The aim of the work is to validate the high-resolution CFD model by comparing its results with the measurements. While the aerodynamic design approach is applied in a particular study for a factory building, it is also applicable in residential houses [31] and for most of the built environment, i.e., settlement climate simulations [32], but the main objective is to set a standard for small European enterprises (SME) with need of a production hall for the ventilation cost reduction.

One of the biggest challenges of the 21st century is to avoid the irreversible rate of global warming, and to restrain the harmful tendencies which are responsible for it. The objective of the Paris Agreement [33] was signed by 195 countries to keep the increase of global average temperature rise below 2 K above pre-industrial levels. In accordance with this goal, the European Union created a Road Map [34] to reduce the greenhouse gas (GHG) emissions by 80% until 2050, compared to the 1990s. However, the global energy consumption raised by over 50% in the last decades, despite the similar ambitions of the previous climate assignments. In addition, the future scenarios show no differences either: in 1998 Schmalansee et al. [35] forecasted in their prognostication at least 200% increase in CO_2-emissions between 1990 and 2050. In 2012, Akashi et al. [36] still estimated over 50% increase in the GHG-emissions during the same period.

The built environment is responsible for 20–40% of the global energy consumption, where the heating, ventilation, and air conditioning (HVAC) system has a share of over 60%. Moreover, due to global warming, the cooling energy demand will further expand. Hence, the natural ventilation (NV) techniques should have a more significant role to reduce the buildings' energy intensity. Beside the energy saving potentials, the Passive Air Conduction Systems (PACS) have advantages to achieve the acceptable indoor air quality (IAQ), contrary to mechanical systems (MV), which are often responsible for the sick building syndrome's development in many modern buildings [37].

It can be observed from the tendencies, that solely the political alignments and the legal regulations are not sufficient to achieve a sustainable future; therefore, it is needed to pursue and to introduce groundbreaking new technologies, which could even over fulfil the current environmental legislations.

NV options serve obvious solutions in agricultural buildings, since they possess frequently huge single space interiors, where robust design principles work efficiently, and the 'occupants'—

animals and plants—are usually more sensitive to MV. Coelho et al. [38], investigated green houses' ventilation in Madrid, where different opening configurations were compared. Based on their results, the bigger the opening areas were, the lesser temperature differences developed between indoors and outdoors, which is desirable, because green houses are usually overheated during summer periods. However, this behavior needs to be taken into account, where the internal temperature should be lower than the external. Numerous studies were conducted with huge scale buildings with animals. Tomasello et al. [39] created a validated computational fluid dynamics (CFD) model for future studies of NV optimization. Nosek et al. [40] investigated the impact of atmospheric boundary layer (ABL) in a cattle barn with wind tunnel simulation. Based on their result, the geometries and sizes of openings had the highest impact on the efficiency of natural ventilation, and the heat sources of the cows and other machines were negligible. Rong et al. [41] observed a similar case of a dairy cow building with CFD simulations, concluding that even 60% differences can occur in the air change (ACH), depending on the wind incident angles to the façade openings. They also recognized that the modeling of plant canopy can reduce the air velocities through the opening more than 29%.
There are only a few examples of NV in industrial buildings, though they have similar geometries to agricultural buildings. A thermal buoyancy driven ventilation was assessed by Tanasic et al. [42] in a cardboard mill hall. Fresh air entered the building through the façade and left on top of the roof. Based on their proposal with heat recovery systems, approximately 1140 t CO_2 emission could be saved yearly. Kistelegdi and Baranya [43] appraised the performance of a PACS in a plastics industry hall during the design phase, where they compared four different tower geometries from 12 wind direction in wind tunnel model tests. The best version achieved 210,000 m^3/h volume flow rate, which equals 82 h^{-1} air change rate. Mazzarón and Canas studied in more papers [44–46] the thermal behavior of traditional wine cellars with wind chimneys. Typically, the temperature was stable in the underground cellars in summer and winter periods, and the chimneys were suitable to extract the stale air without changing drastically the internal relative humidity or temperature and altering negatively the maturation of wine. These studies provide promising results to design a PACS with wind towers in modern wineries as well.

Bahadori [47] firstly paid scholar attention to the vernacular wind catchers in Iran. These so-called "baud-geers" caught the wind on their top openings and drove it down to the interior, thus securing the fresh air supply and the cooling of the overheated internal structures. Saadatian et al. [48] studied thoroughly the transition of traditional wind towers in the Middle East into modern examples. They concluded that not enough scientific results are available to specify modern wind towers and PACS and their exact geometrical parameters. Hughes et al.[49] investigated the specifications of modern wind towers and after a deep literature review they came to the conclusion that it is hard to compare the different techniques, because usually they are assessed only in relation to MV, without comparing them to each other as well. According to Khan et al. [11] the PACS equipped with wind towers can achieve 300 l/s volume flow rate. If these NV system setups correspond to the required ACH values by the local or e.g., ASHRAE regulations, the PACS can maintain an acceptable IAQ-level. Omrani et al. [50] reviewed the available technologies for aerodynamic studies, whereas CFD simulations turned out as the most cost and time effective option. This fast developing tool is able to provide reliable results, and an adequately detailed model could be also used for comfort level assessments [51].
Wind towers can be divided into two major groups, according to the movement direction of the ventilation air current: updraft (UD) and downdraught (DD) systems. Most of the UD towers' mechanisms are also based on the thermal buoyancy effects. Takayama et al. [52] presented a museum complex, which was designed from a former factory, where the thermal buoyancy in

the old chimney induced the ventilation. This PACS could achieve 3 K cooler temperature than the external summer air temperature of 29 °C. The stack effect can be found in the wind induced UD towers as well, but the wind towers can perform approximately 76% stronger air volume flow rate and therefore the buoyancy is usually more like an emergency option for calm [8]. The UD movement is forced in many cases with help of a 'Venturi-shaped' plate on top of the towers. The compressed external wind currents under this 'Venturi' objects induce a depression zone, which can extract the air from the tower. Lim et al. [53] optimized the NV of a domestic house in Malaysia with CFD simulations. During their research, they achieved a 14,000 m^3/h volume flow rate in a two-story building with approximately 130 m^2 floor area. A 20 × 20 × 50 m 'Venturi'-shaped roof structure was investigated by van Hoff et al. [54] in CFD and wind tunnel tests, whereas they integrated deflector wings into the depression zone. They could not improve ventilation performances, because the deflectors created too high resistance, and the wind was not able to create force under the 'Venturi'-shaped roof but bypassed it.

On the other side, the operation principle of DD towers is quite simple: the openings are arranged on top of the wind towers or roofs and they face towards to the approaching wind, and the caught fresh air is forced down to the interior. Badran's [55] research was based on the ancient Jordanian wind catcher. According to his results, above 4 m height there are no significant improvements in the performance of the towers in domestic buildings, compared to the traditional 9 to 15 m towers. Sadeghi et al. [56] ventilated an average medium-density apartment building with DD towers, which could provide in the warmer periods (external temperatures > 23 °C) by 1725 more comfort hours than window openings. Saif et al. [57] improved the IAQ in classrooms with modified wind catchers and have met the ASHRAE requirements under Kuwait's climate conditions.

The vernacular wind towers frequently combined the two ventilation methods [58,59] with dividing walls in the towers, so on the windward side an over pressure zone forced the fresh air down in and on the leeward side an under pressure zone extracted the stale air out. However, Mohamadabadi et al. [60]showed in their study the flaw of this construction: a short circuit is generated below the tower, so the fresh air almost immediately leaves the interior behind the inlet, without mixing with the interior air.

Currently, the most developed regulations are created by the American Society of Heating, Refrigerating, and Air-Conditioning Engineers (ASHRAE). The ASHRAE 62.1 and 62.2 [61]considers the topic of mechanical and natural ventilation and IAQ. It provides appropriate sizing values for the design of MV systems as well as simple NV systems (e.g., one- or two-sided window ventilation, etc.). However, there exists no calculation or modelling guidance for unconventional complex PACSs. Only simplified, approximated equations, rule of thumb table-data, as well as general calculation and simulation description is provided. A similar legislation created by the European Union, the EN 15 251 [62], quantifies the minimum requirements of acceptable ventilation in non-residential buildings. Hungary has its own laws to regulate ventilation designs in buildings as well—the TNM 7/2006 V.24 [63], however it does not contemplate NV. Its new modification will force dwellers to use MV in buildings as well. The EN 15,251 legislation was considered in this study because its validity and general applicability in the EU.

The literature review outlines well the need for spreading NV in both agricultural and industrial buildings. A good founding is provided by vernacular tower structures, but in the last decades, the investigations were more focused on the justification of the PACS against MV systems. Currently, their relevance is meanwhile proven, and their application is inevitable because of the global warming and its negative effects. This research became necessary because in the design phase of a new industrial building, it was impossible to collect satisfactory information from the literature to properly create not just a working, but also a specified and precisely scaled

NV system in given boundary conditions. It became clear that there is a deficiency in studies concentrating on comparison of different PACS, which could be helpful for architects and engineers to choose the appropriate PACS with optimal parameters for the particular building application. To fill this gap in this phase, a UD and a DD PACS were proposed and juxtaposed in a modern prototype winery.

In this study, one of the investigation's focus is set on the fresh air inlet structure and its formal design parameters, which are originated as wind catchers from the ancient Iranian, Middle-East and Egyptian territories. Bahadori [47] mentioned them first, and offered it for consideration as a new/old option instead of mechanical ventilation (MV). The main element is a vertical structure – wind tower – that has a 'wind catcher' geometry on top. It can harvest the predominant wind flow (one-sided wind catchers) or capture the wind from all directions (two or more sided wind catchers) and force the air to flow down to the interior, thus providing fresh air, and improving indoor air quality (IAQ). Hughes [49] and Jomehzadeh [51] write about the history and development of wind catchers in a thorough way by reviewing geographical locations and climate aspects of vernacular wind towers, together with contemporary examples from architectural and scientific point of view. Finally, they suggest the application of wind catchers in modern PACS, and they support this idea with the detailed evaluation of numerous modern wind catcher geometries. Dehghani et al. [64] wrote about the evolution of wind catchers as well, the work not only collects the available data and offers it as a base knowledge for the next generation, in fact it creates a new special industrial wind catcher geometry based on their own conclusions. Heidari et al. [65] investigated the vernacular earthen architecture of Iran using CFD simulations. The paper classified the houses by their typology, and based on the results a guideline was created that can help to avoid unwanted air movements, positively affect IAQ and optimize air change per hour (ACH). Badran [55] collected information about the traditional Jordanian wind towers, whose heights are between 4 and 15 m. It is stated that the towers already provide enough fresh air for a two story building if the towers are only 9 m high, enabling to save construction material and time. In addition, based on the results, with evaporative cooling approximately 9°K temperature decrease is possible in the towers in the Jordan valley. Mohamadabadi et al. [60] discussed the aerodynamic operation of a rectangular wind catcher with six sub-sections under different wind incident angles. The different sections conduct the airflow up or down simultaneously, depending on the wind direction and the evolving pressure zones around the towers. The research used wind tunnel model experiments and CFD simulations to evaluate the towers, and it pointed out that this combined towers without any wind dependent control can have a short-circuit on the bottom, where the entering fresh air immediately leaves the interior without mixing with the exhaust air. Zarmehr et al. [66] took an ancient Persian water reservoir as reference model in their research. In a complex geometry analysis seven different modifications were tried out and compared. The most promising version achieved 15 m/s air velocity inside the towers, and produced approximately 8°K cooling, showing that it is possible to improve the vernacular base model, however many of the alterations did not enhanced the PACS's ventilation performance. Calautit et al. evaluated the cooling potential of single-sided [67] and multi-directional [68] wind catchers with integrated heat transfer devices with CFD simulations. The outcomes of the paper were positive: the single-sided geometry achieved 8-12°K cooling with only 15% decrease of air velocity, and the multi-directional wind catcher reached similar level of effectiveness. Long et al. [69] proposed a complex PACS in a visitor center of a National Park in Utah, USA. The PACS contained wind catchers, Trombe-walls, elevated exhaust (outlet) points and evaporative cooling etc. 67% energy savings are achieved, and the visitors think about the wind catchers as an amenity of the building. This is important, because the integration of these techniques into the architectural concept is crucial to make NV more popular among architects as well as

contractors and occupants. Balabel et al. [70] investigated the inlet opening angles effect on a partial-cylinder wind catcher geometry and different locations of the tower in a given building. Their findings show, that the higher opening angles can achieve better results, and the wind catcher has better performance between 20.55 – 37.37 5% when it is behind the building due to the incoming wind, compared to the other versions. Haghighi et al. [71] proposed a combination of wind catcher and solar absorption chiller, integrated in a two-story building. The system could cool down the internal air by 10-20 °K. Beside the cooling potential, an urban scale investigation was conducted as well, by combining three similar buildings related to the occurring wind direction. The results were analyzed considering also geometrical differences, e.g. the lower towers produced less ACH. Chew et al. [72] approached the topic from a different way: in urban environment, different wind catcher geometries were integrated to the top of buildings to conduct down the airflow from the roof level to the street canyons. After multiple alteration in water channel model measurements, the improved design of a wind catcher with closed sidewall enhanced the maximum near-ground wind speed in the canyons by four times. Alwetaishi et al. [73] could reach a 12 °C temperature reduction in the region of Saud-Arabia inside an underground room via evaporative cooling, which are commonly implemented to wind catchers.

These studies proved that wind catchers are not only used sufficiently in the ancient era, but they are able to satisfy higher needs, and can be combined with modern techniques to achieve higher, optimal level of IAQ. However, the use of wind catchers is only a guiding principle of a PACS. The determination of the right geometry based on the local functions, building shape, structure and dimensions, urban texture and meteorological data is essential for further performance improvement and savings in financial-, energy-, environment and time resource. Afshin et al. [74] described the behavior of a traditional two-sided wind catcher under different wind directions. Based on the CFD results, the air stream direction changes in the tower if the wind incident angle is higher than 55° (0°=orthogonal to the wind catcher's inlet). If the wind direction was parallel (90°) to the openings, the wind catcher reached the highest ACH, because in this case both the tower sections extracted exhaust air from the interiors, therefore the ventilation's cross section was doubled. Benkari et al. [75] applied two simple wind catcher shapes to a semi-opened atrium. The version with curvy transaction to vertical walls delivered better ACH performance, and it was successful to provide fresh air for the atrium's whole area. Ansar et al. [76] combined wind catchers with solar chimneys, and the PACS's different parameters were systematically changed (e.g. cross section). According to the conclusions, not all geometrical change improves the performance, and it is highlighted that danger of frictional losses threats, if the shape design is not created with proper blending and smoothing. Sarjito et al. [77] compared different wind-cowl variations with CFD simulations. The most effective version with an extended baffle had 79.4% mass capture efficiency, which was five times higher than the weakest option. Alsailani et al. [78] conducted a comprehensive parametric CFD study of wind catcher topology by investigating six properties' thirty-three variation. The results showed approximately 23% difference between the best and worst scenario, and it was raised further to 29% when guide vanes were implemented to the model. Varela-Boydo et al. [79] had also examined parametrically the shapes of wind catchers, nevertheless, in this study the parameters were investigated in a combined way. There were 174 scenarios of 28 versions solved in CFD simulations. The wind catchers were based on traditional two-sided towers (one side is inlet and the other is outlet), therefore the short-cut problem mentioned by Mohamadabadi [60], is possibly active in these cases too. Nonetheless, very detailed and gap-filling insights were created, and it is offered as a 'how to and not to do' guideline for wind catcher engineers.

Among the available research, two principal trends prevail: one part of the studies consider concrete, complex building use, climate and urban circumstances (e. g. tests in more wind direction) but the tested ventilation structure domain has mostly low level of detail and the number of the examined cases are rather low. The other trend includes investigations without exact, detailed building and neighbor structures and further boundary conditions (e.g. tests in only one wind direction) but the examined ventilation structure domain has higher level of resolution and the number cases are higher as well. All research work models relatively small building and neighborhood areas in form of simplified geometries due to the high level of fluid mechanical complexity, mesh generation issues, computation capacity and time requirements.
During the design stage of a prototype winery, boutique hotel and panorama restaurant facility, appropriate literature data were found on the proven functionality and workability of PACS, however, sufficient information about the NV structures precise sizing, scaling and geometrical parameters, in particular given building boundaries were not available. According to the quality and quantity of the gained results from literature, the outlining knowledge about shape design of ventilation structures is apparently incomplete. There is a scientific need for building a wide and thorough knowledge about wind catcher topology, which functions as guideline in such situations. The purpose of this study to expand this field with new versions and results along with the reviewed authors. Therefore, in a previous phase [80], PACS versions with different air conduction directions were proposed and compared in the winery industry building project. A down drought (DD) PACS including a wind catcher inlet and an updraft (UD) PACS with a 'Venturi' outlet tower were compared. The results suggested that on a site with no prevailing wind situation, DD wind catchers are more favorable against the uni- or bidirectional UD 'Venturi' towers, since the DD system possesses an omnidirectional behavior. Although the study offered a solution to decide between different PACSs and other valuable information was found to describe the behavior of a DD and UD PACS, it has not helped to specify the detailed dimensions of the system's 'engines': the wind catcher inlet and the 'Venturi' outlet. However, the following questions remained open: Which detailed geometry versions offer better solution for the chosen PACS? How and what kind of topology of natural ventilating structures should be chosen for a DD PACS in an industrial building to achieve the highest possible ACH and thus best cooling and natural IAQ for the wine process and storage technology? Aim of particular study is to reply these questions, which are still not satisfactory answered by the reviewed literature. At the same time, reasonable structural and architectural design aspects are to be considered during the shape modelling and optimization process.
CFD simulation supported development of wind catcher shape topology in a Passive Air Conduction System (PACS)

Aim of particular study is to reply these questions, which are still not satisfactory answered by the reviewed literature. At the same time, reasonable structural and architectural design aspects are to be considered during the shape modelling and optimization process.

5. The complex analysis of the industrial integration of PACS systems' potential

My dissertation is essentially based on my three main publications:

- Development of Wind Catcher Shape Topology in a Passive Air Conduction System (PACS)", *Buildings*, 2022
- Ádám László Katona, István Ervin Háber, stván Kistelegdi. "Comparison of Downdraught and Up Draft Passive Air Conduction Systems (PACS) in a Winery Building", *Buildings*, 2021
- Ádám László Katona, Huang Xuan, Sara Elhadad, István Kistelegdi, István Háber, High-Resolution CFD and In-Situ Monitoring Based Validation of an Industrial Passive Air Conduction System (PACS), *Energies*, 2020

5.1. The base model of the study

5.1.1. Materials and Methods

The applied investigation method, consists of a high-resolution CFD model experiment, with the main aim being to provide an appropriate initial basis for PACS development in industry halls. The procedure was designed by the following aims:

- Real building monitoring: As a first step, an implemented prototype industry building was monitored since 2015 (5 years' database) to gain in situ measurements of its production hall's ventilation properties and the unique chimneys' aerodynamic characteristics.
- High-resolution CFD model: In a second stage, a high-resolution CFD model is created to be calibrated by the measured air velocity and air temperature values. During geometry creation, mathematical solver code selection (turbulence models), appropriate boundary conditions are indispensable. In order to achieve an accurate model validation, all relevant details of the interior and the exterior should be modeled, i.e., the terrain, vegetation, furniture, occupants, equipment, and lighting appliances are defined with aerodynamically reasonable simplifications.
- Manual measurements: Besides the integrated, automated monitoring system, timely, limited manual measurements are necessary to capture a detailed airflow pattern and the thermal behavior of the investigated production hall.
- CFD model calibration: In the final stage, calibration of the air temperatures in the ventilation towers, as well as the air volume flow in the exhaust chimneys and the total air change ACH in the hall, takes place in the CFD model.
- Assessment and evaluation of the proposed PACS: The validated CFD model provides high-resolution visualization about the evolved external and internal airflow pattern characteristic of the proposed PACS. The result analysis enables development of the first generic knowledge to further improve PACS for sustainable buildings.

5.1.2. Prototype Building

Natural ventilation in the middle European climate is not a common technique; even in Hungary it is neither applied in the building industry nor included in university curricula, so there is a strong need to have best practices for similar industrial buildings in the wider Central European area. A natural ventilated industrial building (Figure 1) has been built in Southern Hungary, Komló, designed by the Energy Design Group of the University of Pécs. The location is considered as a temperate oceanic climate—Cfb climate zone—by a 1 km resolution Köppen–Geiger classification [81]. The name can be confusing but the mild summer and milder winter can be valid for higher latitudes as well, especially when situated immediately poleward of the Mediterranean climate zone, as is the case here. The site is located on a north facing slope, where the vegetation is limited to grass, only a few buildings and small patch of trees can be found around the building.

The building can reach a positive energy balance as a result of the thermal and CFD-simulation-based ENERGIA DESIGN® planning method [82]. It includes numerous techniques: passive architectural strategies as climate-zoning-based space organization and orientation, NV, strategic building body shaping, structures, materials, wall–window ratios, orientation, further active systems (solar thermal system, earth-probes, heat pumps, soil–air heat exchanger and the originally planned PV-system). The construction of the building was completed in 2012, taking up 2515 m^2 useful area. The production hall with 612.5 m^2 net floor space is placed on the ground floor and connected through 2 levels with the roof by three oversized 'chimneys'.

(a) (b)

Figure 1. (**a**) Experimental reference industry and office building (RATI Ltd.) with passive ventilation towers and wind accelerator 'Venturi' deflectors; (**b**) production hall with adjacent ventilation chimney opening.

The subject of the first investigations is the NV system of the prototype building, which consists of individually developed ventilation wind towers and wind deflecting structures, which ventilates and cools the most important part of the building, the central production hall, and also contributes to the positive energy balance. In this way, a passive air conduction system (PACS) is created in the hall, combining the unidirectional solar chimney principle [83] with updraft ventilation and a depression-generating wind tower system (Figures 2 and 3). The wind tower principle is partly based on the vernacular Malquaf towers [68], while the special airflow deflectors, the 'Venturi' structures—attached to the top of the towers to accelerate the wind flow—apply a bionic principle, based on the convex form of a penguin as a boundary layer accelerator [84].

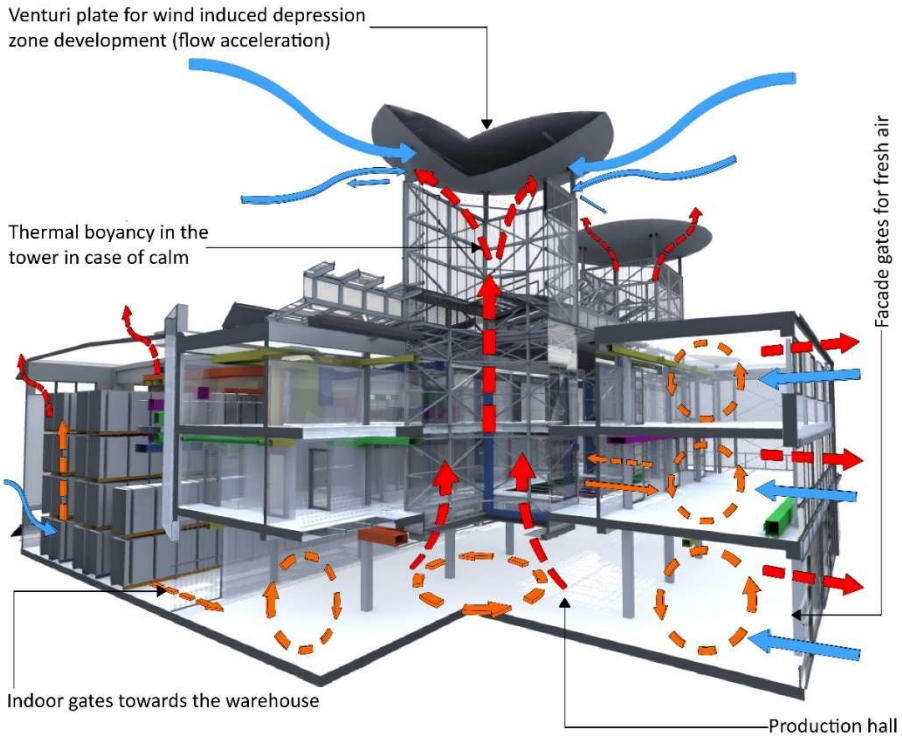

Figure 2. The passive air conduction system (PACS) concept of the prototype building.

According to this concept, the driving force can be wind, solar gains and internal heat loads, generating continuous upward flow (stack effect) from the production hall to the chimneys. Fresh air flows into the production hall via three motorized gates in the north façade. The production hall is directly connected to the warehouse by two industrial gates as well. Through these gates, additional, indirect fresh air post-flow or air change (ACH) can take place in the production hall. The towers are also responsible for the natural lighting of the production hall and the atrium, which is penetrated by the towers. When furnished, the aerodynamically effective volume of the relatively low production hall was significantly reduced by placing machines and shelves. The PACS is operated during the transitional seasons and at mild summer for daytime ventilation (approximately 6 months), as well as on hot summer days for nocturnal ventilation (passive cooling, approximately 2 months). Since a polymer molding process for the automotive industry takes place in the production hall, it is important to have proper ACH, to provide fresh, clean air and high indoor air quality (IAQ) for the employees. The gates at the towers' top are controlled by the building management system (BMS) according to different air temperatures in three different zones in the production hall, to air temperatures at the towers' top, to weather conditions (wind velocity, rain, storm), to time schedules and all of these factors' interconnections. If one of the temperature zones in the hall increases its temperature above a particular set point, the associated tower opens with 30% intensity. In case of further warming in the hall, after each 2 K temperature rise, the appropriate tower opens with 60% and 90% intensity, respectively (Figure 3c).

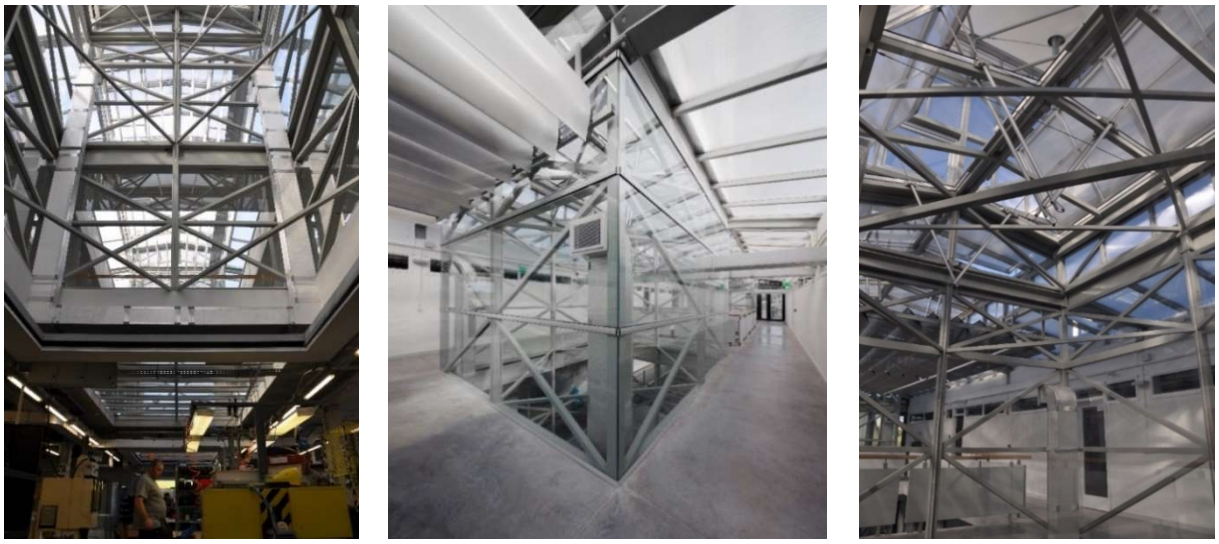

(**a**) (**b**) (**c**)

Figure 3. The passive air conduction system (PACS) in the implemented building. (**a**) Steel–glass–polycarbonate tower with bottom opening above the production hall; (**b**) central atrium penetrated by a tower; (**c**) upper tower opening with 60% intensity.

The ventilation performance was already investigated during the design phase by low-scale wind tunnel tests, which were compared to CFD simulations. The results showed that the difference in the wind tunnel measurement and the CFD simulation is around 10%, which is suitable for design purposes [43]. The wind acceleration factor below the 'Venturi' structures resulted in a promising, high-efficient passive solution for NV systems.

5.1.3. Instrumentation

As part of a research collaboration between the owner and operator RATI Ltd. and the University of Pécs (PTE), the university has added a complex mobile monitoring system (MMS) to the existing building management system (BMS) in the pilot building. The BMS provides users with the ability to control general building automation which contains 300 sensors. The second system, the MMS, includes more than 750 data points and allows the research group to collect flow data from the PACS, energy-related data from the heating, ventilation and air conditioning (HVAC) system, and indoor environment comfort quality (IECQ) in the different rooms. The physical characteristics of the building have been monitored by the research team between the period 2015–2020. The measurement of the thermal and flow conditions of the production hall is crucial for this study, in order to calibrate the CFD simulation model and the comfort and energy system modeling for further research investigations. In the framework of continuous data collection, air velocity measurement was carried out with Dantec Comfort Sense Mini CTA (constant temperature anemometer) hot wire probes (which can measure velocities between 0.05 and 30 m/s with accuracy of 2% between 0.05 and 1.0 m/s and 5% between 1.0 and 5.0 m/s, respectively); the air temperature was measured with TESTO 6621 sensors, with the accuracy of 0.5 °C in temperature. Figure 4 shows the built-in, continuous measurements in the PACS. At a height of 3.0, 5.0 or 7.5, 10, 12.5, and 17.0 m, the towers are equipped with air temperature and relative humidity measuring sensors to record temperature gradients, heat flows, etc. Additionally, in each tower, two CTA

probes were installed, the lower one at hall height (at 3.5 m) and another one at the chimneys' top height (at 17 m).

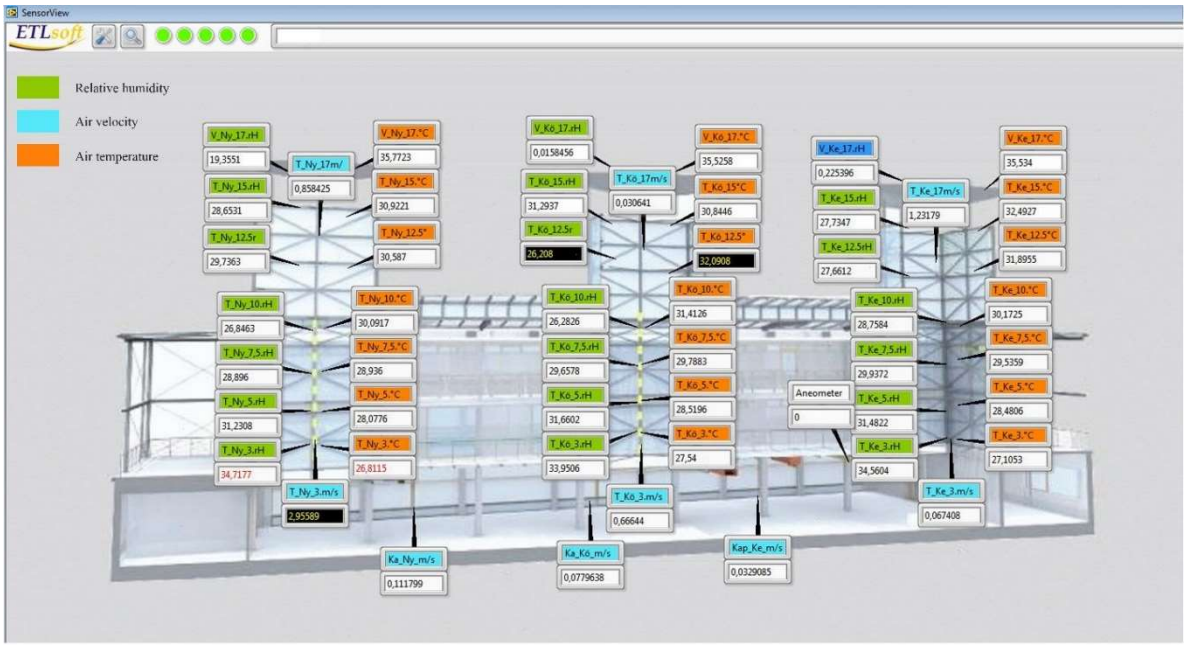

Figure 4. Software interface screen of the MMS monitoring system. Air temperature and relative humidity at different heights of the towers, airflow velocity at 3.5 and 17.0 m height of the towers, airflow velocity in the production hall and at façade gates.

The external wind direction, wind speed, and temperature is recorded by a Vaisala XT520 Weather Station with ultrasonic sensors in a National Instruments CompactRIO field data acquisition and processing device. The measurement range and accuracy of the weather station is the following: wind speed: 0 to 60 m/s; ±0.3 m/s; temperature: –52 to 60 °C; ±0.3 °C. The measurement tool is installed at the top of the 'Venturi' structure above the west vent-tower (Figure 5) in the free atmospheric wind flow and the total height of its position is 21 m above ground level and 4 m above the 'Venturi' structure of the tower.

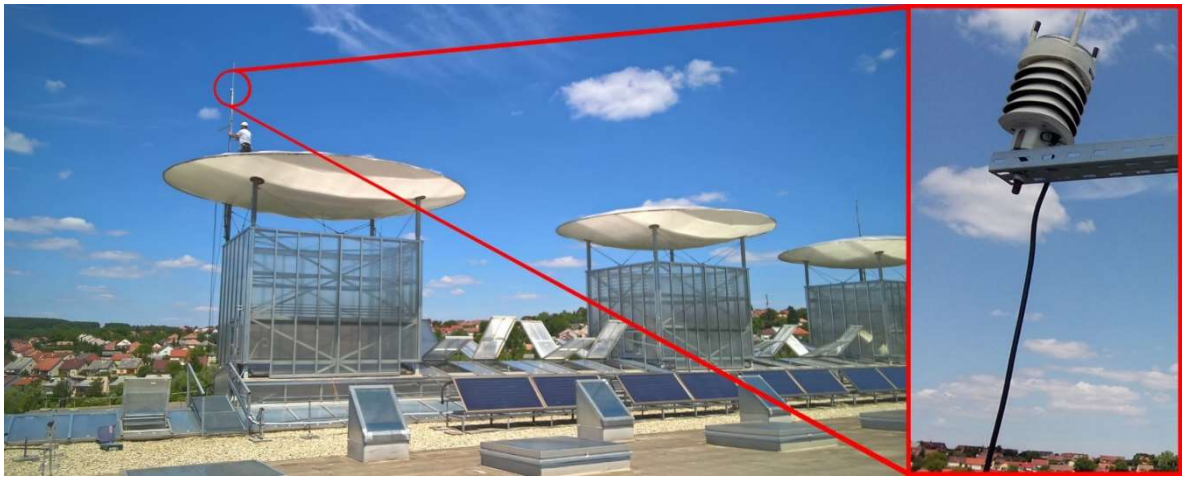

Figure 5. Installed position of Vaisala XT520 meteorological weather station on the west ventilation tower.

For the purpose of this study, instantaneous values were required for the validation of presumptive flow simulations, so a brief, 3-hour operation period of the production hall was recorded in working hours, taking into account lighting function, occupant position and metabolic heat production, tools, machinery, and power. In addition to in situ continuous MMS measurements, manual measurements were also required to integrate the effects of infiltration through air ducts, facade joints, and exterior and interior windows and gates. The manual measurements were carried out by the following strategy: the air change was induced dominantly by the suctions effect of three wind towers in the production hall. All the openings were closed and the air handling units (AHU) were shut down during the measurements. Therefore, the fresh air sources were only infiltrations around the building envelope openings and the internal gates and doors, as well as the air ducts' supply inlets of the mechanical ventilation system. Despite the AHU being shut down, the air duct inlets were considered as inlet source as well, because indirect access to outdoor fresh air is provided by a special passive soil–air heat exchanger tunnel system. This subterranean air duct system was constructed as a pre-heater or pre-cooler of the mechanical ventilation. This means that the measured temperatures were not influenced by any forced and tempered ventilation. The infiltrations and the air duct inlets were not integrated to the MMS; hence a manual measurement was necessary. Since the CFD simulation represents aerodynamic phenomenon in a capsuled short period of time, therefore the measured data were collected in a short time as possible (approx. 2–3 hours) to finish the assigned measurements in the hall. Simultaneously, the MMS saved data in a minute frequency, to enable to collect detailed, averaged monitoring data. A Testo 480 handheld multifunctional meter was applied with telescopic air temperature, relative humidity, and anemometer (hot wire resistance probes) flow rate meter for infiltration air velocity (volume flow) and air temperature measurements, with the following specification: temperature: –20 to 70 °C; ±0.5 °C and velocity: 0 to 20 m/s; ±0.03 m/s; range and accuracy, respectively. Volumetric flow rates were measured at the ground floor openings in accordance with ISO/DIS 19455-1(en) planning for functional performance testing for building commissioning" using the equal area method for the entrance to a rectangular duct. Since each tower cross-section takes up approximately 5.2 × 3.9 m, calibration of the automated, integrated MMS anemometers in the towers in 3.5 m height were necessary: here, manual air temperature and velocity measurements were carried out within a raster, consisting of 25 sampling points per tower.

The perimeter infiltration (porosity) of the hall's envelope structure could be determined by measuring air velocity and temperature at all external and internal openings (façade gates, internal doors) and calculating the volume flow values at each opening perimeter (Table 1 and Figure 6). In order to exclude effects of mechanical ventilation, the air handling units (AHU) were switched off during the typical occupation/production hours at the time point of measurements. Table 2 and Figure 7 assess the measured 'passive' inflow rates through the supply air duct-inlets, caused by the pressure difference in relation to the production hall. Exhaust air could only exit the building through the three ventilation towers. This work is typical for transition and early summer operation periods: during daytime only exhaust airing takes place through the tower openings and during night cooling by fresh air flows in via façade gates and exhaust air leaves through tower openings. Due to the principle of energy and mass conservation, the outflow measurement values through the towers should agree with the inflow into the hall [85]. Regarding the manual metering results, it is apparent that the porosity infiltration plays a considerable role in inflow intensity, while the air duct inlets have almost no impact on the airflow characteristic of the hall.

Table 1. Measured infiltration volume flows and temperatures through the envelope openings and perimeter in the production hall.

Measured Point	Filtration/ Airflow Via	Airflow [m3/h]	Air Temperature [°C]	Direction of Airflow	Total Airflow [m3/h]
.	N wall	148	27.7	IN	24,088
.	NW gate	3430	26.5	IN	
.	N wall	140	25.9	IN	
.	Central-N gate	3110	26.3	IN	
.	N wall	372	25.1	IN	
.	NE gate	4170	26.3	IN	
.	N wall	236	26.7	IN	
.	E staircase door	300	26.3	IN	
.	E office door	407	25.8	IN	
0.	Autom. SE gate	5120	25.7	IN	
1.	Man. S gate	934	24.9	IN	
2.	Man. S gate	746	25.6	IN	
3.	Man. S gate	1308	25.4	IN	
4.	Man. S gate	854	25.1	IN	
5.	Autom. SW gate	2136	24.8	IN	
6.	W staircase door	540	25.4	IN	
7.	W office door	120	25.4	IN	
8.	W workshop door	17	25.9	IN	
9.	W wind tower	8029	26.5	OUT	24,088
0.	Central wind tower	7557	26.6	OUT	

1.	E wind tower	8502	26.9	OUT

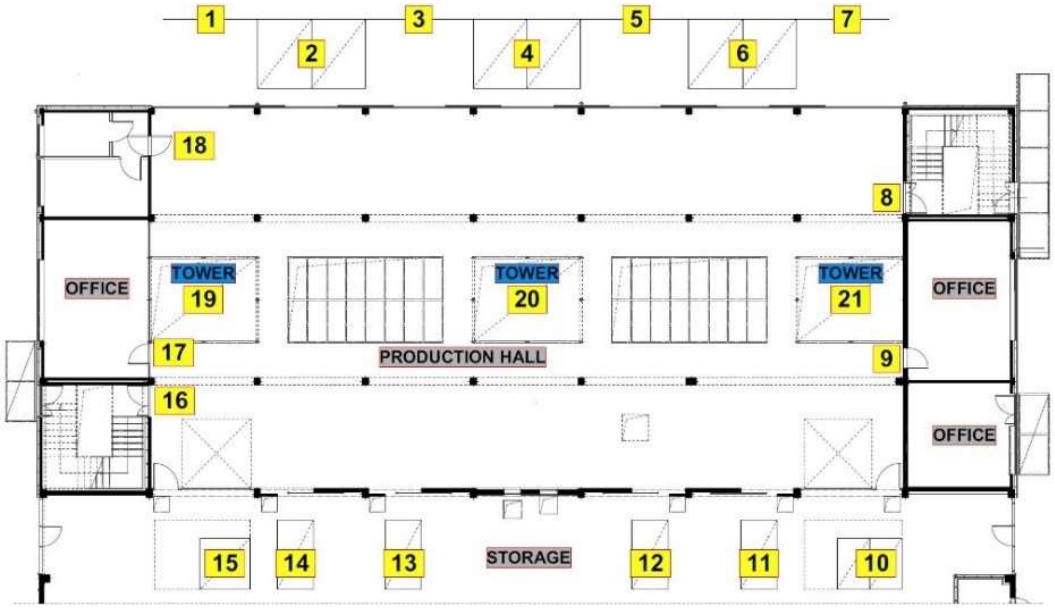

Figure 6. Location of measurements of infiltration volume flows and temperatures through the envelope openings and perimeter in the production hall.

Table 2. Measured air flow rates and temperatures trough air duct inlets.

Passively Induced Air Flow From		**No.**	**Air Flow [m^3/h]**	**Air Temperature [°C]**	**Direction of Air Flow**
Fresh Air through Air Supply	East part of air duct	1.	5.76	31.63	IN
		2.	3.96	25.1	IN
	West part of air duct	3.	11.76	24.88	IN
		4.	7.8	25.23	IN
		5.	1.32	26.07	IN
		6.	1.44	27.63	IN
		7.	5.04	25.88	IN
	Air duct from wind tower—west	13.	55.5	24.2	IN
	Air duct from wind tower—central	14.	24.5	25.78	IN

	Air duct from wind tower—east	15.	132.5	26.21	IN
Air Extraction From Technology	Tech. extraction—North	8.	37.26	35.83	OUT
		9.	12.96	32.73	OUT
		10.	6.48	32.73	OUT
	Tech. extraction—South	11.	41.58	30.93	OUT
	Glue machine extraction	12.	4.52	28.05	OUT

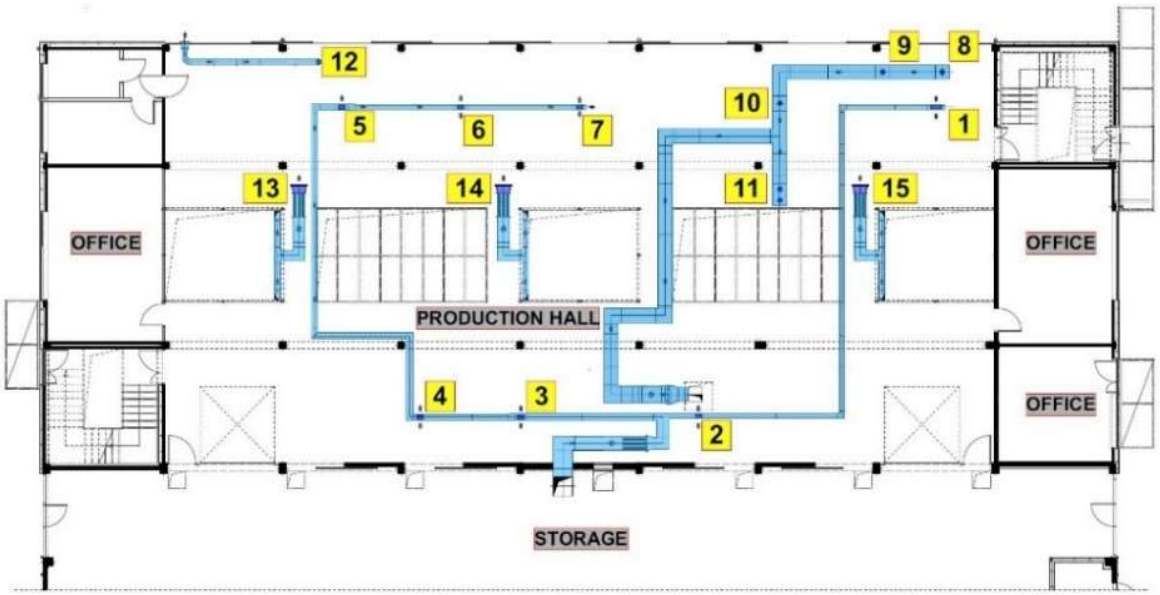

Figure 7. Location of air flow rates' and temperatures' measurements trough air duct inlets.

5.1.4. The CFD Model

In order to analyze airflow characteristic and temperature distribution, fluid dynamics simulations (CFD) were carried out, using ANSYS FLUENT 17.1 as equation solver. Besides wind-driven airflow phenomena, the thermal buoyancy driven airflow effects (stack effect) and thermal qualities of the PACS will be examined as well. The surrounding terrain and the building geometry was overtaken from the architectural design (final plans), and remodeled according to the CFD specifications.

A highly detailed 3D-model has been built; every single furniture is placed in the hall, mostly in simplified representation as a cuboid. The model contains heat sources as well: all lamps and instruments and their heat losses and people's heat dissipation (Figure 8 and Table 3.). For each obstacle that possesses certain internal heat gain with different heat intensities (W/m^3) were dedicated corresponding to the automated and manual monitoring in the production hall. The heat source values are contained in Table 3 for the machines and the worktables.

Figure 8. Internal heat gains from occupants, equipment and artificial lighting in the production hall.

Table 3. Internal heat gains from occupants, equipment and artificial lighting (W) in the production hall.

Heat Sources [W]			
No.	Name	Technology [1]	Lighting [1]
1.	Vacuum machine	not operating [2]	-
2.	Vacuum machine	4400	-
3.	Vacuum machine	not operating	-
4.	Vacuum machine	2100	-
5.	Vacuum machine	not operating	-
6.	Disk-type milling cutter	not operating	-
7.	CNC machine	1980	-
8.	CNC machine	not operating	-
9.	CNC machine	not operating	-
10.	Table (equipment)	4 × 40	6 × 46
11.	Table (equipment)	6 × 58	6 × 36
12.	Table (equipment)	6 × 58	6 × 36
13.	Table (equipment)	4 × 58	4 × 36
14.	Table (equipment)	4 × 58	4 × 36

15.	Table (equipment)	38	2 × 20
16.	Table (equipment)	2 × 38	2 × 36
17.	Table (equipment)	2 × 38	2 × 36
18.	Sitting occupants	8 × 150	-
19.	Standing/walking occupants	8 × 200	-
20.	Hall lighting	-	102 × 35

[1] Calculated heat losses, by the manuals of equipment given by the operators; [2] Some machines did not operate under the period of measurements.

The geometrical discretization has been followed by dividing the flow field for numerous cell size domains to have accurate values where it is needed, and the model size was fitted to the computation limits with almost 9.5 million cells in volume. The most detailed is the production hall; the remaining inner rooms and spaces are not important for the research questions (Figure 9). Different leaks were constructed around the façade gates (as an effect of the inaccurate construction), having adjustable porosity properties in order to simulate the infiltration phenomena through the façade [86]. According to boundary conditions assessment (manual measurements), the air duct system's supply air inlet volume flows were modeled as well. The discretized geometry consists of 0.2 m average cell size elements inside the building. The external space was divided to diverse volume domains, where the average cell size in the near building shell domain is 1.5 m, while the ground holds a 5 layers of prismatic boundary layer for the proper modelling of the important near wall flows, thus the volume mesh is an unstructured hybrid mesh with pyramid, tetra and hexagonal elements.

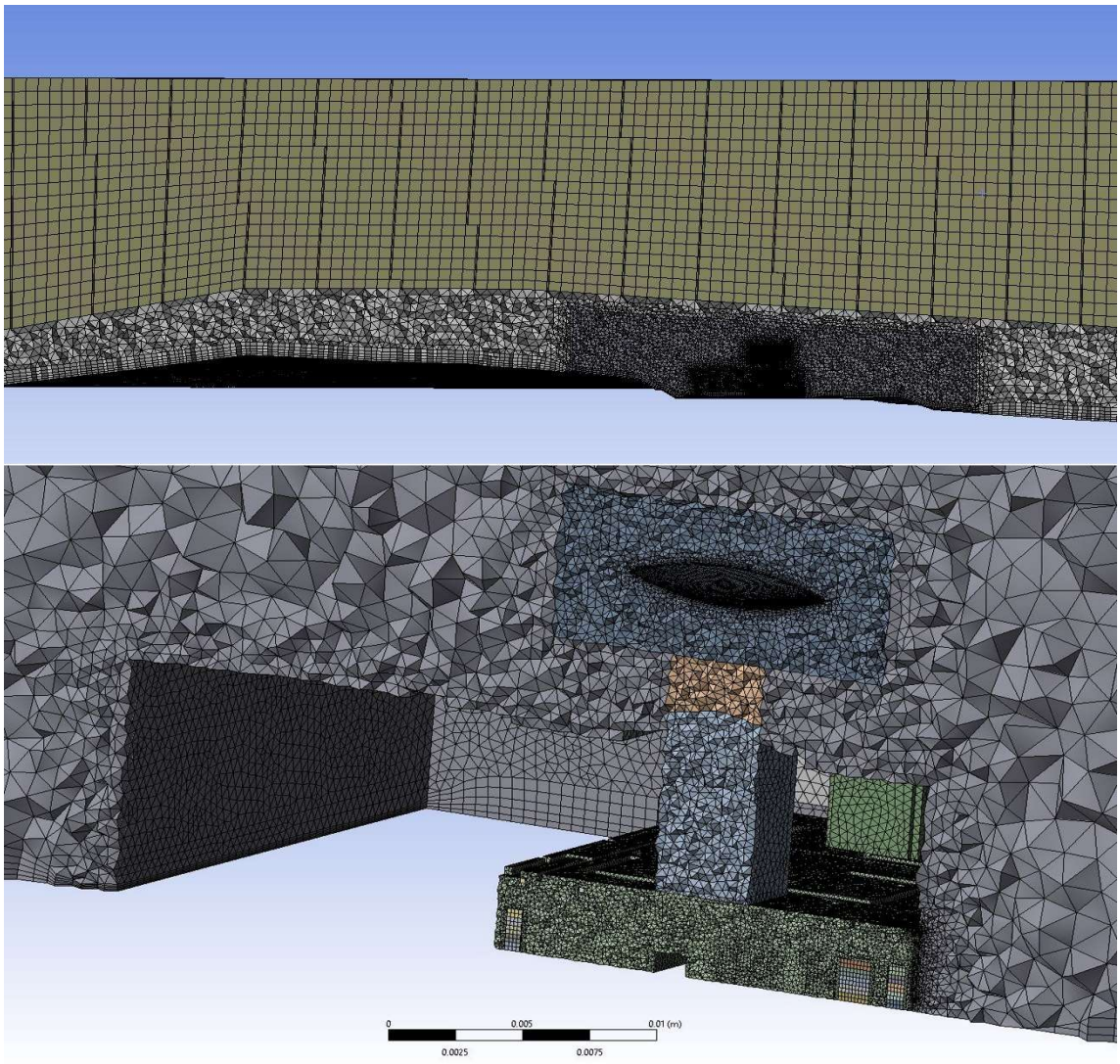

Figure 9. The volume mesh section from far view (top) and close view (bottom).

5.1.5. Boundary Conditions

For validation purposes, nine wind directions were recorded on 32 different days during the summer. However, to manage this simply, only the prevailing wind direction case is presented in this study, while the other datasets were recorded for overall validation. The validation was based on the NW wind direction, which was the most relevant wind direction during the boundary-condition-assessing measurements (Figure 10).
In this particular case, the measured average wind speed amounted 4.06 m/s, which was chosen as a basis for the wind profile adjustments at 17 m elevation from ground. The simulated wind profile is based on the following equation (1), presuming that the wind velocity reaches 3 m/s at 10 m height.

$$v_{mag}=0.7102\cdot\ln(z)+1.9361, \quad (1)$$

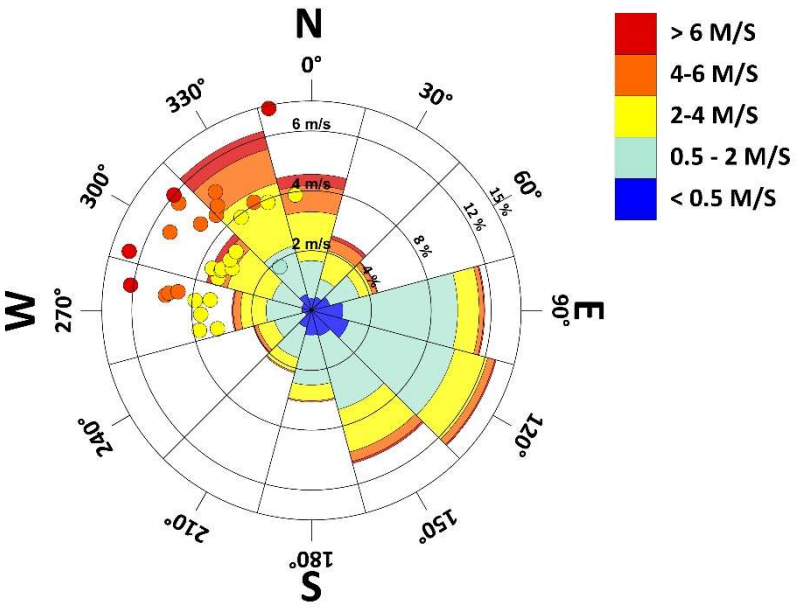

Figure 10. Wind speed frequency (%) with accruing wind directions and velocities in yearly resolution showed by segments and during the validation measurement hours showed by dots (m/s).

The temperature was measured individually at more points as at the weather station (ambient temperature) and in the production hall (three measurement points) and in the towers (3 x 6 sensors, Figure 4) to set the initial values. As Figure 8 shows, heat sources such as lamps, machines and workers in the hall were determined with position and geometry, whereas these objects were handled as porous boxes with different air tightness based on measurements [87]. The viscous model is based on the previous experiences; a stable solution was chosen for transient solution (with initial steady state calculation), with energy transport modelling included. As shown in the literature research and own experiences, k-Ω turbulence model is well suited for this kind of investigations, therefore in the design phase simulations this turbulence model was used. Reaching a steady state situation after 10,000 iterations, the simulation was modified into transient calculation method for accurate realistic results.

5.2. Results of the validation process

5.2.1. Validation of the Reference CFD Model

Figure 11 shows the cross section of the model (terrain and building) with the developed air flow around the building as an overview of the flow field. The initial comparison for the validation was derived from the average velocity magnitude in the cross section at the wind velocity meter (Figure 12a). The results show 0.16 % of deviation compared to measured data, which can be accepted as an accurate result [6]. As the second reference, the air temperature differences were highlighted (Figure 12b), and in accordance with the results, the energy transfer simulation method can be stated as acceptable, with no need for further statistical analysis, while the difference from the measured values shows a value lower than 1%. In an engineering application, this result can be used for further joint processes.

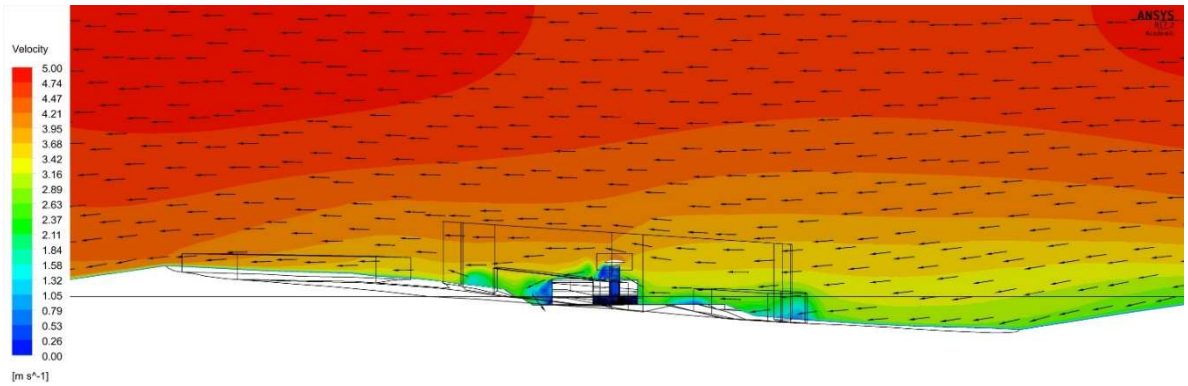

Figure 11. Air flow field in the CFD simulation model, velocity contours and vectors (m/s).

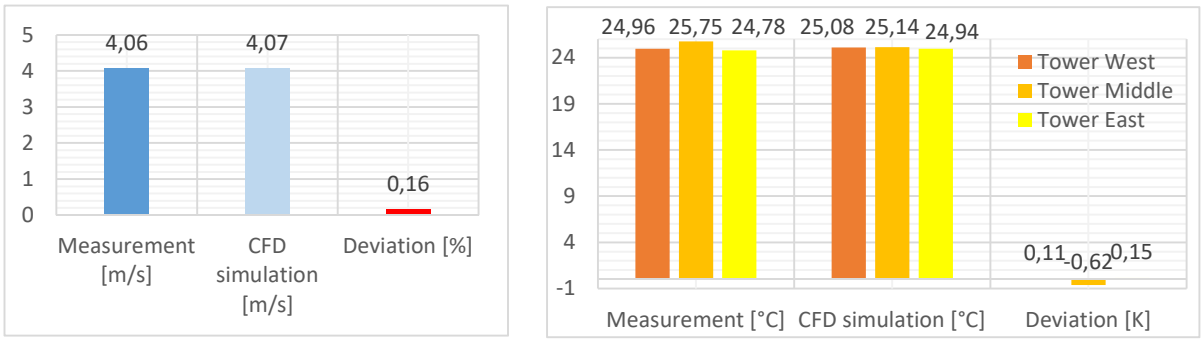

(a) **(b)**

Figure 12. Measured and simulated wind velocity (a) and air temperature (b) comparison in the three ventilation towers.

Figure 13 demonstrates the air velocity distribution at the bottom opening of the towers in 3 m height, while the comparison between the manual and automated velocity measurements is shown in Figure 14. The automated MMS measurement shows significant deviations from the average value of the detailed manual measured results: 11.3% at middle tower, 33.4% at west tower and 42.44% at east tower.

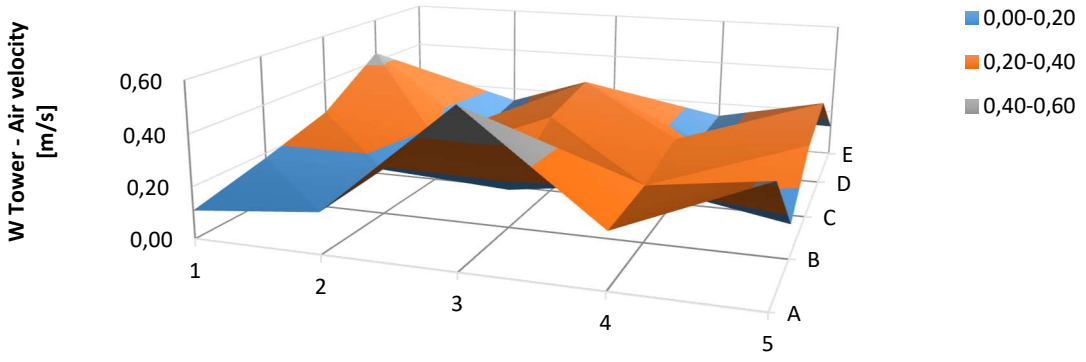

(a)

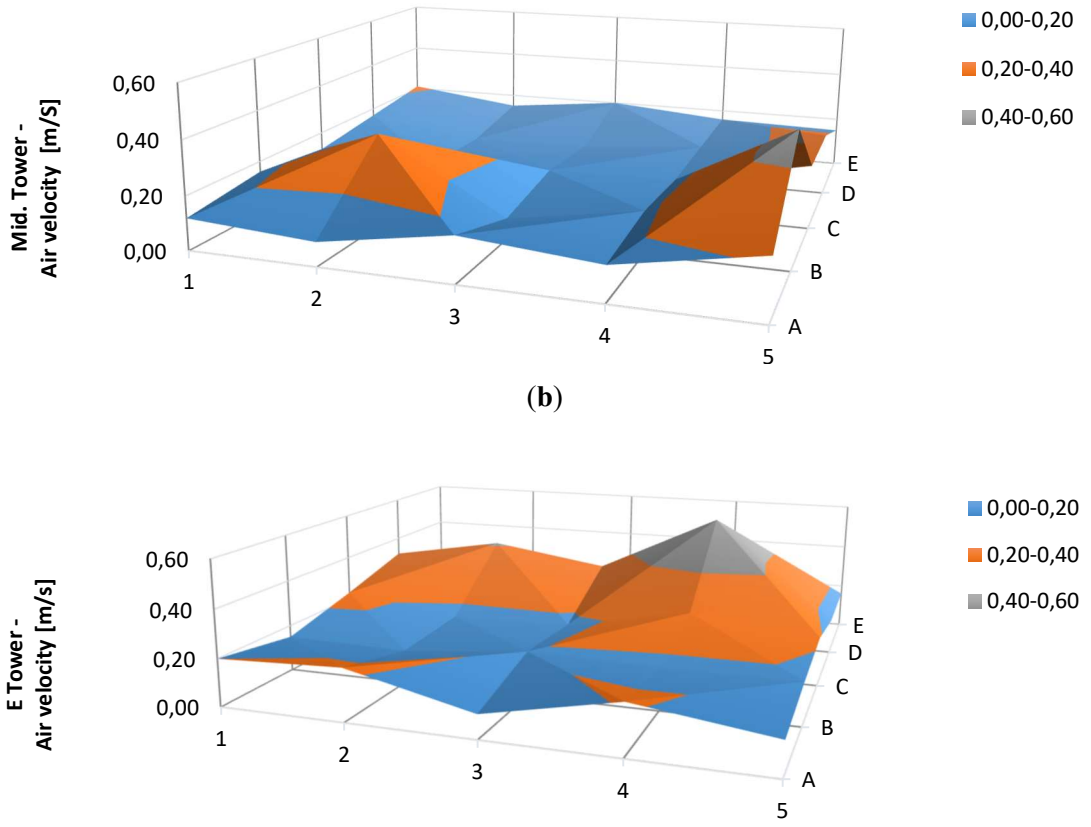

Figure 13. Manual measurement results in 25 sampling points per each tower about air velocity in the bottom inlets in 3 m height.

The hand measurements demonstrated that the automated anemometer's metering and sampling correctness is inaccurate due to occurring complex airflow turbulence in the tower, which cannot be assessed by only one metering sampling point. However, the continuous anemometer measurement can deliver a time-dependent, approximated picture about the airflow characteristic of the towers and the hall for general monitoring purposes. However, the error values are virtually important, since they provide useful correction factors for the recalculation of measured airflow results (Figure 14) to achieve an appropriate basis for the comparison with the CFD simulations. These corrections were made accordingly in the following volume flow comparison.

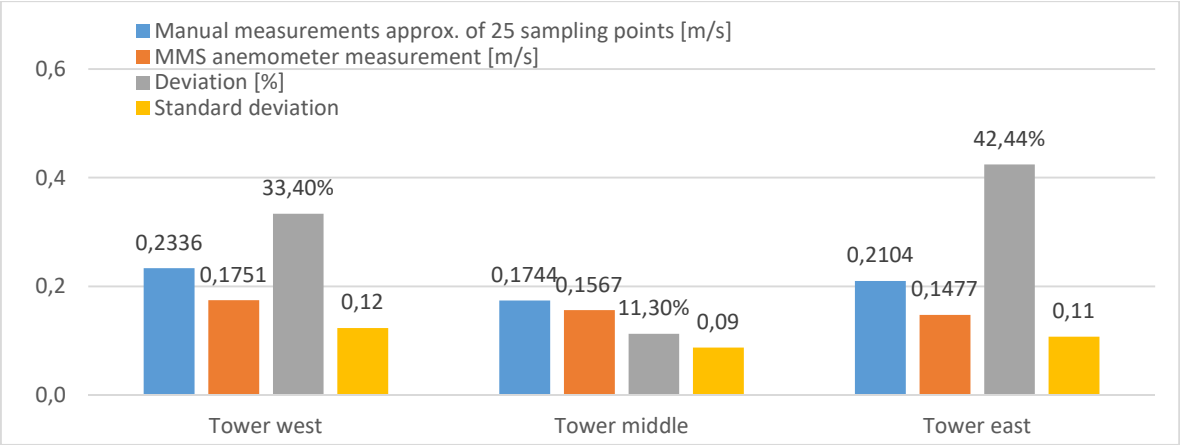

Figure 14. Comparison of hand measurement results in 25 sampling points per each tower (mean value) and MMS automated anemometer measurement of 1 sampling point about air velocity in the towers' bottom inlets.

Next, the ventilation of air volume flow rate was analyzed at the three towers (Figure 15). Regarding the total volume flow rates, a disagreement of 6.18% occurs. The detailed comparison at each tower's airflow characteristic delivers higher deviation between 13–17% in both positive and negative directions due to the following correlations. In the simulations a constant wind flow is provided form NW direction; according to that, a constant airflow system can be developed in the model. Since the wind direction changes continuously, there is no constant wind direction in reality, so the wind direction can change even every minute. To avoid this problem, only wind direction data were taken into account between north and west. In case of a rapid wind direction change from north to west, airflow acceleration will be induced in the wind exposed west tower. During this, in the east tower—which is located now in slipstream—the airflow stops not immediately, but rather continues according to the previous N wind's momentum to stream forward in the moment of measurement. This air movement does not change the measurement values significantly but shows the appropriate distribution as lightly distorted.

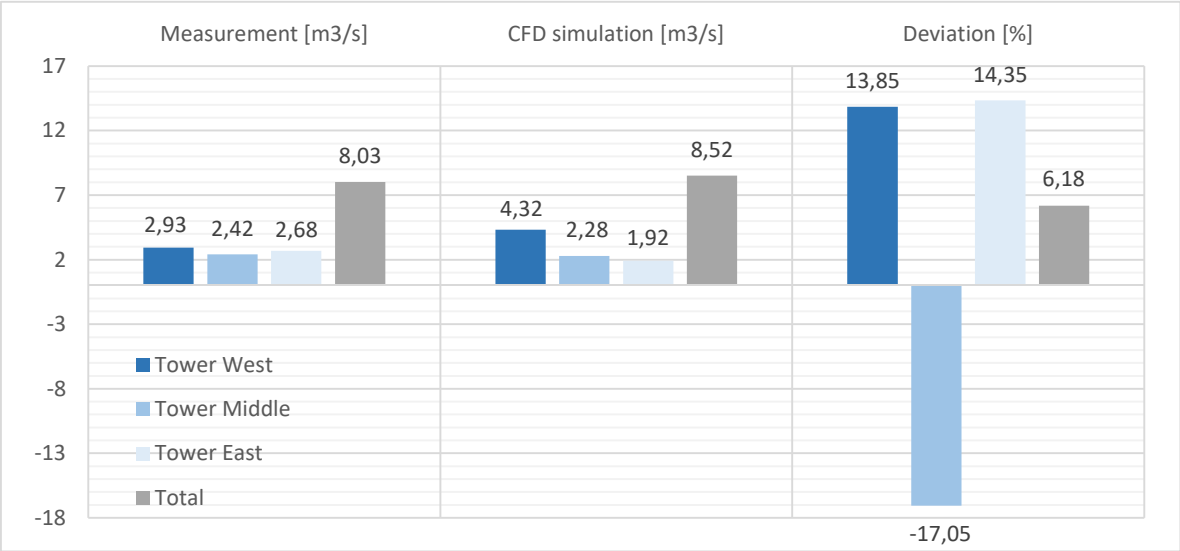

Figure 15. Measured and simulated air volume flow comparison in the three ventilation towers.

Due to the uncertainty grade of the measurement technique in such time dependent cases, the deviation values—regarding the complexity of the fluctuations and, as a result, the variation in measurements and the variation in measured and calculated values—show by all means an acceptable validation of the CFD model. Based on the result comparison, the CFD simulation model can be acknowledged as a validated, calibrated CFD model that follows reality in an accurate way and is available for further development of up- and downdraft ventilation systems, also in a generalized form.
Since the model was similarly adjusted from other wind directions, giving similar accuracy rates, the focus was put on the inside flow field.

5.2.2. Evaluation of the PACS Efficiency

The pathline diagram (Figure 16) demonstrates the efficient and comfortable ventilation of the production hall in accordance with the boundary conditions of the validation measurements: during typical working hours, the gates of the north façade were closed and the doors of the towers were 100% open. The PACS is able to ensure 30,646 m^3/h volume flow rate, which means an ACH of 11.98 1/h in the production hall (the total volume contains the tempered air volumes of the three towers also). The PACS can achieve approximately 9.3 times higher ACH than the required value according to the EN 15251 standard of indoor air quality [62] (because the standard does not concern industrial functions, as mentioned in the introduction, the given values for conference rooms were used, because the occupant density was similar to the ventilated hall). In addition, the air distribution of air is well mixed in the hall, ensuring a homogenous ACH without stagnant zones. The suction effect in the chimneys starts an upward flow, which helps to drive in outdoor air through the façade construction filtration. The air flowing in the chimneys develop large swirls, suggesting that, for the purpose of increasing flow velocity and ventilation efficiency, this tower system has too large cross-section dimensions in relation to the hall's volume and geometry as well as related to the building's shape and dimensions. This can be seen as a result of 'to be mistaken for security', by oversizing the towers with a safety margin.

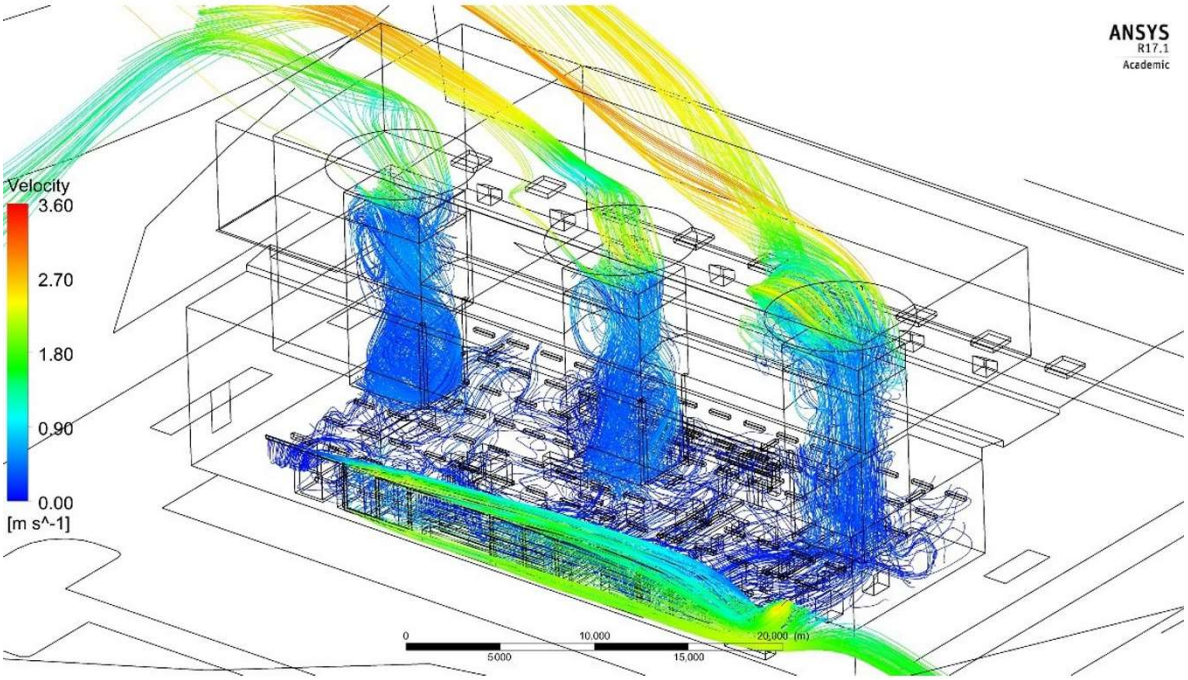

Figure 16. Airflow characteristic in the production hall with three updraft ventilation towers, velocity pathlines (m/s)—validated CFD model of the implemented Hungarian reference building.

At the initial wind direction, we can follow the tower efficiency by monitoring the pressure field at Figure 17b demonstrating decreasing efficiency in this specific wind direction. Figure 17a shows the decelerating velocities in the chimneys moving from right to left, while the pressure diagram (Figure 17b) shows that the suction power of the depression zone behind the towers is gradually decreasing, following the wind direction. In this case, when the wind approaches the building parallel to the longitudinal axis of the hall, the towers have a slipstream-effect on each other; therefore, the towers behind each other possess less suction power. Consequently, the 'ideal' wind direction means currents perpendicular to the longitudinal axis of the building, i.e., wind direction from N. In this wind direction case, no slipstream situation would evolve, and hence the efficiency would increase, resulting in a better ACH in the production hall.

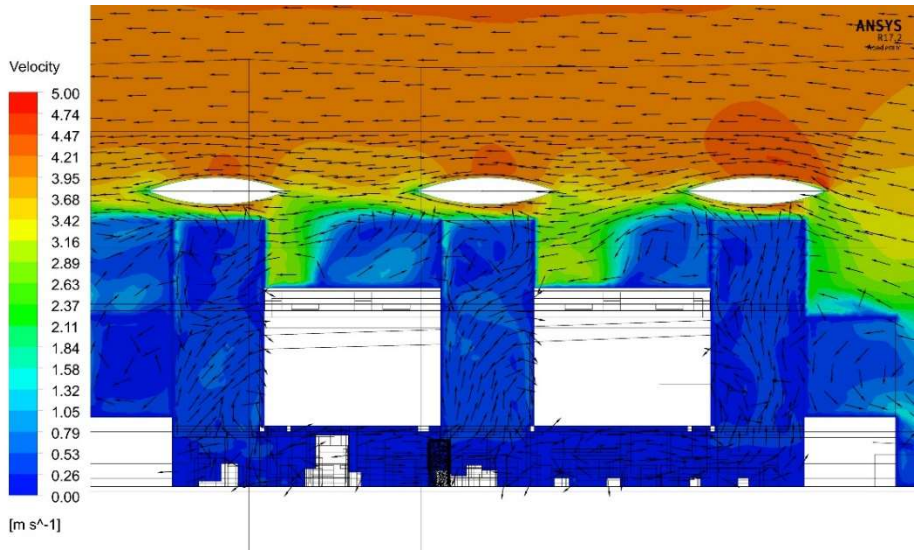

(**a**)

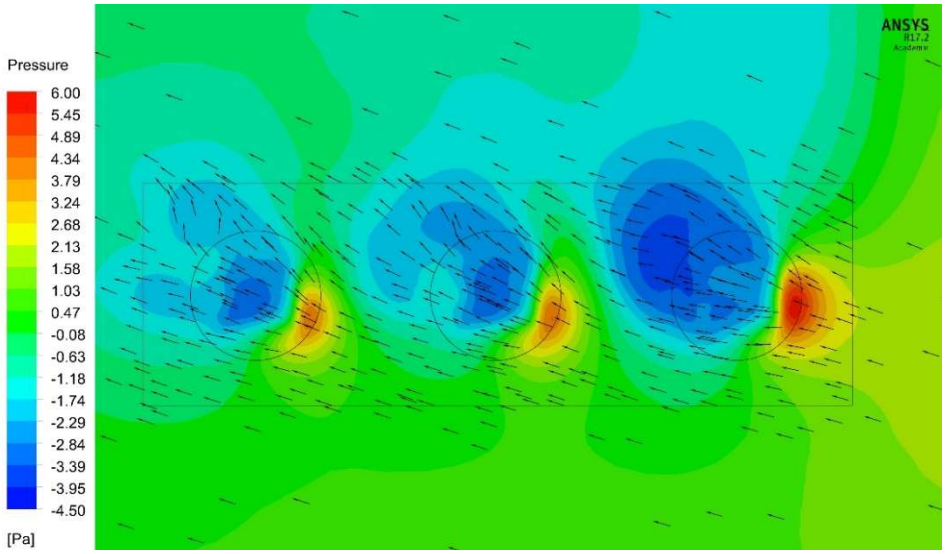

(**b**)

Figure 17. Longitudinal section through the hall with flow velocities (top) and pressure field at the 'Venturi' plates (bottom).

Figure 18 shows the internal conditions of the production hall. According to the figure on the top, there is no draft inside the hall, to the detriment of the PMV-index and to the benefit of the DR-index according to EN ISO 7730 and EN 15251; only the exhaust air inside the chimney starts to accelerate. There is an efficient wind acceleration effect to observe: the wind velocity of approx. 2.5 m/s is accelerated to approximately 5 m/s between the chimney's top opening and the 'Venturi' disc by developing here a depression zone (Figure 17–18). Further, the wind strikes perpendicular to the right outer wall of the tower, slows down in vertical direction (from 4.06 to 2.4 m/s) and, as a weakening force, it decelerates the unobstructed higher, horizontal currents. Underneath the 'Venturi' plate, below the occurring velocity maximum, there is a small air drop into the chimney, suggesting that the draft booster geometry is far from the chimney opening. The figure at the bottom illustrates that the flow of cooler outside air inside the hall prevents overheating in the comfort zone (indoor space from 0 to approximately 2 m height) due to the heat generated by occupants, artificial lighting, and the equipment. While the air temperature in the comfort zone remains below 26 °C, the overheated area with 26–28 °C is only visible in the red-stained air layer below the ceiling, between 3.0–3.4 m height.

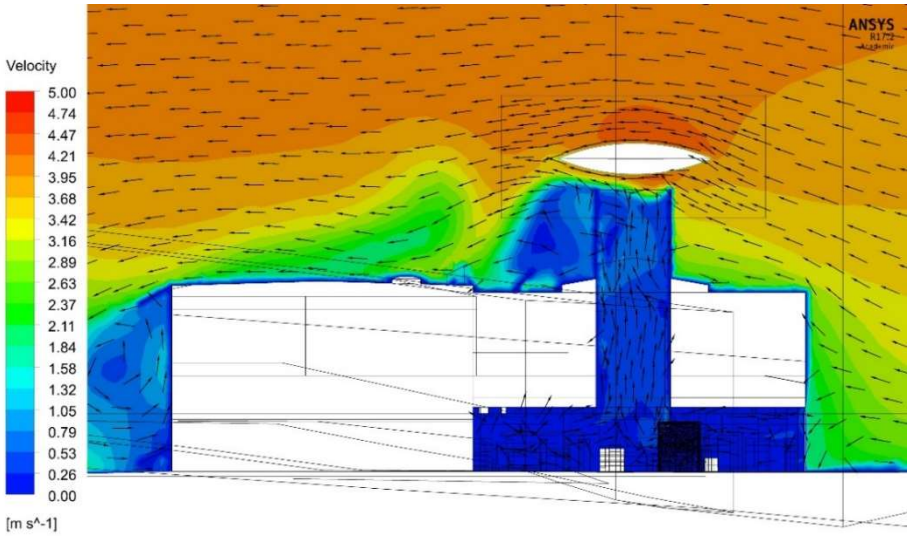

(**a**)

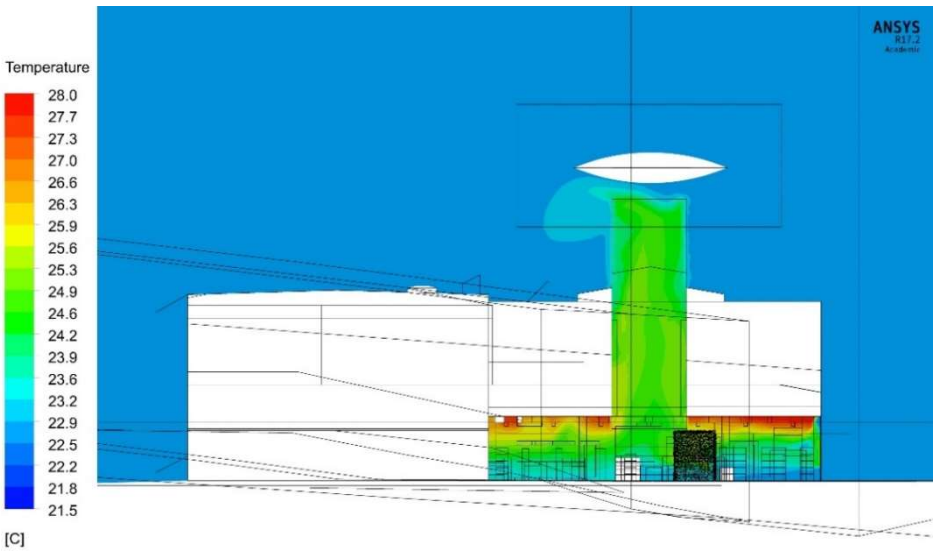

(**b**)

Figure 18. Cross section through the hall with velocity contours and vectors (a); air temperature distribution (b).

5.2.3. Conclusions of the in situ measurements and validation

Through the experimental measurements in the tested industrial building, the functionality of the proposed special-type PACS has been proven. Furthermore, the achieved high ventilation efficiency rate confirms the advantageous aerodynamic approach of the ENERGIA DESIGN® planning method, applying fluid mechanics calculations, wind tunnel tests and CFD modelling to develop working PACS in buildings.

The comparison of CFD simulation showed that experimental measurements revealed almost identical local air temperatures and wind velocities, while flow rates closed up the measured values with acceptable error rates.

Since deviations between measured and calculated data are primarily due to changing wind direction and the consequently delayed wind momentum effects in the measurements, the model can be acknowledged as validated, providing an initial model for new research experiments in the form of case modifications.

Besides quantifying the efficient functionality of the proposed PACS, the results demonstrated specific external and internal airflow characteristics, which revealed the following novel conclusions and development requirements regarding PACS system properties in middle-sized, single-story industry halls under temperate oceanic climate, i.e., in cases of common European SMEs with approximately 500–1,000 m^2 floor space:

The **high-resolution CFD model** of the tested building predicted the PACS performance with sufficient accuracy, and thus the aerodynamic planning process could be appropriately supported. Therefore, high-resolution CFD modelling is recommended in order to reliably predict the complex natural airflow phenomena in sustainable building design;

Smaller than planned **chimney cross-section** dimensions (5.2 × 4.9 m) would hold promise for more economic structure solutions by still maintaining the necessary air exchange rate for daytime ventilation as well as for night-cooling. The narrower chimney cross-sections could decrease the generated up-draught vortexes (lateral distribution of the air currents' kinetic energy) in the towers, and thus a more efficient wind draw could be achieved. With the help of

detailed CFD model support, the building industry standard ‘safety margin over sizing effect’, and therefore investment costs can be reduced significantly;

Finding 1

The ENERGIA DESIGN® planning method was proposed by Kistelegdi in 2013. The proposed method was used during the design process of the RATI Ltd.’s new industrial complex. The building contains a complex Passive Air Conduction System with three wind towers. A high-resolution Computational Fluid Dynamic model was developed for investigating the building ventilation performance and compare it with in situ measurements. The validated model showed that instead of three wind towers only two could have been sufficient to maintain acceptable comfort level in an approximately 600 m2 industrial hall with 4.5 m height and light industrial occupancy. These results highlight the importance of detailed complex aero dynamical simulations in the design phase, therefore, it can save significant amount of energy and money.
The thesis approves the novelty and pioneer ways of the Energy Design® method, however the possible improvements were clarified by the newly obtained results.

The deaccelerating effect on the approaching wind velocity, caused by the slowed-down upward flow along the chimney shaft’s vertical wall, could be avoided by designing the **tower’s wall in tilted position**. An approximately 45° slope shows a promising concept (arithmetic middle between vertical and horizontal surfaces) that needs to be quantified in future CFD experiments. Firstly, in this way, undisturbed circumstances should be created for the entering wind flow into the zone between the ‘Venturi’ disc and the tower’s top outlet opening, to ensure the generation of an appropriate under-pressure zone. Secondly, this solution should further increase the wind velocity due to its ‘nozzle-effect’;
In order to ensure an optimal depression zone (acceleration) development at the chimney’s top outlet, the **‘Venturi’ deflector plate’s position** plays a key role in the creation of an efficient draw effect. Arranging the deflector structure closer to the tower’s top outlet opening gives promising indications: it would prevent relapse and increase the ventilation suction effect;
Variations in the **shape and size of the ‘Venturi’ disc and** the corresponding **roof structure/chimney-tower** open a new field of wind acceleration and ventilation optimization in PACS. Questions regarding the tilt angle of bottom surface of the ‘Venturi’ structure, height of the chimney above the roof surface, tilt angle of the tower top opening geometry, as well as he dimensions of the top opening chimney gate, must be answered in iterative future CFD investigations;
The intensity of the wind tower vent-operation changes according to their **relative position** to the building and to each other. It is worth arranging them in correspondence with the general wind-microclimate. To avoid weakening the ventilation capacity of the towers in wind shaded positions, it is recommended that they are not too close to each other in a given wind direction parallel to their straight arrangement axis-line. A more random arrangement is needed, whereas the distance between two towers must be great enough to prevent slipstream effect. Evidently, further CFD model tests are necessary to give precise feedback about the according performance of the diverse tower arrangements. In the current study, the least effective—most often slipstreamed—middle tower could be left out from future design: the two lateral towers provide a sufficient ACH of 8.72 1/h, 6.7-times higher than the regulatory required 1.4 1/h ACH by the EN 15251 standard.
In conclusion, the following statements are suitable for a setup of a sufficient PACS of a typical SME: two towers are able to achieve the required air quality level already and their dimensions are acceptable at approximately 5.0 × 4.0 × 17.0 m (width x deepness x height). For a reliable

updraft ventilation those should be equipped with 'Venturi' deflector structures over the chimneys. The 'Venturi' plates should have lateral cantilevers with a deepness of approximately 0.5 times the min. diameter of the chimney. The required area related PACS ratio is 0.10 (10% of the net floor space is required for appropriate NV) and the necessary volumetric PACS ratio is 0.31 (31% of the space volume is required for appropriate NV). The ratio between hall and chimney height is approximately 1:5. Nevertheless, these dimensions can be specified by further studies.

In the future this validated CFD model is suitable to investigate the influencing factors of major geometry changes, arrangement variations and different types of PACS's operation principles. Valuable results could be exploited about the geometry settings of the towers, such as different heights, cross-section shapes and dimensions, or a vertically varied tower design, for instance. These results would affect the efficiency of a PACS, as well as the architectural appearance of a building. One of the most important parts of a wind tower is the opening at the top, and, in this case, the Venturi shaped deflectors. With different variations in these 3d-deflector objects (geometry, horizontal and vertical positions) a whole generation of Venturi objects could be developed in the future. Thus, an easily applicable system would be created, which can be used in different climatic (unidirectional or omnidirectional towers, depending on the prevailing wind direction), topographic (urban, rural, etc.) or aesthetic (city regulations, customer demands, etc.) situations. A problem of multiple interest was discovered during the study: the number and the horizontal arrangement, as well as the locations of the chimneys related to each other and the buildings, can significantly affect the efficiency of the PACS. The simulation results should be also used for comfort rate validation as well.

In the future this validated CFD model became suitable to investigate the influencing factors of major geometry changes, arrangement variations and different types of PACS's operation principles. Therefore, valuable results could be exploited about the geometry settings of the towers. These results have shown that the buildings PACS, which was designed by the ED method, were not fully optimal, because the achieved ventilation rates (8.72 h^{-1}) suggested that only two towers would have been sufficient to create acceptable IAQ in the production hall. With this modification the construction would have been faster and cheaper, extra interior space would have been freed, and a clearer and optimized PACS would have been applied to the building. The results are not devaluing the ED method significance, but shows the importance of high resolution CFD simulations even in the design phase for cost and energy efficiency.

5.3. System comparisons of different PACS solution with identical boundary conditions

5.3.1. Case study building and Site

The design of a new winery was started in 2017 in Villány, Hungary (Figure 19). The site is located in the border of the temperate and Mediterranean climate zone; according to the Köppen-Geiger climate classification it is considered as a Cfb—temperate oceanic climate [81]. There was no possibility to perform in situ measurements during the design phase; therefore, the typical weather data was produced by the Meteonorm® database from a five-year average. Because there is no physical weather station in the town, interpolated data was required. The distance weighted interpolation is calculated from the six nearest weather stations with similar latitude and altitude and satellite data by the software itself [88].

(**a**) (**b**)

Figure 19. (a) Design visualization rendering and (b) the final building under construction.

Based on the adaptive comfort model calculations of de Dear and Brager [89], an outdoor temperature interval was defined as the first criteria for suitable NV hours during the year from the Meteonorm. The second criterion was the wind speed, because too high air velocity can cause draft effects for occupants, therefore the upper limit was set to 8 m/s. This value is originated from my maintenance experiences in a very similar PACS in an industrial building, in Hungary [90]. Based on these parameters, 3639 h were found during an average year, being acceptable for NV. Chen and al. [91] found in their simulations 3294 NV compatible operation hours in Düsseldorf, which location possesses the same Köppen-Geiger climate classification and similar altitude than in the site in current study.

The industry section is represented by a traditional cellar and a modern production hall in the building—both subterranean spaces. The ventilation in these two rooms should be solved by PACS. Two different solutions were considered exploiting the wind as resource: a DD and a UD PACS.

On the one side, the PACS of the basement halls should ensure as hygienic IAQ as possible, reflecting today's modern, high-tech winery requirements. On the other side, the PACS should control the relative humidity and the air temperature in certain wine production technologically preferred internals for as long as possible throughout the year.

In both cases, a UD directed wind tower provides for exhaust airing, under a pyramided roof, which helps to transfer the horizontal winds over the flat roof to the tower opening. The fundamental difference between the two systems is the driving force for the air movement in

the interior. In case of the UD PACS, the tower is equipped with a previously described 'Venturi-plate' and the formulated depression zone under it is the main wind driven operator. The fresh air is originated from two underground industrial gates on the opposite site of the building (Figure 20a). The updraft tower structure can be found in the DD PACS version also, but the fresh air is delivered by a separated modern wind catcher (Figure 20b). On top of the DD wind catcher a special chimney crown is designed, which operates similar to the traditional 'baud-geers'. The over pressured zone on the opening of the tower is introducing and forcing down the fresh air to the interior.

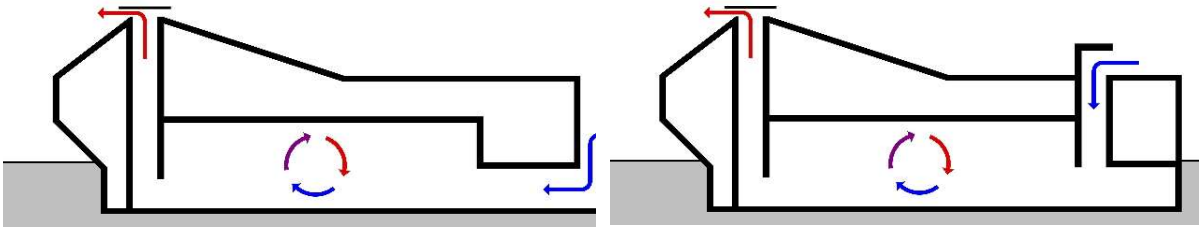

(**a**) (**b**)

Figure 20. The two investigated PACS method: (**a**) updraft (UD) and (**b**) down drought (DD).

Since the modeling of the surrounding (e.g., vegetation, buildings) can significantly affect the aerodynamic circumstances [41,92] two sites were considered, one with two direct neighbors and the other with more neighbor buildings but in further distance, respectively. Here, the scientific opportunity was occurred to investigate the effects of the different neighborhoods on the PACS of the winery under the same weather conditions. The territory is an agricultural area on the boundaries of Villány, where the dwellers usually cultivate grapes, so the vegetation is mainly formulated by linearly organized vineyards, with an average of 2 m heights (Figure 21).

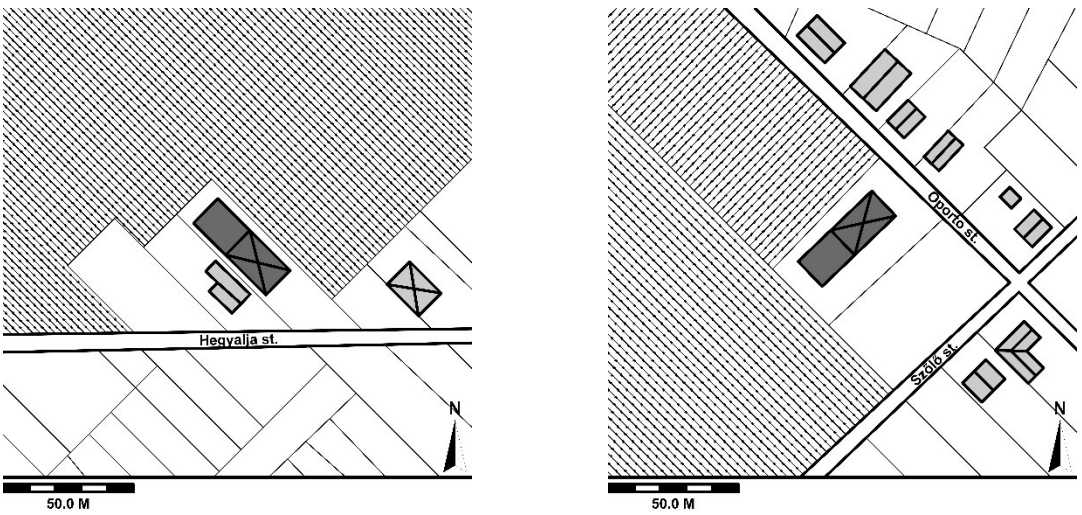

(**a**) (**b**)

Figure 21. Construction sites with the new winery building (dark gray); neighbor buildings (light grey), vineyards (hatch). The X marks the pyramid with the UD tower in two different locations: (**a**) Site A – lower density with closer neighbors; (**b**) Site B – higher density with further neighbors

Figure 22 displays the wind speed frequency sorted by the wind incidence angle. The yearly average wind velocity is 2.73 m/s at 10 m height, and it is increased above 5 m/s in less than approximately 15% of the year. The figure shows that the northern and western directions are more frequent (around 60% of the total year). However, leaving out the remaining incident angles from the PACS investigations, approximately 1500 NV compatible operation hours would be lost. In order to provide an effective NV in as much operation hours yearly as possible, an omnidirectional design of PACS was crucial.

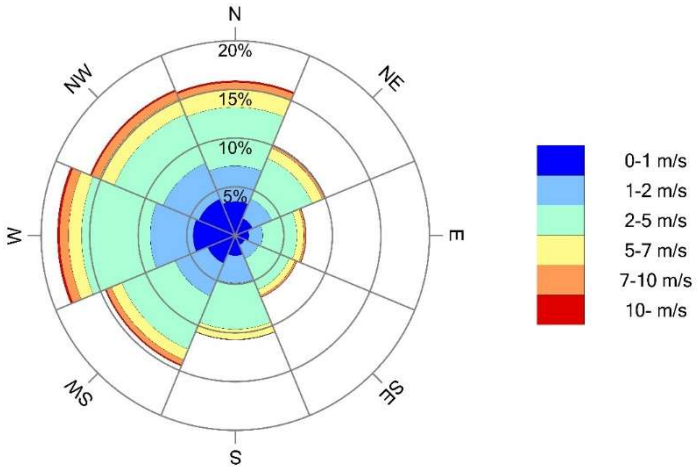

Figure 22. Wind velocity frequency (%) sorted by incidence angle.

In the case of the UD PACS, the symmetrical geometry of the 'Venturi'-object and the pyramid top opening provides for omnidirectional behavior (Figure 23a). In the DD PACS case, the wind catcher's chimney crown is equipped with deflectors in line with its diagonals, dividing the cross-section of the tower into four equal segments (Figure 23b). During ventilation, only the actual wind facing segment will be opened, and a building management system (BMS) is required to respond to the changing wind scenarios.

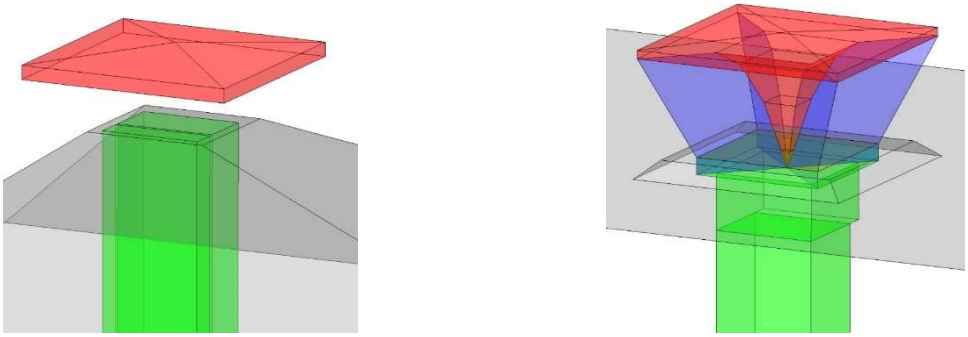

(**a**) (**b**)

Figure 23. (**a**) 'Venturi' plate structure (red) as deflector of the outlet tower (green) with lifting (closing) mechanism; (**b**) Omnidirectional chimney crown geometry (red) on top of the inlet tower (green) with diaphragm deflectors on diagonals (blue).

Two adjacent underground rooms were designated for NV operation. The smaller is a one story-high classic cellar with 100 m^2 floor area and 331 m^3 air volume, where the wine maturing procedure takes place in oak barrels. This traditional winemaking process needs stable relative humidity and temperature; hence the NV will be used under strictly regulated conditions in order to avoid vacillating IAQ and unwanted evaporation or damage of the wine. Airflow control is ensured in the cellar by moving louvres in the lower part of the ventilation tower. There will be no constant working activities, but the room will be opened for guided visitors, because the facility serves as a combined boutique hotel as well. The larger neighbor space is a two-story production hall with irregular cross section, 167 m^2 floor area and 906 m^3 air volume. There will be constant work through the year and it is also open for the visitors. According to this occupancy behavior, there could be over 30 people at once in this room. According to the EN 15251 [62] regulation, 3.5 L/s/person is the minimal air change rate for an acceptable comfort level in a non-domestic building (the regulation does not concern about industrial buildings, but the occupancy density could be equivalent with e.g., classrooms). In this case, at least 798.84 m^3/h volume flow rate (VFR) is necessary, which means 0.882 h^{-1} ACH in the production hall. The wine processing takes place in closed steel tanks, hence only the human need was considered. The PACS's role is more significant here, since here the relative humidity and temperature control range is wider than in the cellar, meaning that the production hall can be more frequently naturally ventilated during the year. Therefore, the production hall's results were crucial to the final decision. The two towers are situated at the opposite end of the hall, and between the two spaces. To prevent stale air mixing or backflow, the UD and the bottom of the DD tower were divided according to the proportion of the volumes of the cellar and the production hall (Figure 24).

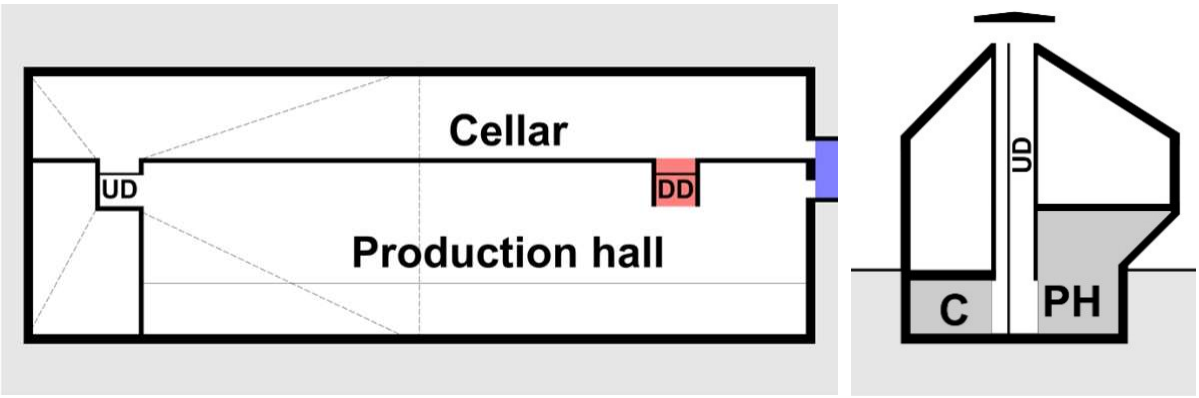

(**a**) (**b**)

Figure 24. (**a**) Floor plan, red shows the DD inlet tower, existing only in the DD PACS version; blue shows the ground zone inlet, existing only in UD PACS; (**b**) Section of the natural ventilated spaces

In summary, four main sub-models were created: two PACS model versions (UD and DD) were calculated in two different environments. All off the models were 'blown' by the wind with eight different incident angles for a detailed understanding of the created systems. In total 32 CFD simulation cases were solved and evaluated.

5.3.2. Simulations and Model Set Up

The comparison of the two PACS was brought off in a CFD simulation framework. Based on cost and time efficiency, CFD is one of the most widely used tools available for aerodynamic

purposes. That is proved by Huang [93], whose scrutiny shows that 70% of the reviewed papers used CFD solvers. His investigation was not limited to NV cases, but according to the results, it can be stated that RNG k-Ω and k-ε models performed best of all cases. Numerous other studies have concluded similar insights [15,18]. Coupled indoor-outdoor simulation scenarios were created for the complex understanding of not only the PACS performance but its environmental situation, as its importance was stated by Mohamed et al. [94]. Leaning on the literature and on the my previous experiences [90], the k-Ω model was chosen to perform the simulations of the described problem. As solver code, the ANSYS® Fluent 17.2 application was used. Simulations reached a steady state after 2000 iterations, thereafter the calculation was modified into transient solutions, whereas 200 additional time step was calculated until it finally converged (1 time step equals 1 s and contains 10 iterations).
The flow volume was discretized by applying a finite volume method (FVM), whereby in the nodes of created cells the solver software computes the physical parameters. Accuracy of the results depends on the well-chosen dimensions of the resulted mesh of FVM. Two steps assure the quality of the generated grid. First, I worked on a CFD model validation including in situ measurements of an existing building, whereas the gained experiences served as basis for the constructed mesh's discretization in the current investigation [90]. Table 4 describes the structure of the grid, created with ANSYS® Mesher. The differences between the two cases are coming from the geometrical discrepancies, and it is clear that the current study concerns a smaller domain. The representative cell size decrease rate ranged between 1.5 and 2.5, as the whole domain and the major dimensions as well.

Table 4. Representative cell sizes of the generated meshes.

Region	Validated Mesh	Current Mesh
Total domain size	500 m × 500 m × 100 m	200 m × 200 m × 80 m
Atmospheric	6 m	4 m
Macro environment	3 m	2 m
Micro environment	2 m	1 m
Near building walls	0.5 m	0.3 m
Towers/openings	0.3 m	0.1 m
Interior	0.2 m	0.25 m

The second pillar of grid's quality is to define the error range of the created mesh. To prove the validity of the results, the guidelines that were specified by Celik et al. [95] were followed. Their work is based on the Richardson extrapolation, which is widely accepted to evaluate the errors of the discretization. The grid independency test was carried out with three different resolutions, including 2.034, 4.397, and 9.504 million cells, respectively (Figure 25). The fine-grid convergence index was 0.45% and 1.24% for the fine and medium grid. Since the latter discretization has also acceptably low error range, the medium grid was chosen for the simulation to save calculation time. The detailed calculations of the errors are described in the Appendix A.
The 2.73 m/s average wind velocity, taken from the Meteonorm database, pertains to a height of 10 m. Since the air velocity depends on the distance from the ground, the change of velocity can be described with a wind profile, which was generated as a user defined function (UDF) in

Ansys® Fluent, based on the works of Balogh et al. [96,97]. The vertical alteration of the wind velocity was not only modified by a general terrain topology on the inlet boundary, but the local terrain differences and their roughness constants were also taken into account.

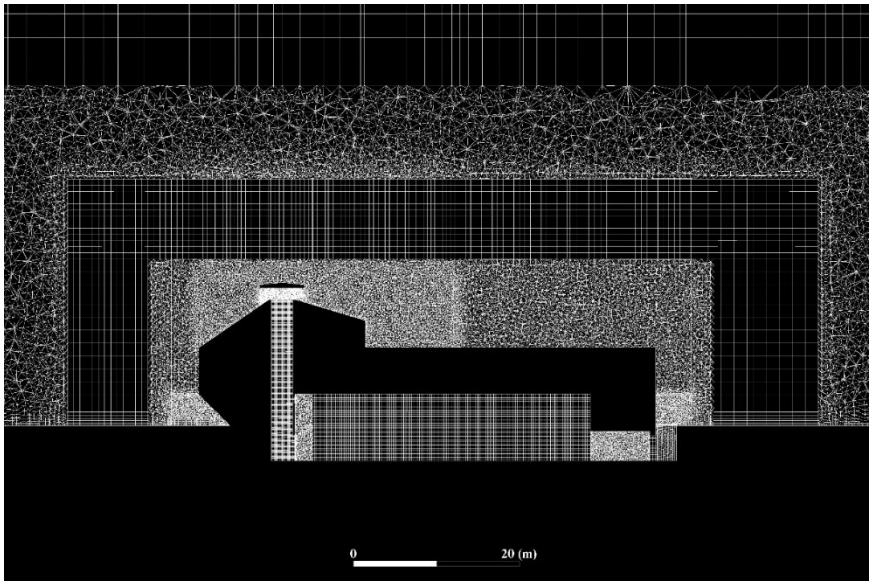

(**a**)

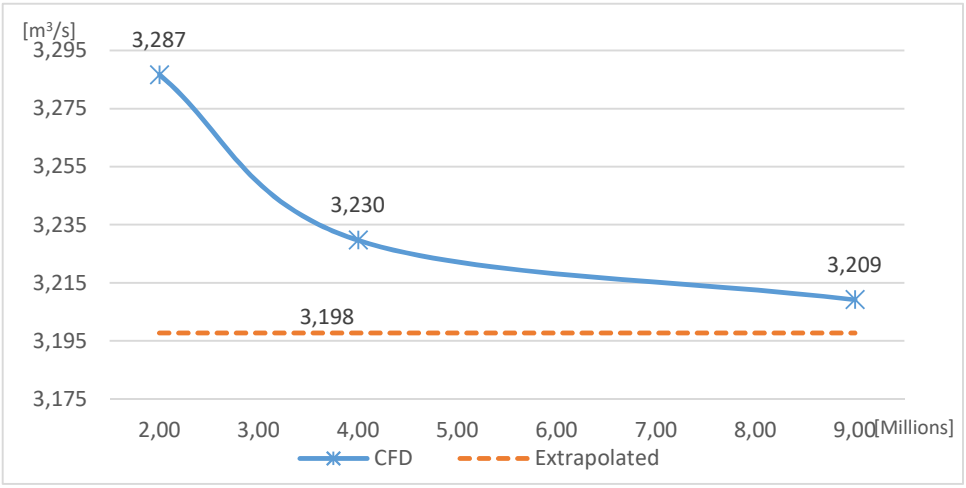

(**b**)

Figure 25. (**a**) Visualization of the highest grid resolution with 9.3 million cells and (**b**) grid refinement results of the three different grid resolutions, concerning ACH [m^3/s].

5.3.3. Limitations of the method

The CFD models were created to evaluate and compare the ventilation performance of two PACS and gain general insights about their behavior compared to each other. Due to the fact that the facility's spaces are non-constantly occupied, model discretization was not optimized for indoor air quality estimation. Therefore, the internal fresh air distribution may be not satisfactory in all scenarios. Because of the same reasons, temperature and humidity were also

not considered, although it is stated that for wine making these two factors are not negligible, especially in the traditional cellar. These IAQ performances will be incorporated in the next CFD investigation steps, complemented by time dependent temperature and humidity based opening control studies using thermal simulations. The main concept of this particular study was to satisfy the requirement for as high as possible volume flow rate, hence the highest day and night ventilation efficacy. In case of short, temporary time intervals, during which high ACH is not desired (e.g., harvest season or IAQ controlled time periods), it is possible to reduce the performance with adjustable dampeners.

5.4. Results

5.4.1. Scenario Site A—Lower Density, Closer Neighbors

Since no exclusive prevailing wind direction could be identified, and the building's geometry is asymmetrical, the two PACS versions were simulated under eight wind directions: four parallel and orthogonal to the main axis of the building, and four with 45° rotations, respectively. Firstly, the PACS was investigated on the lower density site with closer neighbors (Site A).

The internal volume flow rate (VFR) is taken as the measuring value of a PACS's ventilation performance, demonstrating the various ACH-values in wind direction dependency (Figure 26). In both cases (UD and DD), the cellar provides higher ACH, due to the simpler and smaller cross-section and smaller volume.

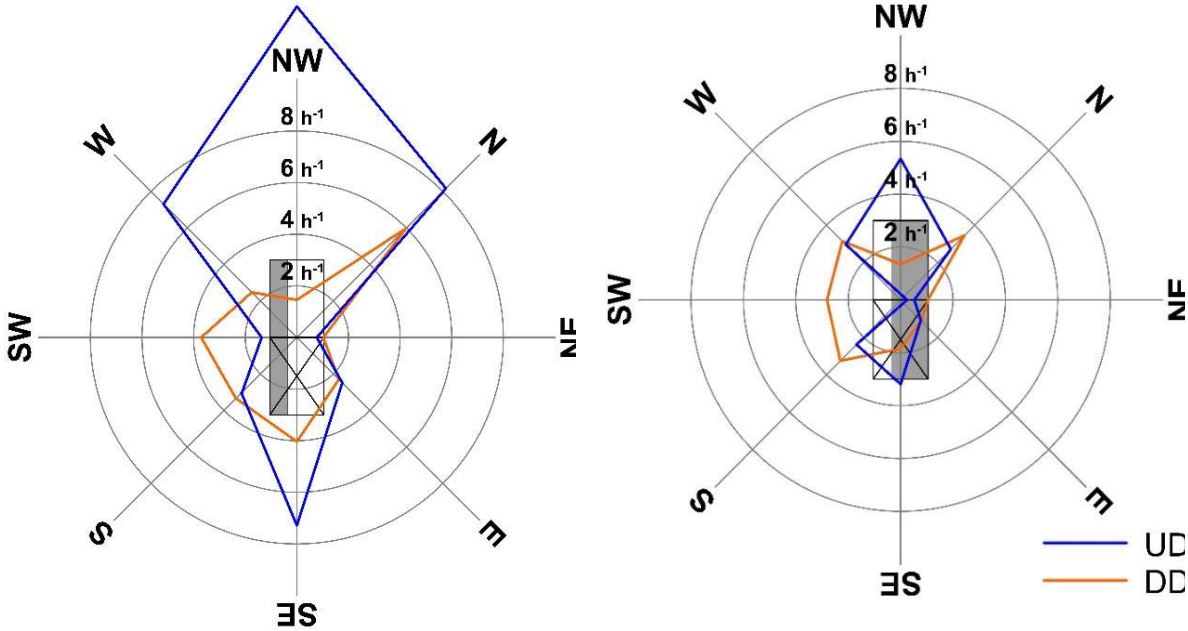

(a) (b)

Figure 26. Results of air change per hour [h^{-1}] (**a**) in the cellar and (**b**) in the production hall where grey shows the mentioned area in the sematic figure of the building—Site A with less but closer neighbors.

When the wind hits directly the underground gates without any object in the way (NW), the highest ACH 5.34 h^{-1} (hall) and 12.82 h^{-1} (cellar) develop. Unexpectedly, the same effect

occurred from the opposite SE direction, 3.18 h^{-1} (hall) and 7.29 h^{-1} (cellar), because a separation zone is formed at the leeward side of the building, generating a back flow towards to the gates (Figure 27).

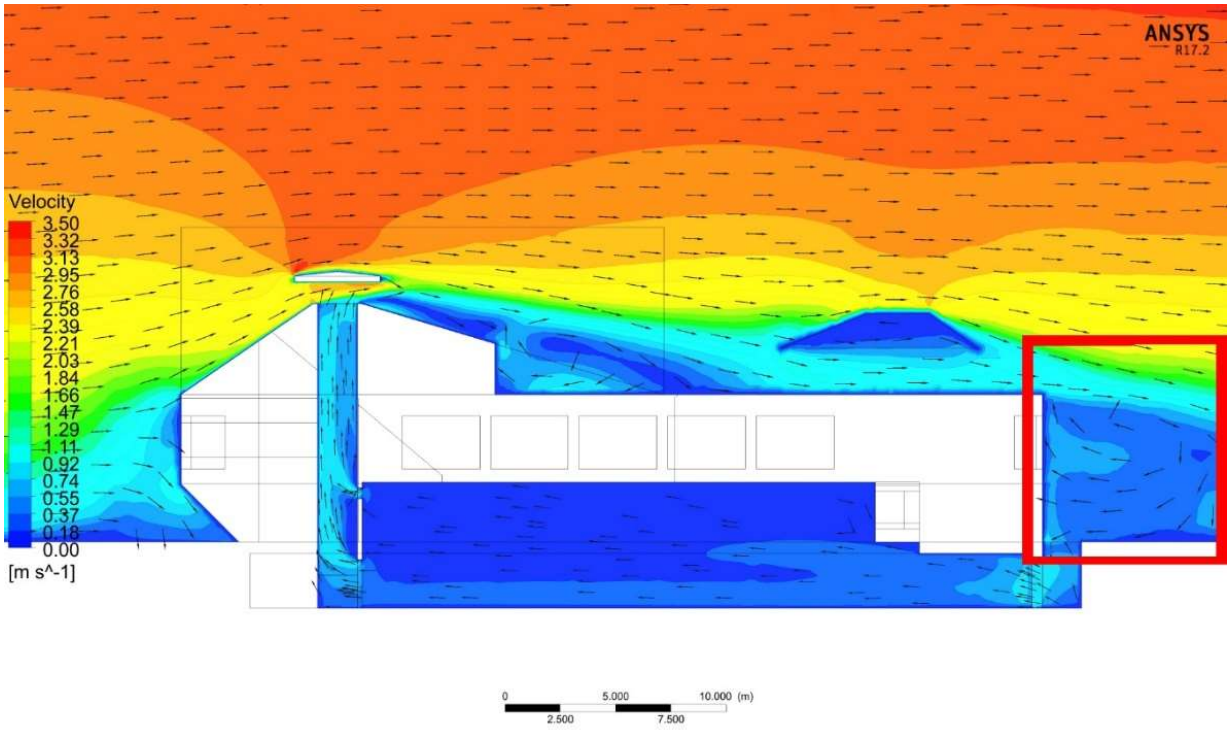

Figure 27. Backflow occurrence behind the building in case of approaching wind direction from SE in the UD PACS (colors and vectors by air velocity [m/s]).

Figure 28 shows the formulated air patterns in and around the winery with UD PACS. In case of the 45° incident wind angles, the UD PACS deliver an approximated performance between the two amplitudes—between 1.09 h^{-1} and 2.96 h^{-1} (hall) and 2.49 h^{-1} and 8.17 h^{-1} (cellar). However, the UD system works at highest efficiency only in incident wind angle parallel to the connecting axis of the UD tower and the inlet openings, while at the two orthogonal direction (SW and NE) it performed poorly: −0.25 h^{-1} and 0.52 h^{-1} (hall) and 1.36 h^{-1} and 0.77 h^{-1} (cellar), respectively. Negative value means that the flow direction in the wind tower turned backward (SW direction), showing very low ventilation efficiency. The main reason for that is the disadvantageous low-pressure zone at the NW end of the building, created by the wind current that bypasses the underground inlet gates, and creates a suction over it, similar to the 'Venturi' plate's effect, but with opposite force (Figure 28b). The more the incident angle of the wind decreases to the longitudinal axis of the building, the more this disadvantageous under pressure zone is weakened and the ventilation efficiency increases (Figure 26). Since the technology hall possesses a 2.74 times larger indoor volume, the achieved ACH rates are approximately 52% lower than in the cellar.

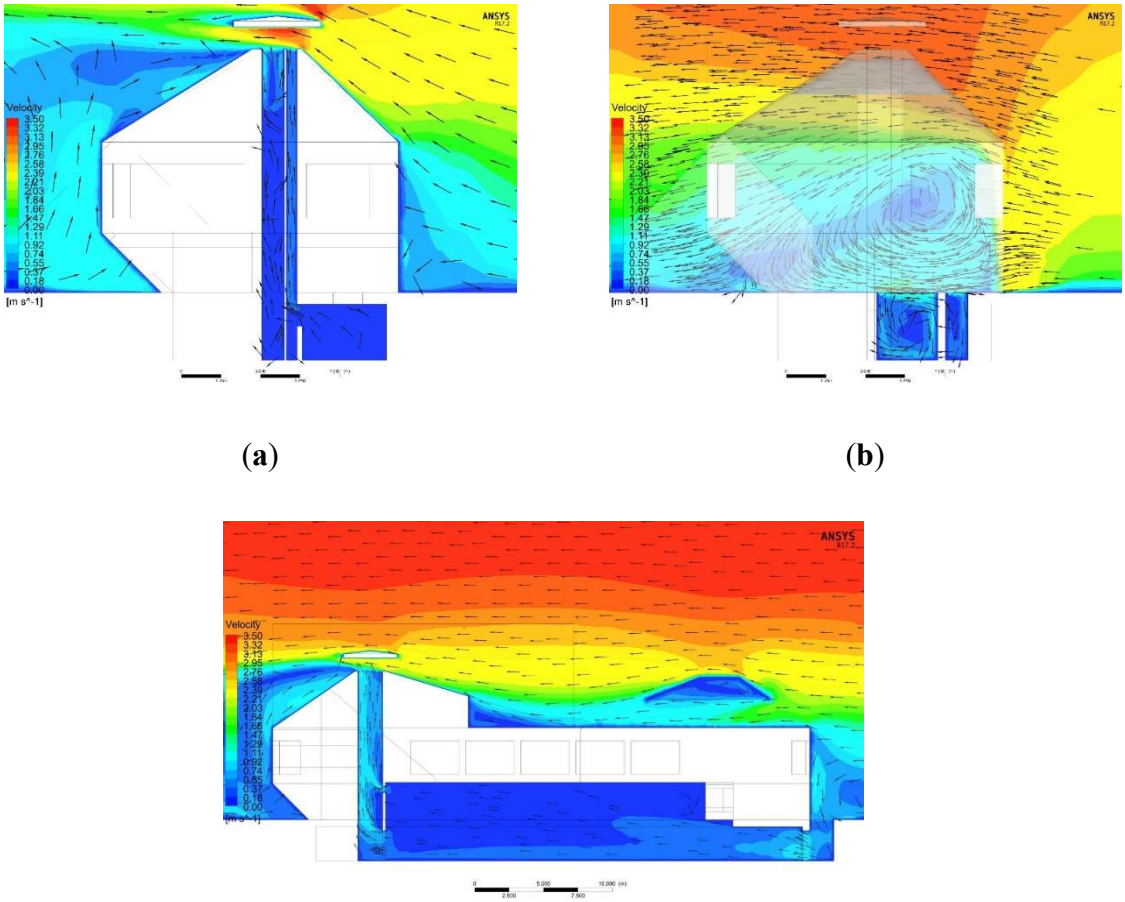

Figure 28. Airflow patterns in the cellar and the industry hall in the case of updraft (UD) PACS (colors and vectors by air velocity [m/s])—(**a**) cross section of the airflow through the UD tower under NE wind direction, (**b**) cross section through the inlet gates behind the building under NE wind direction with counter wise vortices, which are responsible for the negative ACH amplitudes, (**c**) longitudinal section of the airflow in and around the building under NW wind direction; (**d**) 3D streamlines of the airflow under NW wind direction.

Figure 29 demonstrates the air pattern characteristics in and around the winery with DD PACS. This version obtained between 1.04 h^{-1} to 3.45 h^{-1} ACH (hall) and 1.02 h^{-1} to 5.98 h^{-1} (cellar) ACH performances, respectively, with more evenly distributed values, meaning that this system is more independent from the wind directions. Although the highest value is only 64% of the highest result in UD circumstances, there are no extreme ACH minimums. In contrast to the UD, every direction can achieve the required 0.882 h^{-1}, in which ACH was determined by the EN 15251 legislation.

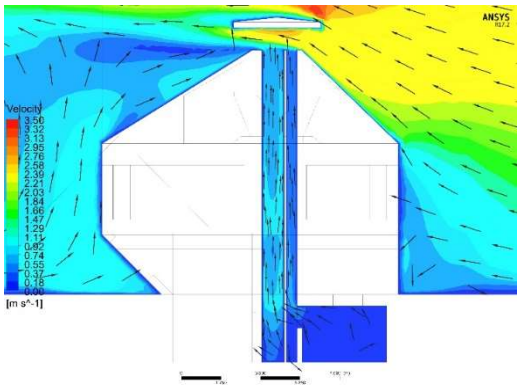

(**a**)

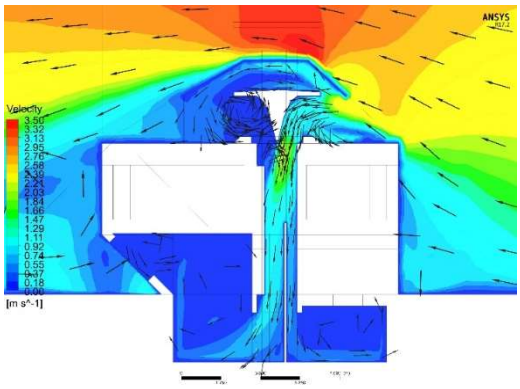

(**b**)

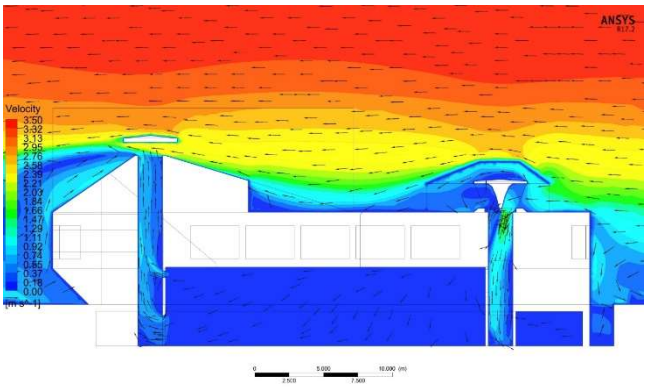

(**c**)

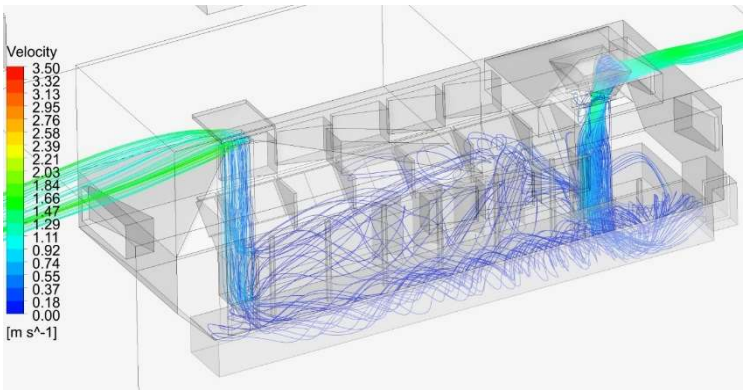

(**d**)

Figure 29. Airflow patterns in the cellar and the industry hall in the case of downdraught (DD) PACS (colors and vectors by air velocity [m/s])—(**a**) cross section of the airflow through the outlet tower under NE wind direction, (**b**) cross section through the inlet tower under NE wind direction, (**c**) longitudinal section of the airflow in and around the building under NW wind direction, (**d**) 3D streamlines of the airflow under NW wind direction.

5.4.2. Scenario Site B—Higher Density, Further Neighbors

During the second experiment, the PACS was investigated with further and more neighbors. All other boundary conditions remained identical to the case in Scenario Site A. Figure 30 displays the air change rates of the two PACS system with the new conditions. The previously obtained ventilation character (Scenario Site A) is recognizable in these cases as well. The UD version is still very effective in the two parallel wind directions (NE and SW) with 4.11 h^{-1} and 3.73 h^{-1} (hall), and 6.72 h^{-1} and 4.98 h^{-1} (cellar), respectively. While the two orthogonal directions (SE and NW) create a mixed suction effect, where 1.54 h^{-1} and 0.08 h^{-1} (hall) and 3.41 h^{-1} and 2.56 h^{-1} (cellar) is obtained, respectively. In SW and NE directions, the missing proximate neighbors had a ventilation amplifier consequence in the previous case (Site A), while in SE and NW directions this has the opposite effect.

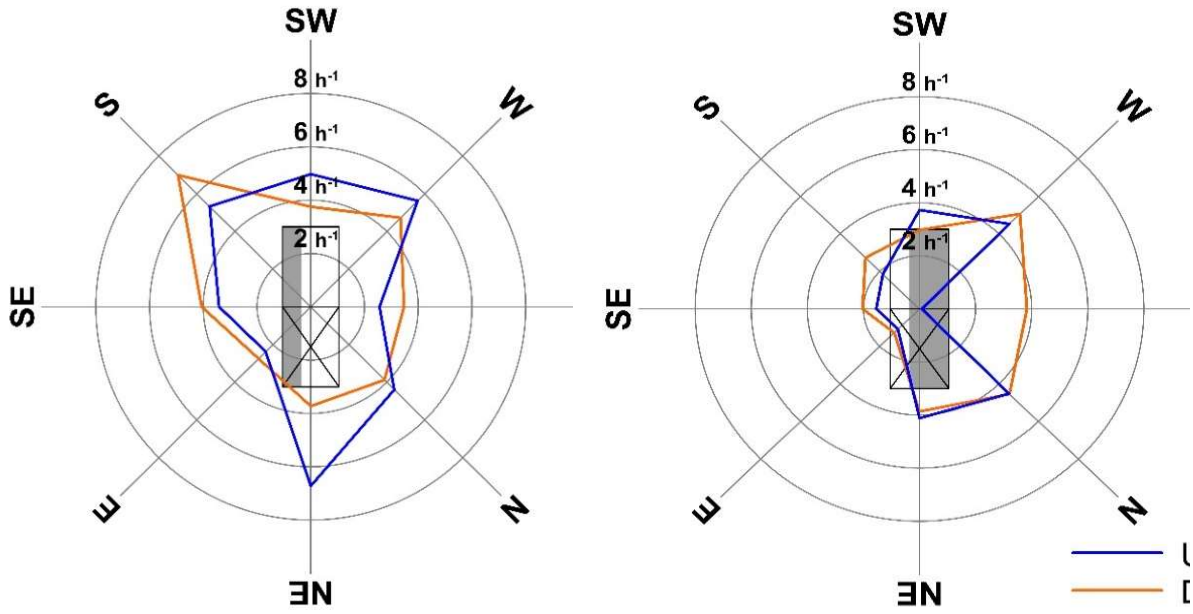

(**a**) (**b**)

Figure 30. Results of air change per hour [h^{-1}] (**a**) in the cellar and (**b**) in the production hall where grey shows the mentioned area in the sematic figure of the building—Site B with denser but further neighbors.

DD version is still a more reliable wind direction independent system with consistent values, and can maintain a good IAQ with fresh air in this industrial facility. The developed ACH is between 1.27 h^{-1} and 5.06 h^{-1} (hall) 2.75 h^{-1} and 6.99 h^{-1} (cellar), which is slightly better performance, than that in the former scenario (Site A), and it suggests that few, but very close, objects can influence the NV performance more poorly than a dense built environment in

greater distance. The obtained results in the DD are in compliance to ACH requirement of EN 15,251 code as well.

5.4.3. Conclusion of the comparison of DD and UD PACS

Previous works validate the acceptability of the NV options comparing with MV. While most available literature report about wind tower investigations in hot and arid climate [47,55,57], particular studies could prove that these NV solutions work in the moderate climate as well and they are able to achieve required ACH levels, as is stated in numerous research [8,11,53,87,90] supporting the spread of PACS.

The UD PACS system performs as a wind direction dependent system, because of the high amplitudes in the ACH. Therefore, it acts more like a uni- or bidirectional solution. It is recommended as a perfect solution for (micro)climate circumstances where prevailing wind directions rule for instance. In contrast, the wind independent DD wind catcher opening can ensure the design of an omnidirectional and efficient PACS. Due to the advantageous, wind exposed installation on the rooftop the inlet structure is able to deflect fresh air into the interior in all incident wind directions (Figure 23). The separation of the UD outlet and the DD inlet delivers great advantage compared to combined in- and outlet PACS, as the latter version can cause ventilation shortcut issues between in- and outlet [60]. The UD system provided an approximately 52% difference in the ACH performance between cellar and hall, this ACH difference shrinks to 26% in the case of DD. This means that the DD system ventilation works more independently from the size of the indoor ventilated space volume. The presented comparison of UD and DD systems is a gap filling contribution in current literature about natural ventilation systems.

In the case of dense neighborhood in greater distance (Site B), both UD and DD PACS perform stronger than in Site A (lower neighborhood density in closer distance) in the cellar and hall spaces, showing that proximity of neighbor buildings and objects—even in weaker density—can influence the ventilation rates. These results correlate with previous works [90], examining and proving significant effects of neighbor objects on the NV performance.

Though in scientific studies multiple valid building NV solutions results were obtained about their effective accomplishments, most of the recent studies usually juxtapose NV with MV systems. In contrast, this phase I compared the performance of two different integrated PACS in one building: a UD and a DD system. Subtracted from the results of the two series of simulation under different locations, the following consequences can be concluded:

It has been revealed that in regions without a prevailing wind microclimate, the DD PACS method works as the more reliable option, because it performs a more balanced ventilation efficiency independently from the wind direction. The UD version is even more effective than the DD but only in wind direction dependent situations when the approaching wind comes parallel to the connecting axis of the outlet (tower) and the inlet (underground industrial gates). The main mechanic behind the difference between the two PACS is the wind direction independency of the inlets, whereas the inlet of the DD system profits from its wind exposure to the incident currents. While the downdraught air direction based passive air conduction system's ventilation is empowered by both divided and wind direction related opening-controlled inlet tower as well as the buoyancy and wind suction driven outlet 'Venturi'-tower, the UD PACS' ventilation mechanism is only maintained by the outlet 'Venturi'-tower in most of the wind direction cases. High ACH rate is only achieved in UD PACS, when the approaching wind have direct access to the inlet, meaning that the ventilation is driven by the overpressure at the inlet and the under pressure at the outlet. This is the case as well when the wind direction is opposite to the previously case and parallel to the inlet–outlet connection axis,

and hence the ventilation is driven by the under pressure at the outlet and the suction effect at the inlet.

Finding 2.1.

An up draft passive air conduction system's ventilation performance has huge amplitudes when the wind direction is aligned with the system's main axis (in case of linear flow between outlet and inlet openings), but the other directions has poor capacity. Therefore, the up draft system can be identified as a bidirectional Passive Air Conduction System.

Finding 2.2

On the other hand, a down draught system has no extreme high ventilation potential in one particular wind direction, but in the same situation, every direction can achieve sufficient performance, therefore the down draught system can be identified as an omnidirectional Passive Air Conduction System.

Based on the above-mentioned information, the DD PACS can perform reliable air change rates independently from the incident wind angle, hence it can be named as an omnidirectional method. Consequently, a UD PACS can be named as a bidirectional method.
Fewer but closer neighborhood, including blunt objects, have stronger negative effect on a PACS ventilation efficiency behavior than a denser but farther built environment.
This research's goal was to provide a guide for engineers, who are aware of this fact, and want to design a specified PACS optimized to the location's boundaries.

5.5. Potential analysis of a spacious building prototype with passive bidirectional ventilation

5.5.1. Background

In just a few years, the rapid economic growth of countries such as India, Arabia, South America, Russia and, not least, China has led to a development in the construction industry on a scale that took centuries to develop in Europe. According to some forecasts, the increase in the floor area of buildings in non-OECD countries will double energy consumption by 2050. One of the world's fastest and most intensive development processes is currently taking place in China. From 2007 to 2015, China's energy consumption generated by the construction industry grew by 63%, accounting for more than 50% of the total increase in China's energy consumption.
In the rapid construction process of the explosive 'Far East Industrial Revolution', conventional European architectural and engineering solutions are not able to provide adequate sustainable concepts and buildings. This over-mechanized international architectural style from Europe and North America is not only causing unprecedented climate and environmental damage in the Chinese built environment, but also causing huge energy demand. Global warming's negative effect in the increase of extremities in weather conditions, such as higher summer temperatures (especially in the urban environment), makes cooling of buildings more and more important. **Cooling demand** globally increased 60% between 2000 – 2010 , while further growth of 150% is expected by 2050 [35]. Today's worldwide conventional cooling systems are mostly based on air-conditioning CFC and HCFC technology, consisting of conventional refrigerants (R134 and R22), which are significantly more intensive (factor 1300 – 1700) per molecule than carbon–dioxide (CO2) in the contribution of global warming. In 2006 the USA air conditioning (AC) consumption amounted approximately 11,5% of the total electricity demand, while

regarding the peak load, air-conditioning made 40% demand on it. Air-conditioning load demands for 40% of peak load during summer in Shanghai. Based on electricity disruption problems caused by air conditioning overload in settlements, furthermore due to high investment costs in expensive electricity back-up generating equipment, alternative refrigerating solutions, as well as more radical alternatives to air conditioning and its electricity peak demand are in focus of strong interest. [98]
Systemizing the different '**cooling without air-conditioning'** solutions, passive ventilation systems with cooling performance occur as an energy- and cost-efficient alternative that can be distinguished basically in two types: updraft and downdraught systems, dependent on the air flow direction. Updraft ventilation uses convective thermal buoyancy of warm upward airflow rates in chimney or tower like structures and in high indoor spaces (halls), due to stack effect. Downdraught ventilation relies on the effect of gravity on a body of cooler air to create a downwards stream of air, circulating air from the active (using water coils), passive (using adiabatic evaporative cooling) or hybrid cooling source to the occupied building zone. Investment savings from 50 to 80% are generated in comparison to AC installations due to ventilator and duct system as well as operations cost savings. LCCA payback period is in Europe approx. 5-15, in India 2-5 years [98].

The most efficient solution, however, is to develop the entire building system into a sustainable air conditioning "installation", rather than upgrading individual mechanical or structural systems. In the field of building improvement, the most important aspect is to improve the large consumer sectors. Based on the Chinese building situation as outlined above, the commercial, public, administration and industrial building sectors are not only the largest consumers, but also have the highest energy consumption growth[98]. Within this building sector, the temperature control (mainly cooling) and ventilation of buildings with large and complex air spaces (atria, halls, non-domestic buildings) are not only causing energy problems but also technical comfort problems. Their average floor area ranges from 5,000 to 30,000 m^2 and the high number of artificial lighting, electrical installations and simultaneous occupants means that internal heat build-up is significant. Combined with the solar heat load, the ventilation, air conditioning and maintenance of these buildings represent a significant part of the building maintenance costs, especially in cases - which are frequent - where the air conditioning system is used for air exchange and space conditioning (heating, cooling). A Swiss study (Fig.1.7) analyses the energy consumption of office buildings: cooling and artificial ventilation account for 60% of total consumption. This is coupled with the need for energy-intensive air dehumidification in the subtropical climate zone with high humidity and solar radiation, which is typical of the majority of China. A study in a hot and humid climate zone examined commercial buildings with air-conditioning energy requirements accounting for 60-72% of total operation.

5.5.2. Concept of the innovative new and modular PACS for industrial buildings

Following research is based on the cooperation between the Hungarian University of Pécs, Szentágothai János Research Centre, Energia Design research group and the Chinese Jiao Tong University Shanghai, Architecture Department. A simulation supported design and research investigation program was elaborated to develop passive bidirectional hybrid ventilation and cooling (PHDC) systems in commercial and industry buildings in warm and humid climate. A Hungarian complex industrial and office prototype building with unique aerodynamic design concept, shaping and operation served as a 'reference lab' for experimental measurements [99]. In a first step, investigations compared the 'pioneer' reference building's CFD model calculation results against monitored in situ measurement data during operation of the real building with three updraft passive ventilation tower, 'Venturi'-wind current accelerator

structures and night cooling system. After calibration of the Hungarian reference building's CFD model, it was used as initial point for further simulation variations. Weather data of the validated, high efficient performing updraft ventilated model should be modified into warm and humid subtropical weather conditions (location: Shanghai), furthermore tower geometries will be transformed into downdraught ventilation and cooling structure variation. The vertical ventilation tower system of the reference CFD model performed high efficiency in both upward as well as downwards direction. Concluding the gained results, the next step proposes the development of a universal, theoretical building prototype (*Figure 31*) with large-scale interior volume under warm and humid climate conditions (e.g. region of Shanghai). The building model dimensions were enlarged from the reference hall's 610 m^2 to 6,050 m^2 net floor space. The concept is based on two primary background insights: Since spacious interiors possess central areas in great distance from façades, frequently natural window and opening ventilation is impossible. Secondly, for most generic ventilation system, applicable in different wind distribution micro-climate situations, are independent of wind direction diversity. In order to meet these prerequisite, the towers should be able to provide both inlet and outlet for ventilation. Therefore, the concept of a bidirectional up- and downdraft passive ventilation and cooling tower system seemed to be optimal, when wind direction independency as well as good mixing and cooling of interior air volume is required. In the monitored reference building a drawback was registered at upstream airflows at the ventilation towers' vertical walls in wind coming direction that slowed down the wind velocity at tower's top. To avoid this contra-productive aerodynamic withstand-effect, the tower geometry was integrated into a pyramid-shaped roof geometry. A prototype unit works with two simultaneously operated similar coaxial ventilation towers: the one is responsible for fresh air supply and the other one for exhaust air outlet. Gaining promising result of the CFD simulations, these prototype units were assembled into a larger modular hall system: a four-unit building comprising 55*110=6,050 m^2 (109*54 =5,886m^2), 33,275 m^3 (32,373) m^3 space. Horizontally, the towers are placed in the middle of the subunits with a certain shift relative to each other. Taken from the reference buildings experience, this 'zigzag' positioning should avoid risk of slipstream effect caused by towers standing in a line.

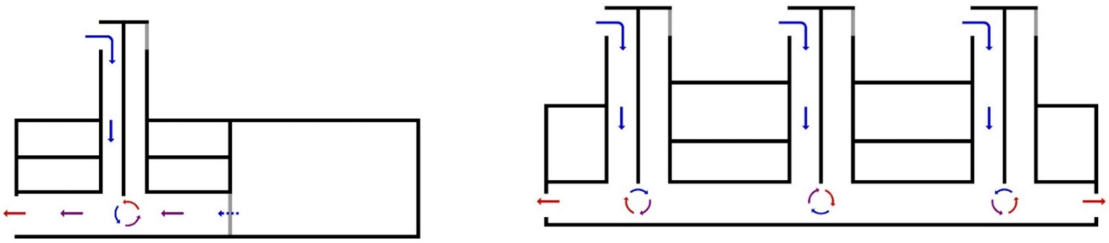

(**a**) (**b**)

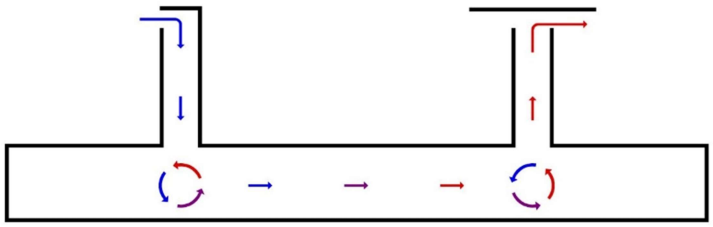

(**c**)

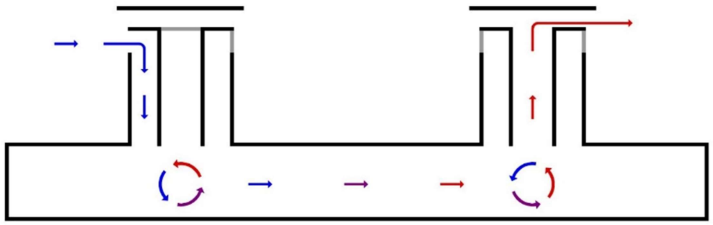

(**d**)

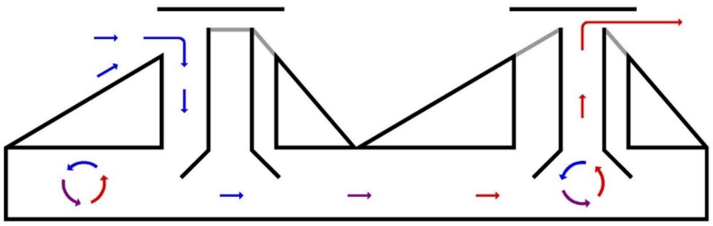

(**e**)

Figure 31: Genesis of the prototype CFD building models: reference buildings updraft ventilation system, reference buildings downdraft ventilation system, prototype model unit, prototype bidirectional large model comprising four units

5.5.3. Prototype basic unit model description

According to previous chapter „2. Research concept", a basic module prototype model was developed that serves as a modular unit for spacious, multi-functional public building functions like event-space, commercial use, convention, conferences, exhibitions, offices, education, industry halls, etc. with greater net floor space. After development of a well-working basic unit module, it should be arranged side by side to create an assembled, large-sized multiple-unit building. The first desired universal building prototype should comprise approx. 6 000 m^2 net floor space with a passive, wind direction independent ventilation system, including cooling possibility in warm and humid climate (location: Shanghai).
Corresponding to the basic unit concept, the validated, downdraught ventilated reference building CFD model geometry was reconstructed. The layout of the module consists of two pieces of 27.5 x 27.5 m square areas with a height of 5.5 m. Caused by air flow reflection, along

the longer sidewalls unwanted recirculation turbulences can occur that would be unrealistic in the assembled, larger end-model. To avoid this, I added a 13.75 m windy buffer zone on each side of the double modules to simulate the effect of the modules being stacked on top of each other. In the empty geometry, I have also included heat-generating units (people, electrical equipment, machinery, artificial lighting) to obtain more realistic values. The resulting floor area (765.25 m2) is almost identical to the production hall (610 m2) of the reference model studied above, and therefore the proportional data for users, artificial lighting and hall equipment were used as a sample. This allowed us to simulate the energy demand and heat production of a real production situation.

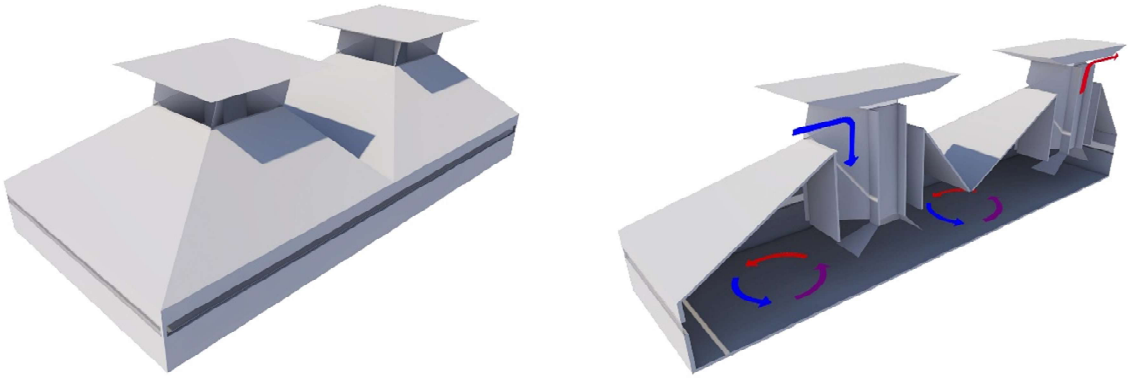

(a) **(b)**

Figure 32 3D visualization about the proposed PACS (a), and a 3D section which describe the main operation of the ventilation through the industrial hall

In order to create a wind direction independent ventilation and cooling system and with special regard to the aim of appropriate jetting flush of the interior space in far distance from façade openings, both fresh air supply and exhaust air extraction should be provided through the roof structure. Considering these requirements, the system must work with two towers simultaneously. The modular units (Figure 33) operate always with two towers pairwise, because the pyramids should work only inlet or outlet at the same time. This means, that the one ventilation tower should be responsible for air inlet (downdraught system) and the opposite 'pair' of it, the other tower should ensure exhaust air outlet (updraft system). The ventilation system consists of 3 x 3 m chimney core tower part for exhaust air outlet and a 2 m wide parametric ring around the core for air supply inlet. 60 cm above the chimneys 'Venturi' disc structures should provide airflow deflection/acceleration. In order to avoid airflow shortcuts below the towers (air would enter and immediately exit the interior), only air inlet or outlet should be possible in one tower, due to an opening mechanism that closes the core chimney (outlet closed: air supply is provided) or the perimeter chimney (inlet closed: exhaust air release is provided).
This can be controlled by a two-position gate, which closes the inlet horn flush with the pyramid side in the output position and is connected to the draft enhancement plate above the horn in the input position, blocking the possibility of exhaust (Figure 33.) The exhaust air flows upwards and outwards in the inner 3x3 m cross-section of the horn, while fresh outside air flows downwards and inwards in the outer 2 m wide ring horn. Indoors, at the bottom of the chimney, inclined deflection hood structures are foreseen for homogenous distribution of incoming fresh air sup

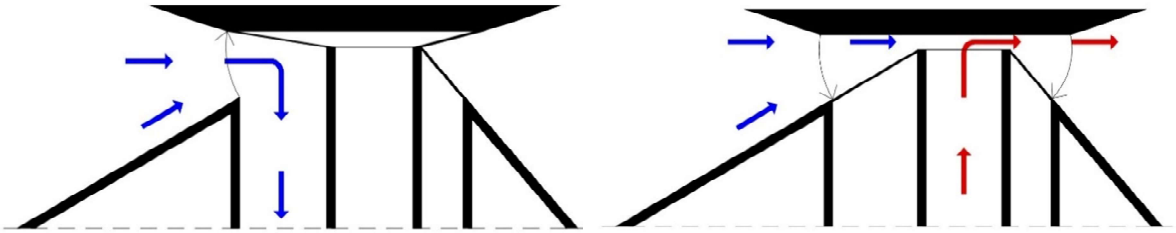

(**a**) (**b**)

Figure 33: Proposed coaxial wind towers different operational settings: (**a**) shows the inlet towers, where the outer shafts of the towers let the fresh air in; (**b**) the center shaft is open, and the 'Venturi' baffle is help to extract the used air from the interior

Horizontally, the towers are positioned in the middle of one half of the module layout, with some offset from each other: with the wind direction perpendicular to the axis connecting the towers, this "zig-zag" placement should avoid the risk of wind shadow effects caused by towers aligned in the approaching wind direction. This can occur when the basic module is arranged in a side-by-side array to create a large building envelope (Figure 34). The concept is derived from the experience of the validation of the CFD model of the Hungarian reference building, which indicated the negative effect of the slipstream effect: the ventilation towers were lined up behind each other in a wind direction parallel to their longitudinal axis, hiding themselves from the approaching wind. In addition, the vertical walls of the ventilation towers recorded a disadvantage in the wind direction, which slowed down the wind speed at the top of the tower. To avoid this deceleration and improve efficiency, a 45° sloped pyramidal roof geometry is supported by each central internal vertical chimney stack. The primary function of the sloped roof planes is to direct the wind to the chimneys without significant deceleration. The spaces created under the pitched roof are excellent for small section rooms, offices, meeting rooms, catering or engineering functions.

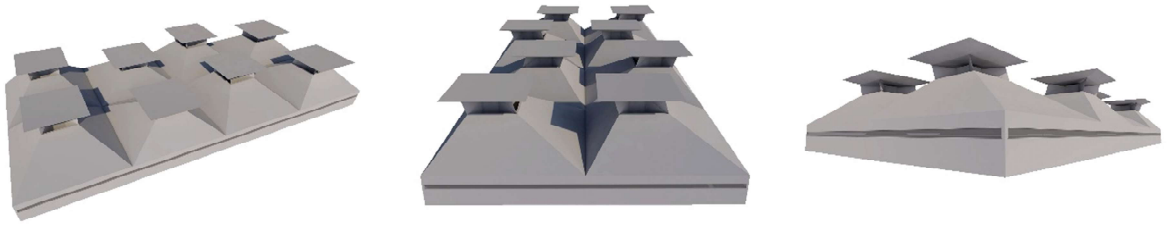

(**a**) (**b**) (**c**)

Figure 34: Complete prototype building model comprising four side-by-sing arranged basic module units

Same boundary conditions were taken into account in following simulations. The site topography remained flat, based on the validated reference model with downdraught cooling system. Dominant wind direction distribution of Shanghai weather data is not considered (only wind velocity conditions), due to our fictive theoretical prototype model, without concrete

construction plot and in this way without knowing the actual wind direction micro climate values. Since wind direction always depends on the micro climate of the given construction and immediate environment, without a concrete, defined planning area the wind direction characteristics are not known. It was assumed that either there will be no dominant wind direction or, in the case of an existing dominant wind direction, it is advisable to place the towers in such a way that none of the main wind directions will be in a wind shadow zone. In the simulations, since the building is axisymmetric, the module was tested in three main wind directions, perpendicular, parallel and diagonal to the axis connecting the towers. Virtually all cases of the ventilation characteristics resulting from all wind direction variations are covered by these three wind direction cases, since the other wind directions would either be identical due to the symmetry of the geometry or the results of the intermediate wind directions can be obtained by interpolation. According to Meteonorm 7 climate database, the wind velocity is 3,5 m/s at 10 m height. Meteonorm 7 data is gained in hourly resolution from standard weather station measurements in Shanghai, meaning the values are not interpolated like climate data for smaller settlements, but directly measured. Mean outdoor air temperature between 6:00 and 18:00 o'clock occupancy hours in summer season is 29,5 °C that is implemented in the CFD simulations.
In each case, the purely wind-induced flow conditions were first investigated and then, if necessary, the geometric or computational conditions were modified based on the results. Finally, the operational usable airflow characteristic wind induction models could be fitted with the internal heat generation and solar heat loads, as well as with a tower-integrated cooling system, which is essential for thermal comfort in subtropical climates. In this way, the ventilation and cooling performance of the complete heat and power models could be tested.

5.5.4. Prototype basic unit model, modified inlet tower with integrated downdraught cooling

The wind induction is complemented by the thermal effect of internal heat sources and solar thermal loads in the following combined airflow and thermal CFD model to develop more realistic airflow characteristics. Internal gains were modelled in the form of occupants, electrical equipment and artificial lighting. As an initial setup, the same internal heat sources from the Hungarian validated CFD model were integrated into the prototype model. Since the dual prototype model has approximately twice the net floor area of the reference building model, the number of appliance units in the prototype model was doubled. In addition, cooling has been integrated into the input tower. The detailed development of the passive-hybrid cooling unit in the form of a whole building mechanical system is the subject of a further research program. In particular, the basic research phase addresses the basic operation of the prototype building model with passive bidirectional hybrid ventilation and cooling (PBHVC), and therefore, as a first step, a theoretical cooling system was modelled in the upper 3 m vertical section of the inlet tower duct. The basic concept of the cooling system is to cool the incoming air so that the cooling air is mixed as it enters the hall space, and the average temperature in the users' comfort zone (lower 2 m high zone) is reduced to below 25 °C [62]. The question was how much thermal energy would have to be removed from the air to reduce the temperature in the interior to below 25 °C, which is considered comfortable in a production hall. To ensure adequate aerodynamic resistance, a general cooling coil resistance was modelled at the inlet perimeter tower (pore jump resistance). This can be characterized as a resistive structure filling 50% of the cross-section and volume, with the power required to cool the air flow through its surface calculated as follows. The calculated cooling capacity has been set as a function of this resistance and the volume, so whether cooling is mechanical or natural, the CFD model volume will show a normal type of cooling coil/calorifer system capable of extracting heat from the incoming air mass. With this solution, both mechanical and/or passive cooling can be modelled

regardless of the method of cooling energy generation. For the calculation of the required cooling capacity, only the wind-induced air flow rates in the towers and openings and the ventilation-induced air temperatures in the interior were considered. The equation used is

$$Q = \Delta T \cdot c \cdot \rho \cdot \dot{V} \tag{4}$$

where ΔT is the difference between the temperature of the ventilated internal space and 25 °C (298,15 K) in K (Kelvin) and V̇ is the air flow rate of the inlet duct in m3/h. Q is the calculated cooling power demand in W (Watts). The cooling power is calculated as the total sum of internal gains (occupants, lighting and equipment) and solar energy load. The desired cooling power is given for each model variation, tailored to the conditions that exist.

$$Q_{\Sigma} = Q_{occ} \cdot Q_{mach} \cdot Q_{sol} \tag{5}$$

$$Q_{sol} = (A_N \cdot G_{N_{max}} + A_S \cdot G_{S_{max}} + A_E \cdot G_{E_{max}} + A_W \cdot G_{W_{max}}) \cdot f_c \tag{6}$$

Table 5 – Internal heat sources

	Quantity [pcs]	**Performance [W]**	**Summary [W]**
Occupants	24	120	2880
Lamps	92	40	3680
Small thermosphere	2	2200	4400
Big thermosphere	1	2980	2980
CNC machine	1	425	425
Glue machine	1	300	300
Saw machine	1	370	370

The results of the calculation show (Figure 35) that the cooling demand is only increased by the faster ventilation hall, so that the cooling power demand is inversely proportional to the flushing rate. The smallest cooling demand occurs for the diagonal wind direction due to the smaller ACH, while the parallel wind direction required 41.6% additional power.

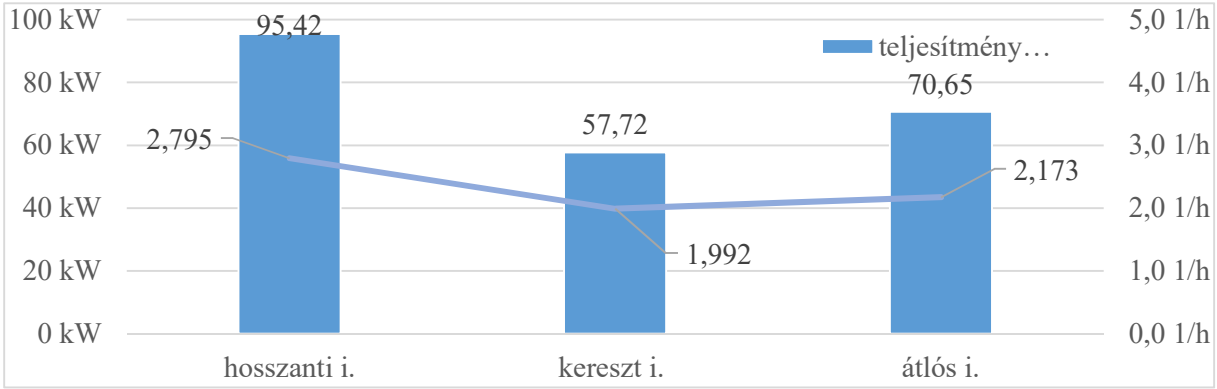

Figure 35. Cooling capacity dependent on air change rate in the three wind direction cases

Fig. 36 show the distribution of air temperatures in the hall interior at a height of 1.5 m in the human thermal comfort zone after activation of the cooling devices in the input horns. The dark blue spots mark the inlet point of the chilled-fresh air with a temperature of 22-23 °C. In parallel and perpendicular wind direction (Figure 36a), indoor air temperatures prevail below 26 °C, while in diagonal wind direction case (Figure 36b) air temperatures around 27-28 °C begin to cause overheating in the hall. The distribution of the incoming cold air confirms the conclusion drawn earlier, i.e. the baffles at the bottom of the horns, have an excessive effect on the air distribution and, although they flush the area behind the critical wind, less air reaches the spaces in front of it.

Figure 37. shows the cooled air temperature distribution in the hall. It shows the height of the cooling equipment inside the chimney, the temperature gradient and the falling downdraught cooled air, furthermore the stagnant warm air volume in the closed tower sections. The temperature distribution of down draught airflow in the inlet perimeter chimney is also indicated. Incoming external air temperature is 29 °C (average outdoor air temperature) that would rise to 33 °C due to internal heat load through equipment, artificial light and occupants. Due to 96 kW cooling power, integrated into the inlet tower, the interior air temperature can be cooled to 24 °C. Entering air reaches 302,15 K (29 °C), while in the first 3 m, where the cooling system is integrated, the air temperature decreases below 295,15 K (22 °C). This cooled air is mixed with interior warm air immediately after entering the hall resulting an air temperature below approx. 297,15 K (24 °C) at 1,5 m height (human comfort zone area). Vertical temperature gradient in the core chimney occurs due to warmer closed perimeter channel beside. As the cold air is trapped against the floor, it is worth considering in the hall design that lower air temperatures, which may be uncomfortable, may develop near the inflow chimney, so the

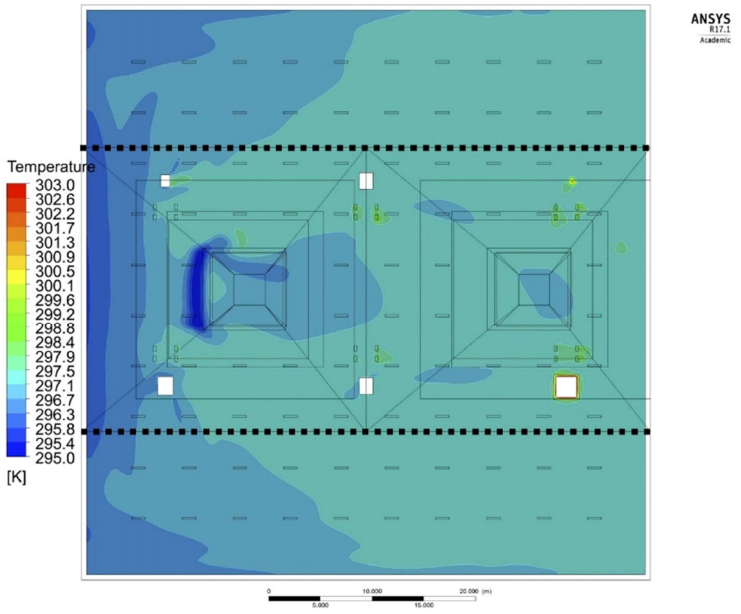

(**a**)

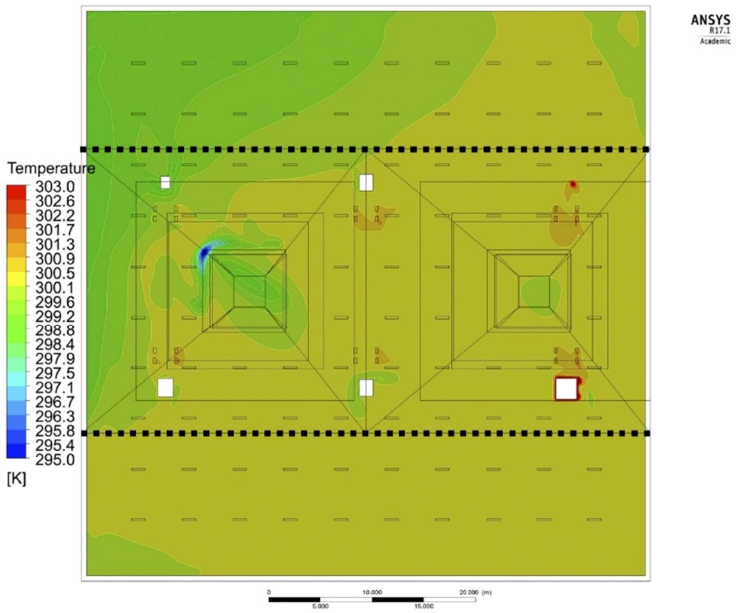

(**b**)

Figure 36: Air temperature distribution (K) in the basic module CFD model with modified inlet towers, horizontal section in 1,5 m height: (**a**) parallel wind direction; (**b**) diagonal wind direction

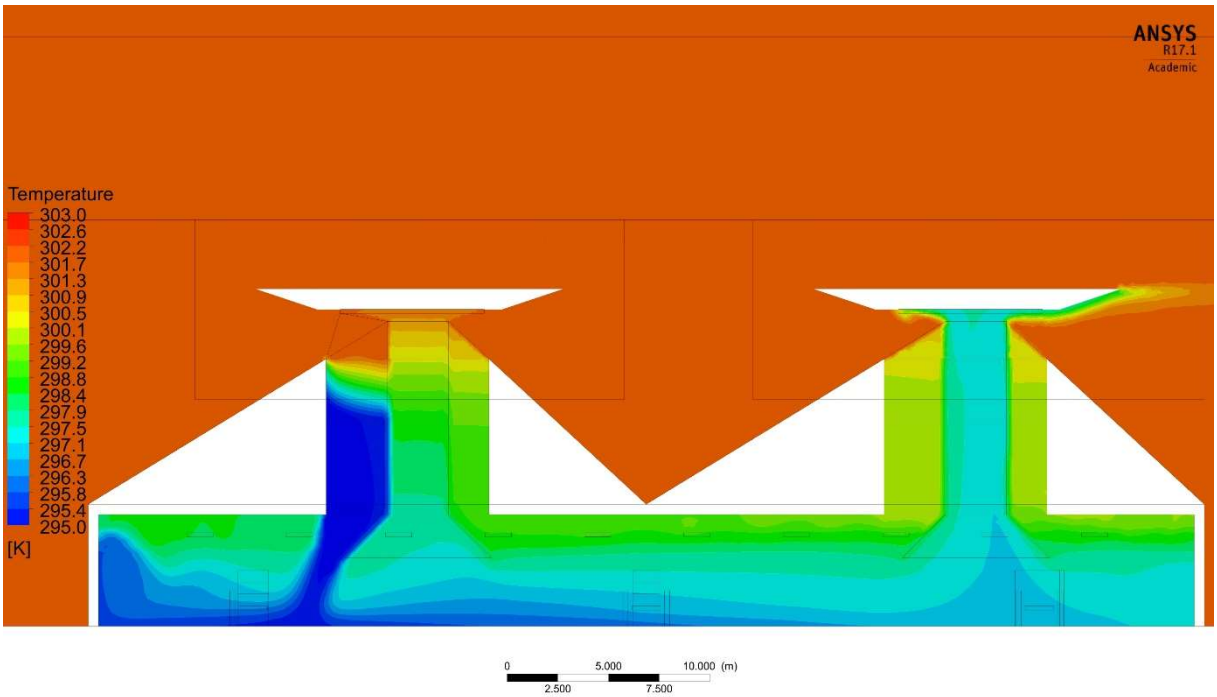

Figure 37: Air temperature distribution, temperature gradient (K) in the basic module CFD model with modified inlet towers, vertical section, parallel wind direction case

Figure 38. a similar cooling effect can be observed from the perpendicular wind direction, Due to 107 kW cooling power the desired average temperature distribution of 298.15 K (25 °C) is achieved, which is considered comfortable compared to the 302.15 K outside. There is no

homogenous temperature distribution in the hall, yet warmer temperatures above 28 °C are only in higher areas (above 4 m height) of the interior to register.

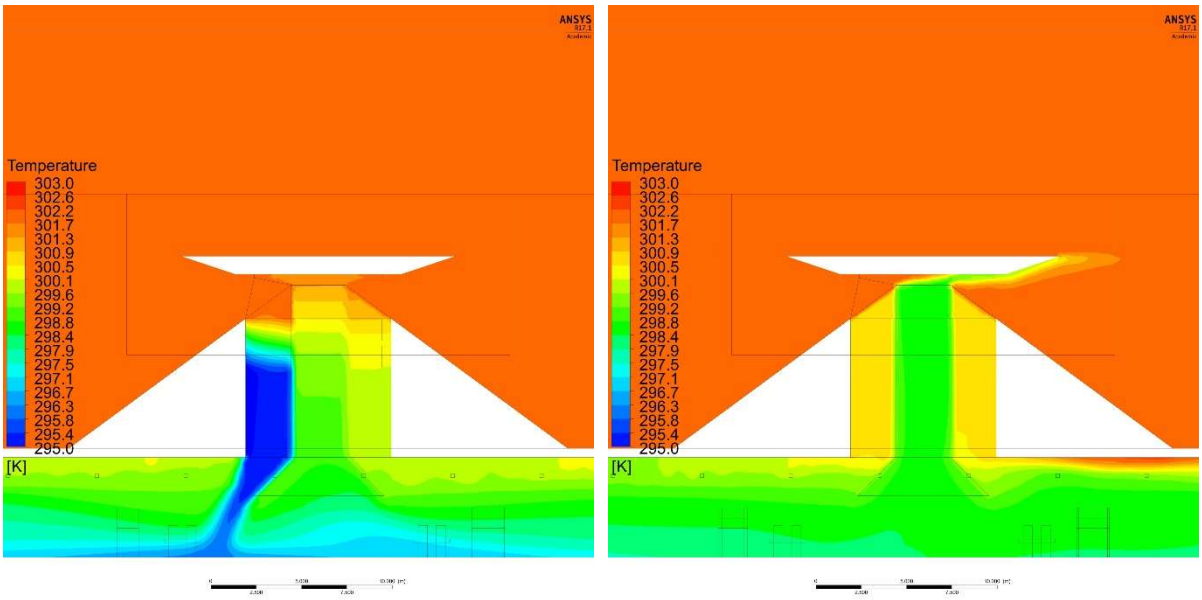

(**a**) (**b**)

Figure 38: Air temperature distribution, temperature gradient (K) in the basic module CFD model with modified inlet towers, vertical section, perpendicular wind direction case, input tower (**a**), output tower (**b**)

Because the baffle effect (20%) of the cooling coil in the inlet tower, the air volume flow was slightly reduced to 29 880 m3/h, and to an air exchange of 2 h-1. A vertical differentiation can be detected inside the closed ejection tower, due to the warmer adjacent tower where the warmer air was stratified (Figure 38a).

The Figure 39. shows the cooling performance along the diagonal wind direction. Warmer temperatures developed in the hall compared to the previous cases. Although the comfort zones at a height of 1.5 m still have values below 300.15 K, i.e. 28 °C, a higher cooling performance is required to maintain a comfortable working environment with this wind direction. It should be noted that heated and spent air at 30 °C is trapped in the outer closed ring of the exhaust horn. This means that in the case of spaces that are not part of the pyramidal hall (e.g. office functions), this used and warm air mass will have a negative impact on the temperature of the people and spaces.

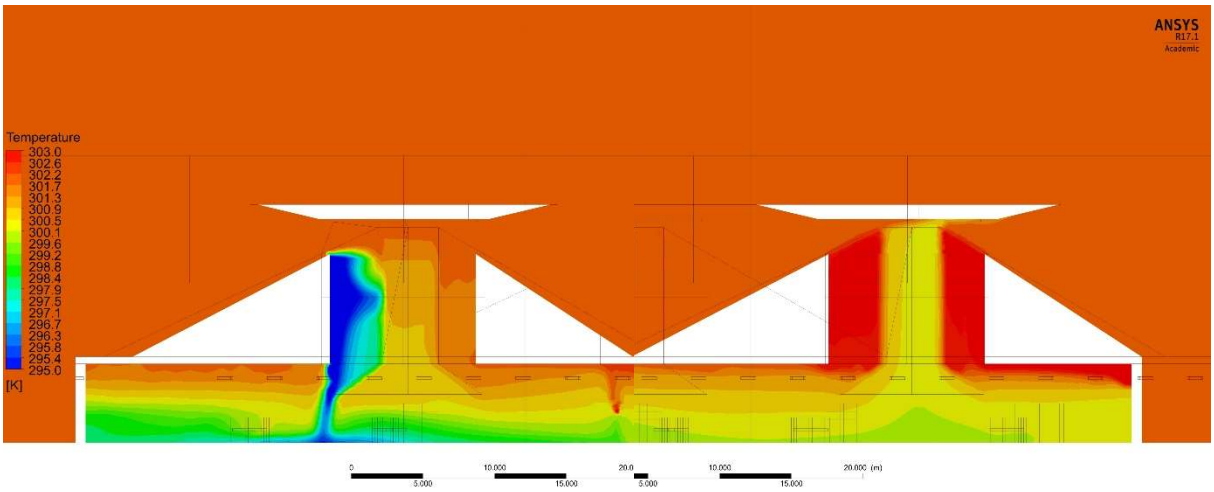

Figure 39: Air temperature distribution, temperature gradient (K) in the basic module CFD model with modified inlet towers, vertical section

5.5.5. Wind and thermal induced performance of the prototype basic unit model

The results make apparent that best ventilation and cooling effects performed in wind direction parallel to the prototype model's longitudinal axis, while in wind directions perpendicular to the hall's longitudinal axis slightly weaker, and in diagonal (45° inclination) angle to the model's longitudinal axis the proportionally worst values were calculated. This is due to the change in the direction of the tower connecting axis relative to the incoming wind direction, i.e. the change in the direction of the substantial internal air flow: the highest air exchange is obtained for the axis parallel to the wind direction, the highest air exchange is obtained for the axis at 90° to the wind direction, with a 21,11 % reduction in efficiency, and a 27,8 % reduction for the axis at 45° to the wind direction. The 'Venturi' structure of the ejection horns to increase the draft coefficient and the lower deflectors of the hall to reduce the draft need to be fine-tuned in future tests. For the diagonal wind direction, the wind catching geometry of the input tower also needs to be improved to increase the wind catching efficiency. With the integrated cooling, the rate of air scavenging was not reduced by orders of magnitude despite the cooling coil drag, so the thermal buoyancy in the hall and output horn was greater than the drag of the cooling coil.

Regarding the temperature distribution characteristics, the results are promising, comfortable indoor thermal environment could be achieved in the hall's interior during cooling. It is suitable for the installation of cooling units to reduce the average daily temperature of the subtropical climate to the comfort level with realistic performance requirements. However, for best, optimized solution further corrections and modifications are required in diagonal wind direction case. Important issue to recognize that this cooling performance were achieved by cooling a double sized space, due to the flaking 'buffer' zones, which double the interior space. One of the cornerstones of the continuation of basic research could be the concrete definition of the technology of such a cooling system, testing of evaporative passive and active solutions, comparison of the operations, efficiency testing. Source-side replacement of cooling performance by natural systems is a primary objective for future research. It is also worthwhile to address the controlled diversion and utilization of cooled air, as well as the recovery of the cold/cooling energy of used but cooled air. Table 6 shows a comparative analysis about the fluid mechanics and thermal performance values of the test CFD models. The system was able

to achieve the highest flushing when the towers were aligned with respect to the wind direction and the lowest when they were locked at an angle of 45° to each other.

Table 6 Air volume flow, desired indoor air temperature and cooling capacity in the three wind direction cases

Wind directions	V [m^3/s] only ventilation	V [m^3/s] ventilation + cooling	T_{ext} [K]	T_{int} [K]	ΔT [K]	Q [kW]
parallel	10,511	11,318	302,15	297,058	5,092	96,09
orthogonal	8,009	7,904	302,15	298,604	3,546	107,07
diagonal	7,500	8,330	302,15	299,273	2,877	77,72

In the prototype designed, a pioneering ventilation concept was developed, resulting in a wind-independent, universally usable horn layout. Since the prototype model is symmetrical, analysis in the three basic wind directions practically covers all important necessary cases. Normally, results in wind directions between the investigated three cases would yield approximately interpolated results. The prototype building's hoods worked efficiently for ventilation and cooling from all wind directions, thus ensuring universal operation. The encouraging results provide 5.0 ACH in a hall with a floor area of 1,512.5 m2.

5.5.6. Integrated bidirectional PACS into the prototype model with enhanced floor area

After successful testing of the primary functions of the basic modules, the units had to be assembled to produce the desired end product of the prototype development, a large, universal, multi-unit building. The well-functioning base unit modules were placed side by side to create the ensemble shown in Figure 40. Four of the prototype model units were assembled to form a complete prototype building model with a floor area of 55 x 110 m and a net floor area of 6,050 m^2 The height of the hall remained at 5.5 m. These dimensions seemed to be the usual dimensions for spacious public buildings for Chinese and international events and industrial functions. The prototype hall is equipped with the previous passive, wind-independent ventilation system, including cooling. The centers of the pyramids are offset in opposite directions from the center in units of two, to allow the towers to operate with as much freedom as possible, independent of the low and high pressure zones of adjacent horns. The internal heat generation outputs and solar heat loads have increased proportionally compared to the previous model and the same environmental boundary conditions are considered in the following simulation. In this case, the geometry was also examined from the three main wind directions (perpendicular, parallel and diagonal - wind directions).

According to the offset placement of the towers (Figure 40), the inlet openings of the perimeter towers differ: towers closer to the windward facade have smaller inlet openings, while towers further from the windward facade have larger inlet openings in the windward direction parallel to the axis connecting the base unit towers. For wind directions perpendicular to the axis connecting the base unit towers and diagonal wind directions, the size of the inlets shall not vary for the towers. These varying inlet sizes are due to the required eccentric geometry of the towers (the pyramids are distorted), which eliminates the wind shadow effect as the towers are aligned in the wind direction.

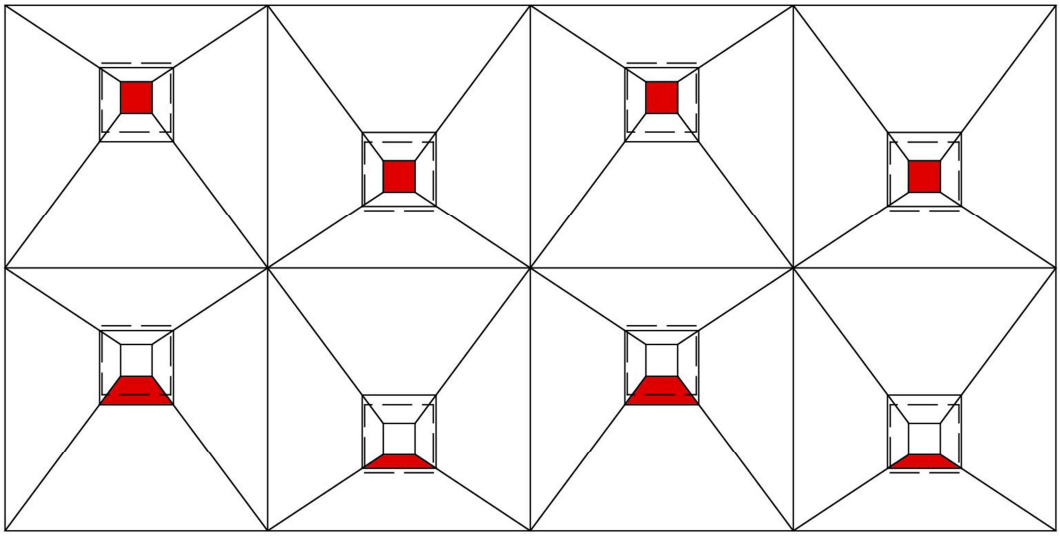

Figure 40: Complete prototype building model comprising four side-by-sing arranged basic module units, top view with inlet perimeter chimney openings (red colored) in windward side (wind direction parallel to tower's connecting axis

5.5.7. Simulation results

The eight towers allow much more permutation in input and output settings. Based on basic logic, we narrowed down the number of runs to 17 typical wind direction dependent, theoretically workable tower opening combinations, and then tested the most optimally working version per wind direction for cooling.

Fig. 41 top shows the resulting flow conditions for a wind direction combination parallel to the base module tower connecting axis in the horizontal plane taken at the height of the horn mouths. The cross-section illustrates the complex flow regime, which can be examined to draw conclusions about its operation. Thick black arrows depict the inlet and outlet horn flows. Wind is entering the figure from the bottom side, hence the windward four inlet towers in first (bottom) tower-row, towers No. 1 - 4 hide the four outlet towers from coming wind currents (second, top tower row, towers No. 5 - 6). A connected airflow correspondence is built up between each double unit's inlet and outlet tower.

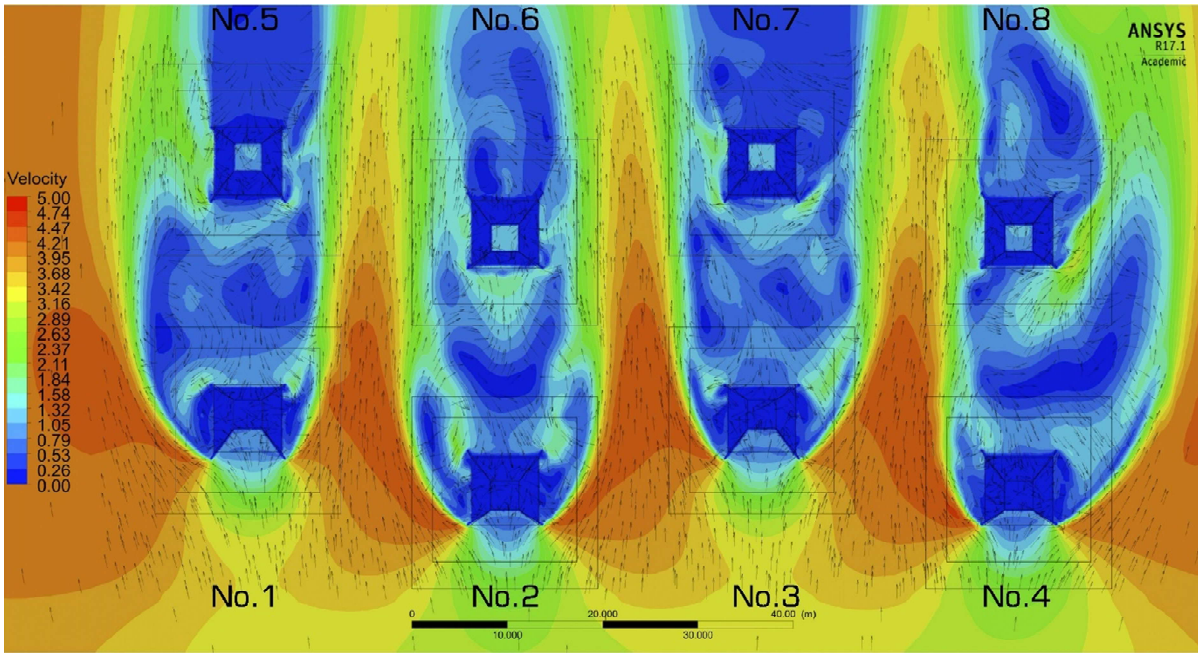

(**a**)

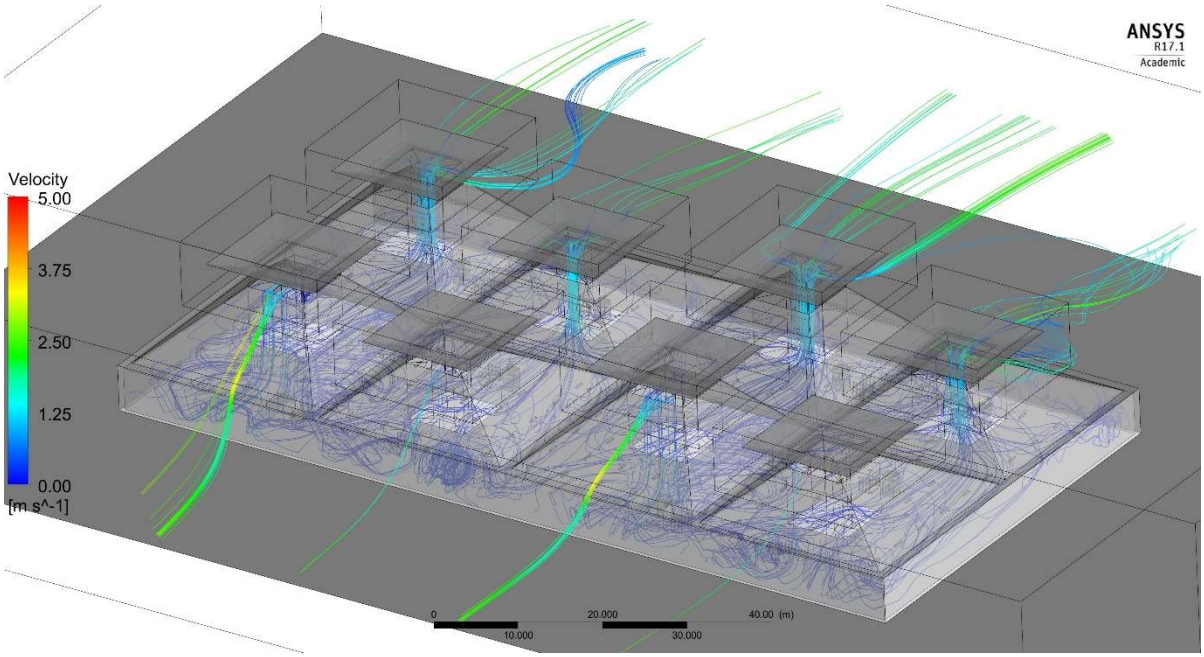

(**b**)

Figure 41: Airflow characteristic in the complete prototype building model, parallel wind direction to basic module units' towers connecting axis, horizontal section in 13,5 m height with velocity contours and vectors (m/s) (**a**), velocity pathline structure (**b**)

Note the variation in fresh air supply to the inlet caused by different sizes of inlet tower duct (Figure 41). Figure 42 shows the effect of different duct sizes: while the incoming airflow enters the hall through inlet chimneys of different sizes, the same outlet chimneys discharge approximately the same amount of air to the outside. Larger inlets deliver 2 times the air volume of smaller inlets. The result of the calculations is 139,500 m3/h inlet and outlet air flow, and thus an air exchange rate of 4.13 h^{-1}. The yarn diagrams (Figure 42b) typically show a well ventilated hall space. Each pair of double-unit towers (inlet and outlet towers) is able to ventilate the entire length of the hall interior transversely, while the windshield facade flanking the interior is about 50% less ventilated.

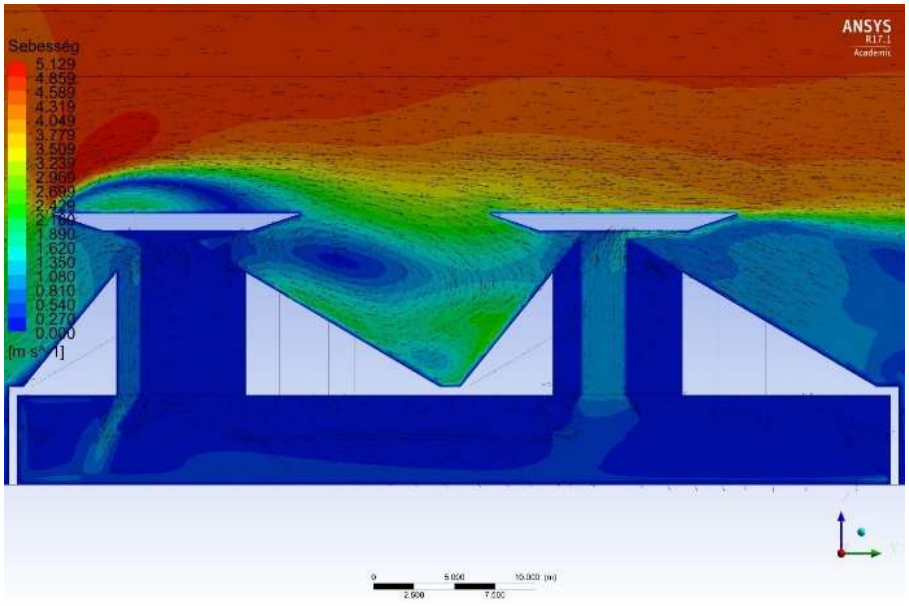

(**a**)

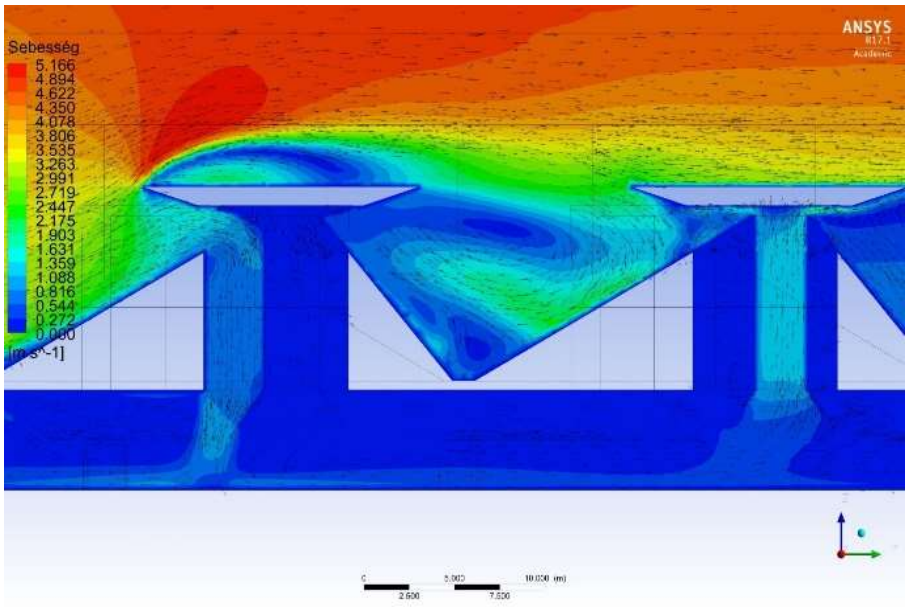

(**b**)

Figure 42: Airflow characteristic in the complete prototype building model, parallel wind direction to basic module units' towers connecting axis, vertical section of windward tower near to windward facade (**a**), vertical section of windward tower far from windward facade (**b**)

Figure 43a shows the resulting flow conditions in the horizontal plane taken at the height of the horn mouths for the opening combination parallel to the base module tower connecting axis. The wind enters the formation from the left side, so an inlet/outlet combination was intended for efficient ACH in the hall. The two windward inlet towers on the left (Nos. 1 and 5) are followed by two outflow towers (Nos. 2 and 6) in the approaching wind direction, creating a ventilation flow through the left half of the building. The next two ventilation chimneys (Nos. 3 and 7), located behind the outlet towers in the direction of the oncoming wind flow, are again responsible for the supply of fresh air, followed by the last two towers (Nos. 4 and 8) on the right side of the building as outlet chimneys.

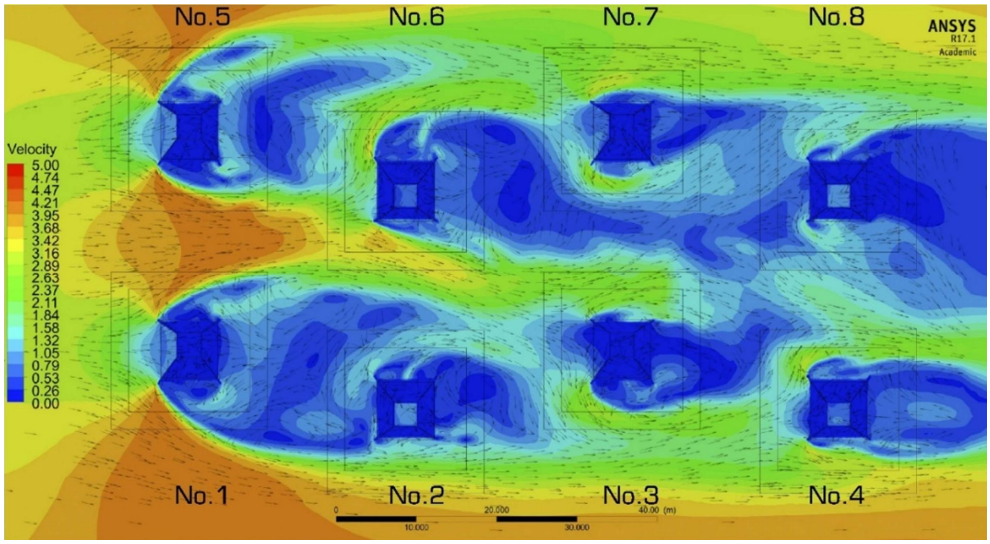

(**a**)

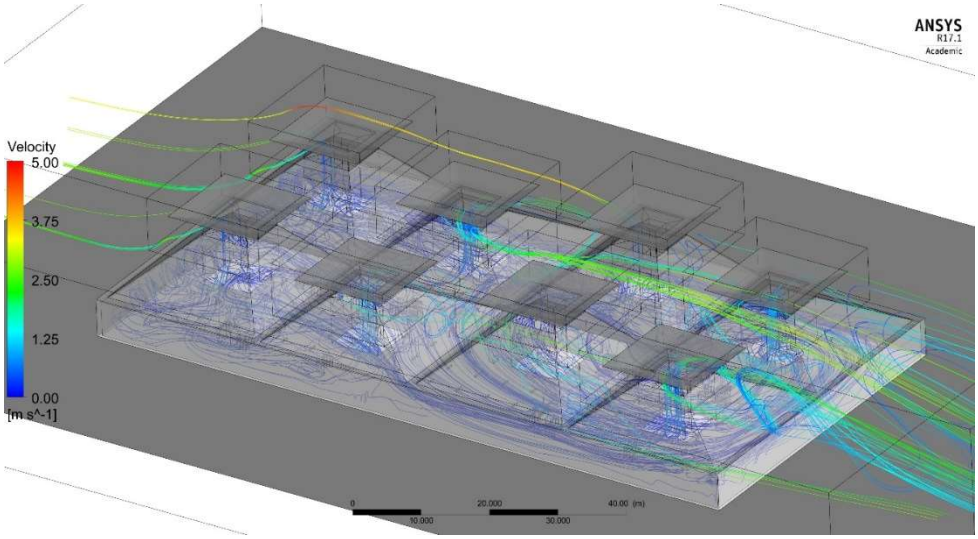

(**b**)

Figure 43: Airflow characteristic in the complete prototype building model, perpendicular wind direction to basic module units' towers connecting axis, horizontal section in 13,5 m height with velocity contours and vectors (m/s) (**a**), velocity pathline structure (**b)**

A continuous airflow correspondence is established between the inlet and outlet towers, despite inlet tower 3 discharging air instead of introducing it into the interior. This effect is caused by

the non-symmetrical tower position constellation. Because Tower 3 is at a greater distance from the edge of the building than Tower 7, Tower 3 is not able to introduce fresh air into the building, but rather draws air from the interior. Although a high-energy wind flow (around 3 m/s) is generated along the longitudinal axis of the building, it does not reach Tower 3 due to the "Venturi nozzle" effect, which accelerates the air velocity between the tower rows. The calculation still results in efficient ventilation performance parameters of 128,000 m^3/h inlet and outlet air volume and thus an air exchange rate of 3.85 1/h. The yarn diagrams (Figure 43 below) typically show a well-ventilated hall space.
Figure 44a shows the resulting flow conditions in the horizontal plane taken at the height of the horn mouths for the base module tower connecting axis for a diagonal wind direction opening combination. The wind enters the figure from the lower left corner, so a special inlet/outlet combination has been envisaged in the hall for efficient ACH. Due to the advantageous windward location of towers 1, 2 and 5 in the left-hand corner of the building and the windward arrangement of tower 4 in the lower right-hand corner of the hall, these towers are responsible for the inlet supply. The remaining four towers act as exhaust ducts. A continuous airflow correspondence is established between the inlet and outlet towers. Compared to Towers 6 to 8, Tower 3 provides 50% less airflow intensity, which is due to the adverse effect of the diagonal tower geometry, as wind flows are dispersed along the sides of the towers. This effect does not allow the high "Venturi" blower efficiency of towers 6-8 to be achieved. The calculation results in efficient ventilation performance parameters of 171,600 m^3/h inlet and outlet air volume and thus an air exchange rate of 5.15 h^{-1}. The yarn diagrams (Figure 44b) typically show a well-ventilated hall space.

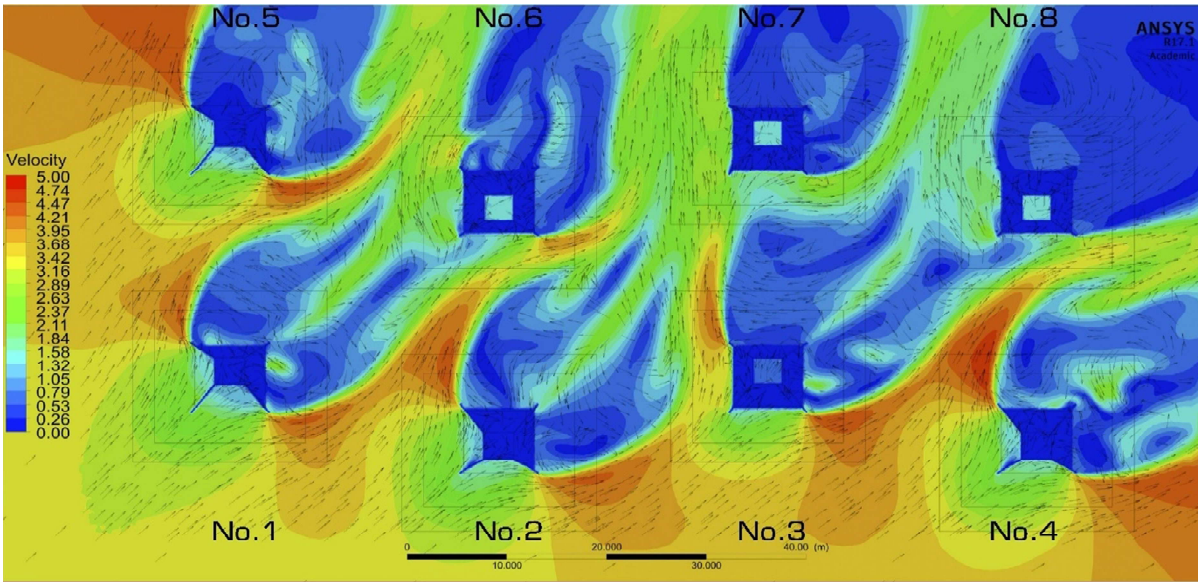

(a)

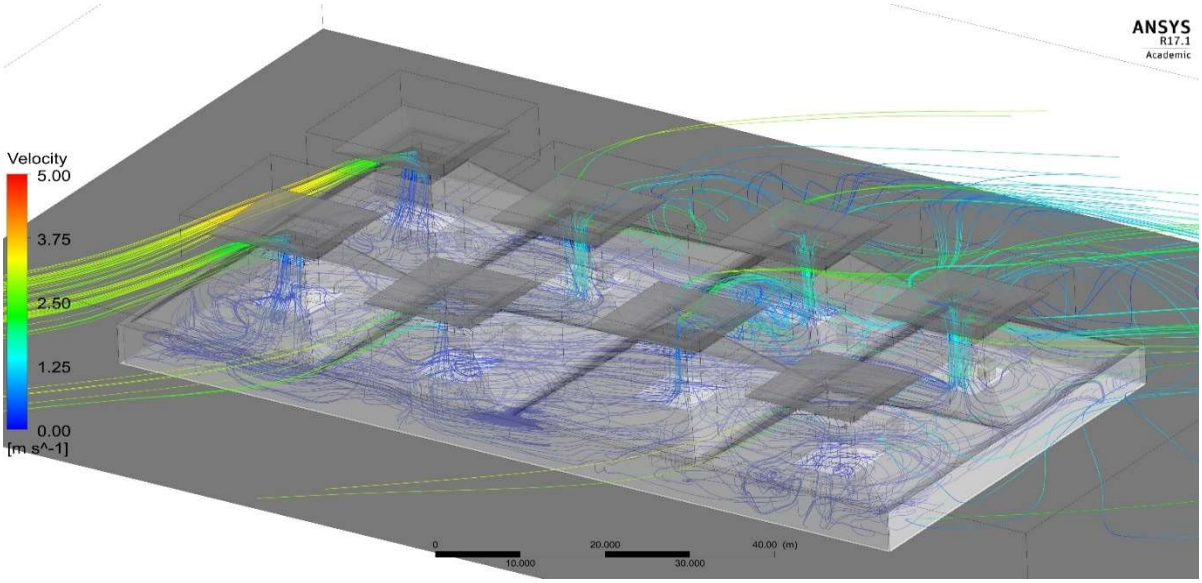

(**b**)

Figure 44: Airflow characteristic in the complete prototype building model, diagonal wind direction to basic module units' towers connecting axis, horizontal section in 13,5 m height with velocity contours and vectors (m/s) (**a**), velocity pathline structure (**b**)

Figure 45 summarizes the wind direction dependent tower trumpet opening combination cases. The base module tower connecting axis-parallel wind direction opening combination cases produce efficient operational ventilation of the prototype building with input and output tower trusses operating as designed. In the parallel wind direction, 4.13 ACH were generated. For a total of four opening combinations for the wind direction perpendicular to the base module tower connecting axis, eliminating wind shadows as much as possible, it is noticeable when examining the opening variations that the tower operation is affected by the distribution of pressure differentials between the pyramids. The most significant effect of this is that for certain horn mouths with initially input gate settings, flow directions, velocities and pressure differentials are developed that convert the horn into an output operation. In this wind direction, the ACH decreased to 3.47 - 3.85 for the two different tower opening constellation cases, approx. 10% air exchange attenuation. This phenomenon can be attributed to the following mechanisms of action:

- Cases 11110000-P1 and 11001100-P1. As the asymmetric horn positions are at different distances from the building perimeter, i.e. from the free wind flow, the second row of intake horns in the wind direction, one of the towers (3 and 6), which is farther from the building perimeter, circulates the air instead of introducing it into the indoor space, and the wind intake mechanism does not apply. These towers are in the wind shadow. The Venturi draught flow between towers 1-4 and 5-8 is not able to induce inflow as it does not reach these towers, which operate in reverse (Figure. 45).

- Cases 01010101-P2 and 00110011-P2: In windward direction, second row towers 2 and 7 behind the intake horns, instead of being intake, eject air because they are in wind shadow. The Venturi draught flow between towers 1 to 4 and 5 to 8 can induce inflow in towers 3 and 6 (Figure 45).

- In the wind direction, a counter flow is formed in the second row of intake horns closer to the outer perimeter. In the wind direction, counter flow occurs in the intake horn in the third row of intake horns farthest from the outer perimeter (outflow

For the incoming diagonal wind direction, the case studies include all possible theoretically conceivable combinations of opening of the wind vane to avoid the wind shadow. In this wind direction, the air exchange ranges from 2.37 to 5.16 ACH, with approx. 20% air exchange in the most efficient case and approx. 20% in the poorest performing case. 43% weakening for a total of six different tower opening constellations. Also in this wind direction, it is a typical phenomenon that certain horn mouths with originally input gate settings develop flow directions, velocities and pressure differences that transform the horn into an output operating horn. This phenomenon is known as
the following mechanisms of action:
As a result of asymmetric horn location, towers closer to the longitudinal central axis of the building, as viewed from the diagonal incoming wind direction, are brought closer to the intake or discharge horns in the wind direction ahead of them, effectively becoming semi-"overlapped" wind shadows. The pyramidal geometry of the inlet or ejection horns ahead of them 'spreads' the incoming wind streams bilaterally, creating a kind of 'Venturi' acceleration, a low pressure zone near the 'overlapped' input horn splice of the problematic rear towers relative to the given wind direction. This reverses the flow and ejection occurs, while the other wind-free horn continues to produce air intake in the problem towers. The results show that this significantly reduces the air supply at these points or even causes a complete blowout. Thus, when several modules are placed side by side, the greatest risk lies in the spacing of the towers (Figure 45). If we look at the shifting of the horn spacing, i.e. the pyramidal peaks towards each other, although it helped to reduce the wind shadow zones in the case of longitudinal winds, the spacing between the horns varies unevenly in the case of oblique winds. Thus, the horns that are spaced at a smaller distance apart, the one that is further back in the wind will be affected by the one in front.

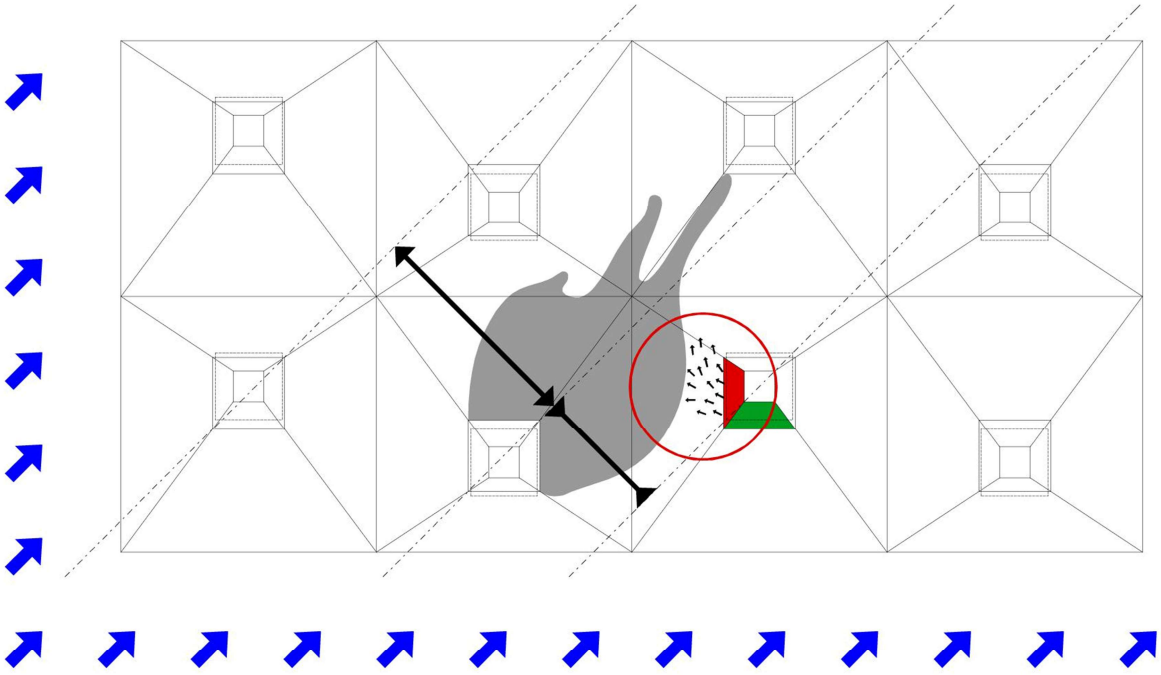

Figure 45: Reason for reversible airflow performance (outflow) in input tower channels, in diagonal wind direction to basic module units' towers connecting axis. "Semi-wind shadow effect" on towers near to longitudinal middle axis of the building.

Despite the reversible flow mechanisms, ventilation remains functional in all cases tested. It can be said that for all three wind directions investigated, a hood opening composition was found that allows efficient passive ventilation to be achieved with the prototype structures. In the most efficient case, a diagonal wind direction of 4.8 - 5.16 h^{-1} (opening codes 00101011 and 11100010) air flushing is obtained due to the design of an optimal, windshield-free input stack composition. The ACH is 3.78 - 3.85 h^{-1} in the perpendicular wind direction (opening codes 00110011 and 11001100) and 4.13 in the parallel wind direction. It can be shown that the newly developed system is operational on a large scale, even with multiple modules in series. The main problem occurs only for the input horns due to the asymmetric horn placement. As a consequence

- wind screened intake horn positions (windward and backward towers) → flow reduction, stoppage
- in addition, some horns are located further away from the building perimeter (from the free wind flow) → inflow reduction, stagnation
- or 'Venturi' draughts between longitudinal tower rows are unable to reach the inflow chimneys → inflow reduction, stoppage
- the tower in front of the windscreened tower 'throws' the diagonal wind currents laterally and thus generates a low pressure zone ('Venturi' acceleration), a suction effect on the wind screened tower horn → inflow reduction, stoppage

Used air ejection horns are always operational. The additional wind direction cases between the three wind directions can be qualified with interpolated ventilation performance values, so the basic ventilation characteristics of the prototype are known. Understanding the behavior mechanism of the input-output towers in terms of tower geometry and positioning merits further research, and the building interior comfort level (draft reduction, thermal comfort) needs to be improved.

5.5.8. Discussion of the innovative PACS implementation's ventilation performance

The first step in the development of a PACS for industrial buildings has been completed, in the form of a modular prototype hall system for the developing Shanghai and Shenzhen industrial area.
In addition to the results of several years of monitored testing of an industrial facility in Hungary, manual measurement data collection and meteorological databases were used to calibrate CFD and thermal simulations of the reference building. The functionality and adaptability of the downdraught system was tested by modifying the validated model of the reference building of RATI Ltd. Once the basic fluid dynamics operability was demonstrated, the development of a new prototype was started by redesigning the validated downdraught CFD model. In order to ensure the internal natural ventilation and permeability of large-scale, high airspace buildings in China, and to cope with the microclimatic wind conditions of the ever-changing building environment, a prototype modular basic unit with a wind-independent PACS integrated into the roof structure was required. As the basic unit showed encouraging results in terms of air flushing and cooling performance, testing of a prototype hall building with a floor

area of nearly 6,000 m^2 could start. The complete prototype wind-induced ventilation characteristic of the four basic units is a high performance passive system that is basically wind-independent. With the theoretical cooling ramp-up, the basic operating mechanism of the system is reliable. After passing the first functional check, the following points and issues require further improvements:

- To what extent is it possible to increase the draft gain of the ejector turret 'Venturi' in the two-tower basic unit model?
- How is it possible to reduce the draught sensation under the discharge tower trumpet indoors in the two-tower basic unit model? The internal "resultant" change in flow direction relative to the incoming wind direction during the throwing and spreading process should be optimized.
- for a diagonal wind direction, what geometric design solution can prevent the wind flow from "dispersing" in both directions, i.e. how can the wind flow be more efficiently captured in the input horn at the corner?
- How viable is an evaporative or other humidifying passive cooling system solution in the input horns under subtropical absolute humidity conditions? To what extent can the relative humidity evolution of the captured log air absorb and cool humidity? A further issue for passive cooling solutions is night cooling, during which high inlet humidity is not a problem, but only lower air temperatures are used to cool internal (to be developed, even mobile) thermal masses (lighter PCM based structures)?
- Which mechanical system is best suited for the input downdraught horn ventilation-cooling solution? Can cold recovery with a water system be efficient?
- To verify the iterability of the flow performance between the three main wind directions, is it worthwhile to verify 1-2 intermediate wind direction cases by CFD runs?
- For ventilation of a complete prototype building, find the appropriate input-output opening code combination for all three wind direction cases. It is worth to increase the power vertical of ACH 3.78 - 5.16 at the following points:
    - Wind shading should be avoided as much as possible. To achieve this, the "narrowing" effect between the diagonal wind direction and the intercepting towers should be addressed by modifying the tower positioning.
    - The increased distance from the side edge of the building to the intake horn in the perpendicular wind direction causes a reversible flow (input becomes output). Here, too, a tower positioning change can improve the situation.
    - The negative, unintended effects of 'Venturi' draught-enhanced flow between towers due to tower positions and geometries (suction effect at input towers in lee and unused inflow potential between longitudinal tower rows) can be improved by design and positioning changes.
    - The theoretical cooling ramp was used to develop a workable downdraught system. **The transformation of input horns into output horns in cooling mode eliminates the cooling effect, so a key development objective is to define the input horns accurately and safely, eliminating reversible flow.**

- In summary, a new PACS building prototype has been developed, whose performance energy saving and environmental (cost and operational) potential should be investigated by coupled dynamic thermal simulation. Applying integrated meteorological boundary conditions, results based conclusions can be extracted about appropriate daylighting system solutions as well as indoor thermal comfort and air hygienic qualities (cooling, ventilation) in a complete summer operation time period. In addition, the needed energy demand of the prototype building will also be calculated using IDA ICE 4.8 software.

- The long-term objective is to develop a modular, prefabricated, flexible product family system that can be applied at low cost in large volume buildings where mechanical ventilation is a key operational consumer. The product family will be developed for different climates, so that the system can be adapted to different climates based on a combination of modules, structures, materials and geometries.

Finding 3.

If the intended ventilated area has huge distances from the façade openings, the most cost and performance efficient Passive Air Conduction System solutions are roof structure integrated vertical down draught and up draft elements.
A new coaxial chimney structure was developed, whereas the down draught principle ensures the fresh air inlet, and the up draft system conducts the stale exhaust air from the interior to the outdoors. The temporary function of a chimney system depends on the actual wind incident angle, which can modify by a building management system. The developed Passive Air Conduction System unit can maintain acceptable air change rate (5.63 h^{-1}) in a 765 m^2 industrial hall and even works efficiently (5.16 h^{-1}) in a multiplied version (8 pieces of arranged basic units) where the area increased to 6,000 m^2.
However, in the large version there can be complications with the suitable opening management, due to unintended airflow directions occurred in the chimneys, due to the flow distribution between and around the towers.

5.6. The questions of *micro level* geometry optimization of PACS' elements

5.6.1. Shape design test variations of the PACS inlet structure

According to the results of the previous study, a DD wind catcher PACS should have been integrated to the new winery building in Villány, Hungary. The prototype building and the PACS is currently in the final stage of the implementation at the construction site (Figure 46), described in detail in [80].

Figure 46. The prototype building under construction with the wind catcher inlet (left pyramid) and the 'Venturi' outlet structures (right pyramid)

The territory is ranked as Cfb-temperate oceanic climate, based on the Köppen-Geieger climate classification [81]. Since no meteorological data were collected on site, the Meteonorm ® [88] database were chosen to generate wind distribution data for the local wind speeds. Because the values did not suggest any exclusive prevailing wind direction, an omnidirectional PACS was selected as solution for future integration into the test reference building. The structure of the PACS is a DD system which include a wind catcher inlet and a wind deflector outlet.
The PACS was integrated in the final architectural plan, - the sections in Figure 47 presents the location of the in- and outlets and chimney structure. The inlet structure is integrated in the flat roof terrace of the restaurant in form of a wind catcher to collect the incoming wind, and force fresh air down to the interior. The stale air is sucked out by the 'Venturi' tower, where the special wind deflector geometry on top of the tower should create a low pressure zone just above the outlet opening. The indicated airflow directions, velocities and volume flow rates, based on the CFD results in the previous study [80]. Now, an inlet structure's shape should be defined that is able to provide highest supply airflow and thus ACH in the two-story high production hall and the cellar in the basement. The position of the investigated wind catcher is indicated in the sections as well.

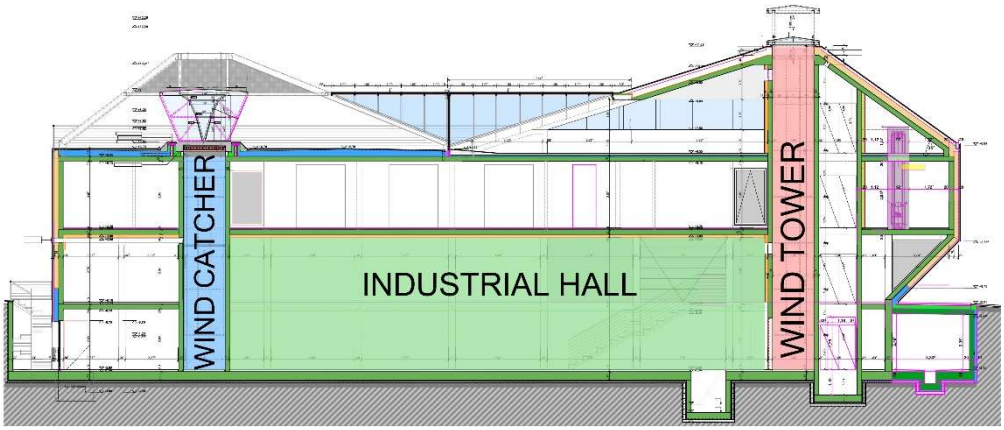

(**a**)

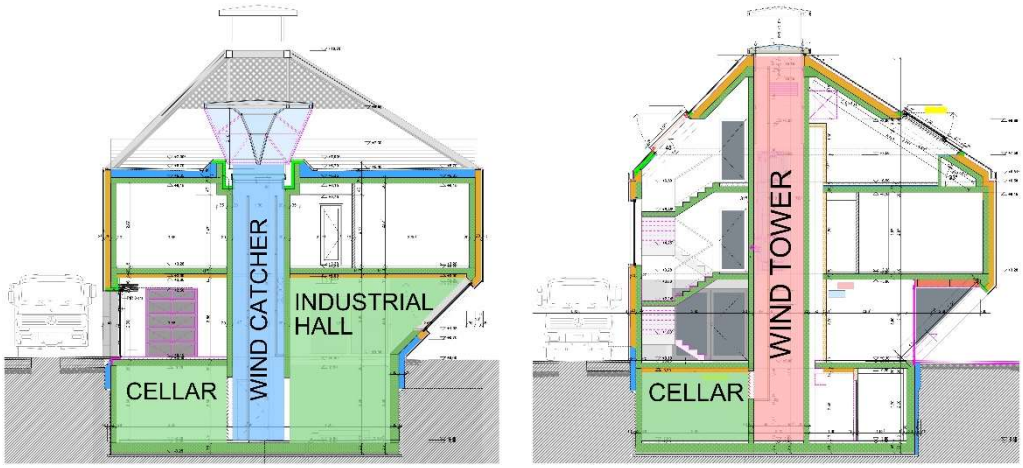

(**b**) (**c**)

Figure 47. The Down Draught Passive Air Conduction System (DD PACS) with in- and outlets and chimney structures integrated in the architectural construction plan with airflow directions, velocities and volume flow rates (based on previous CFD study); (**a**) longitudinal section; (**b**) cross section through the wind catcher; (**c**) cross section through the exhaust wind tower. The reinforced concrete load bearing structure is marked with green color.

Figure 48. proposes the basic boundary conditions for the wind catcher setup. All cases have a rectangular cross section with two separators through the diagonals, hence, four section is created, regulated (opened or closed) by a Building Management System (BMS), depending on the incoming wind's direction. The rectangular chimney section is coming from another study [90], where high performance ventilation towers were achieved in a real-world industry building with an 2000 m^3 technology hall space. According to the conclusions, the tower sections (5.2 x 4.9 m) were over dimensioned (undesired deaccelerating vortices were generated), and thus in the 1200 m^3 winery spaces the chimney section was generally reduced. Particular size was designed as 1.80 x 1.80 m that was together with the rectangular layout and the positions of the chimneys required from functional aspects as well to offer easy integration into the space arrangement and the load bearing reinforced concrete structure of the building. In addition, too close arrangement of the towers to each other created weakening ventilation capacity due to slipstream effect of the chimneys. Therefore, in particular case, only two chimneys are considered to provide higher distance between the openings. The height of the wind catcher is as high as possible to fit into the maximum allowed roof integrated structure dimensions. The walls of the wind catchers were modeled as infinite thin walls, because many modern materials are suitable to create very thin (couple of cm thickness) and thus aerodynamically 'two-dimensional' shapes.

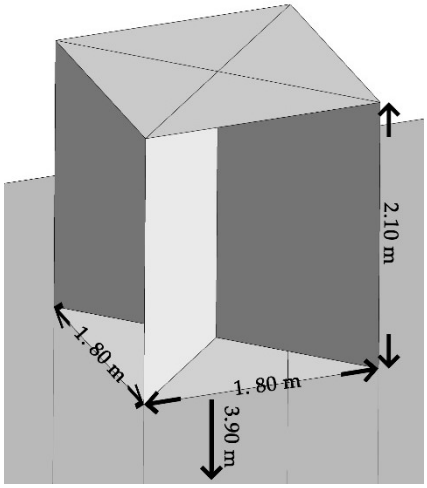

Figure 48. Boundary dimensions of the wind catcher geometry (base case)

For optimal air inlet design, the transition of the entering air movement is crucial, i.e. as little as possible turbulences and vortices are desired to avoid unwanted contra-productive currents against the air supply current direction. Four different geometries were selected based on the work at Ford et al. [98], which should operate sufficiently. The geometry variations are presented on. The first case is the 'empty' wind catcher (base case – Figure 49**a**). The second is the 'circle' (Figure 49**b**), where the radius of the curved inwards and downwards deflecting surface is the height of the inlet openings (right side of the figures). The third one has 'parabolic' curve (Figure 49**c**), while the forth version was equipped with the same wind catcher topology as the third, but the tower's cross section is modified as a hyperbolic bell (Figure 49**d**). The parabola was chosen in the third version's modification according to Ford's design source book [98] and Pearlmutter et al. [5], proposing the parabolic shape as a better aerodynamic option. However, their work was done in a tower with 3.75 m diameter –which means the cross section's area was approximately 3.5 times larger, so for more universal insights, the possible generalization of the results can be advantageous. The ideal curves were represented by segments (left side of the figures), in order to enable easier volume discretization as well as practicality for the construction.

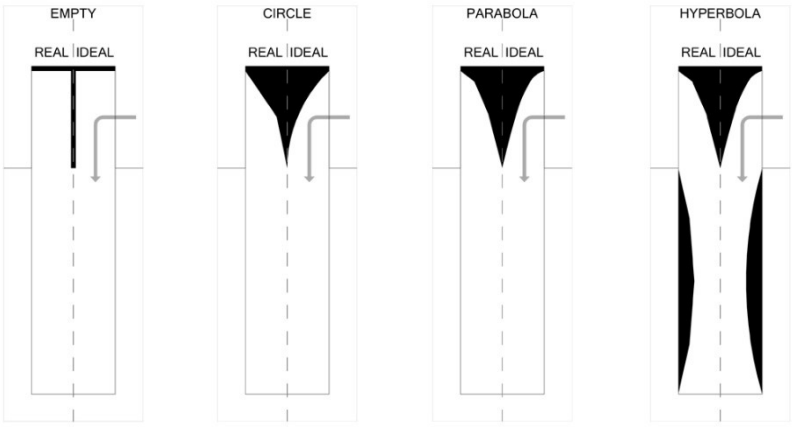

(**a**) (**b**) (**c**) (**d**)

Figure 49. Conception of the wind catcher inlet structure shape; empty' geometry (**a**); 'circle' (**b**); 'parabola'(**c**) and parabola with 'hyperbola' bell in the tower (**d**)

The investigation of the wind catchers is conducted in a simplified version of the original building as the complicated façade and roof (Figure 50a) are reduced to a cubic shape (Figure 50b). Thus, less modelling and calculation time is needed, and a more generic outcome is acquired. Neighbor buildings and vegetation details are replaced with the mathematical modelling of environment's boundary layer: a custom developed wind profile generator calculated the typical wind circumstances with a modified roughness constant[96,97]. The connection between in- and outside with the two towers and the sizes, proportions and geometries of the spaces and chimneys are similar to the CFD model of our previous winery study. The only difference is that the production and storage rooms in the basement are merged in current model to gain the mentioned more generic insights. The connections to the previous study are necessary for the easier validation of the CFD simulations' method, since it has been already performed correctly.
The ventilation outlet chimney consists of the same dimensions and shape as described in [80] in the validated CFD model. The only difference is the geometrical simplifications of the building envelope. Both openings have the same cross section. The height of the exhaust tower's top opening is settled 3.0 m higher than the inlet opening of the supply structure in order to enable as much exposure as possible to the approaching wind in case of the most disadvantageous direction, i.e. coming wind from the direction of the wind catcher.

(**a**) (**b**)

Figure 50. (**a**) Geometry of the original building with validated CFD simulations [80]; (**b**) simplified geometry for generalized results about the wind catcher topology – grey shows the simplified environment, blue the inlet and red the outlet tower, yellow the interior of the cellar, and purple is the investigated wind catcher geometry

5.6.2. Simulations and Model Set Up

The wind catcher geometries were modeled and simulated via CFD software. The CFD simulations are cost- and time effectively modifiable, and the basic infrastructure and its maintenance is more cost-effective as well, this is why it is more widespread than wind tunnel model experiments or in-situ measurements [14,21].
Firstly, a virtual wind tunnel domain was created. Multiple guidelines are proposed to dimension CFD models [22,23,100]. Usually the basic unit of an atmospheric domain is the

height of the building [H] and in this series of simulations, the domain sizes are presented in Figure 51. Since the investigated building is symmetrical, only the three main wind directions' calculation is required: cross (orthogonal to the building's longitudinal axis), diagonal and longitudinal (parallel with the axis). The building longitudinal axis equals with the connection axis between the two chimneys. Due to the approaching wind direction cases, the calculated domain became asymmetrical.

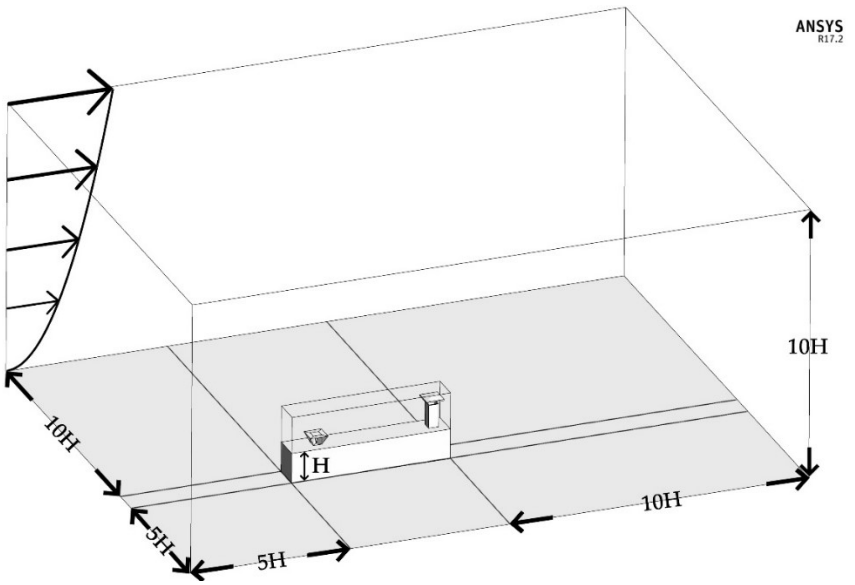

Figure 51. Dimensions of the domain for CFD simulations, H = 6.60 m and it represents the height of the building

The created volume is needed to be discretized by the Finite Volume Method (FVM), whereby in the appropriately densely created cells' nodes the main field variables will be calculated in the CFD simulations. The precision of the results depends on two important aspect of the modelling. First, the CFD results, and the method that tends to achieve precise results should have been validated with manual measurements or already validated literature comparison. This study follows the second option, whereby my previous works [80,90] were taken as reference models including real world measurements, and the representative sizes are shown in Table 7. It can be clearly seen that the previous study's validated mesh sizes (detailed domain) and particular mesh domain dimensions agree. Only the total domain size is smaller in the new research, because here solely three wind directions were investigated with accordingly smaller upwind areas [96,97]. The cell size diversion ranged between 1.5 and 2.5 of the model's discretization.

Table 7. General cell sizes of the simulated meshes.

Region	Validated Mesh [90]	Detailed Domain [80]	Simplified Domain (current research)
Total domain size	500m × 500m × 100m	200m × 200m × 80m	105m x 135m x 60m
Atmospheric	6 m	4 m	4 m

Macro environment	3 m	2 m	2 m
Micro environment	2 m	1 m	1 m
Near building walls	0.5 m	0.3 m	0.3 m
Towers/openings	0.3 m	0.1 m	0.1 m
Interior	0.2 m	0.25 m	0.25 m

The second important aspect of reliability is the 'grid independency', where the quality of the used grid is determined by the widely accepted guidelines of Celik et al. [95] Three different mesh were generated with 353,622; 776,196 and 1,696,657 cells, respectively. The fine-grid convergence index is 1.04% and 0.19% for the medium and the fine mesh (Figure 52.). The medium grid was selected for further work, because the deviance is below an acceptable level. Appendix A discuss the details of the grid independency test's steps.

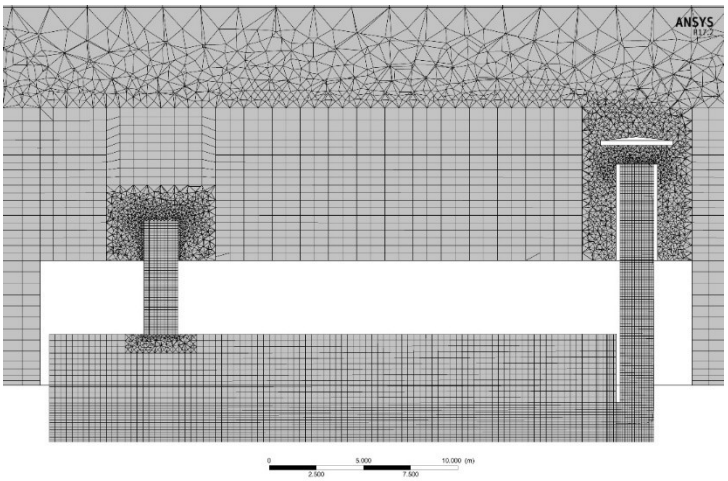

(a)

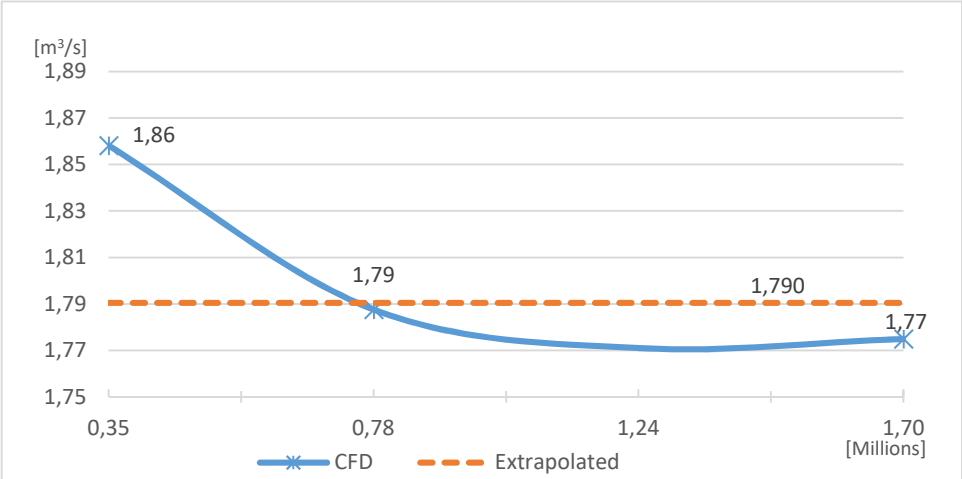

(**b**)

Figure52. (**a**) he selected (medium) discretization (longitudinal section), and (**b**) the grid independency test's ACH [m^3/h] results.

The simulations were carried out in the ANSYS® Fluent 17.2 software. The suitable turbulence model is crucial for respectable CFD simulations, as it stated by Peng et al. [101].They invited 19 CFD engineer team for solve the same problem with their own turbulence modelling method, and the paper found 150% deviances between the different solution methods. Based on my and fellow researchers' experiences [15,60,102,103] the Reynolds Averaged Navier-Stokes (RANS) equations with SST k-**Ω** turbulence model was selected for the CFD. Since, the assessment of the wind catchers' performance is based on the ACH, only isothermal calculations were made and no energy equations solved. One case contained 1,500 iterations in steady state and 1,200 iterations in transient mode (120 seconds, and 1 second has 10 iterations). The transient mode was necessary only in few cases for convergence, but for unified solutions and comparisons, every case was solved with the same settings. The atmospheric wind profile was generated in Fluent, with User Defined Functions (UDF), based on the work of Balogh et al. [96,97]. The air velocity at the height of 10 m was 2.73 m/s (coming from the Meteonorm® database) and the gradual vertical change of the velocity was determined by the local agricultural land (some houses, hedgerows and fences) which were modeled with a uniform roughness constant coded into the UDF.

5.6.3. Results and discussions

The four selected cases were investigated with three different wind directions, which mean a total of 12 scenarios. The three directions are described in section 2.2. The ventilation performances were evaluated in each directions separately, but the final evaluation was made in dependency of the averaged mean values, since an omni-directional PACS is the origin of this study (provided form previous investigation [80] and the wind catcher of this system should work acceptably under all wind situation.
Figure 53. shows the flow fields in the 12 cases of all geometries in horizontal sections around the wind catchers, and Figure 55. presents the same cases in vertical sections. Firstly, the flow fields show great similarity in all cases, whose consequence in ACH can be tracked in Figure 11.

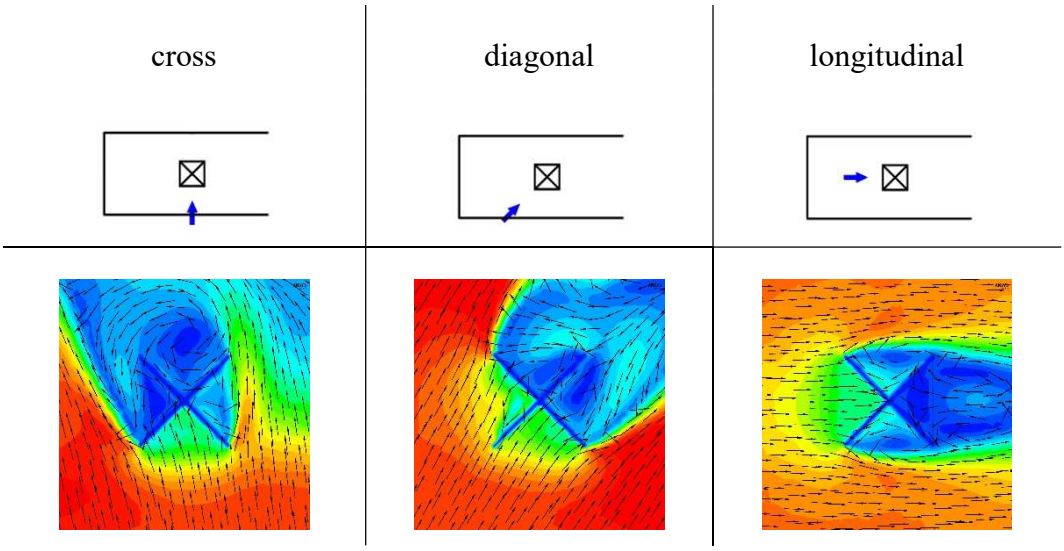

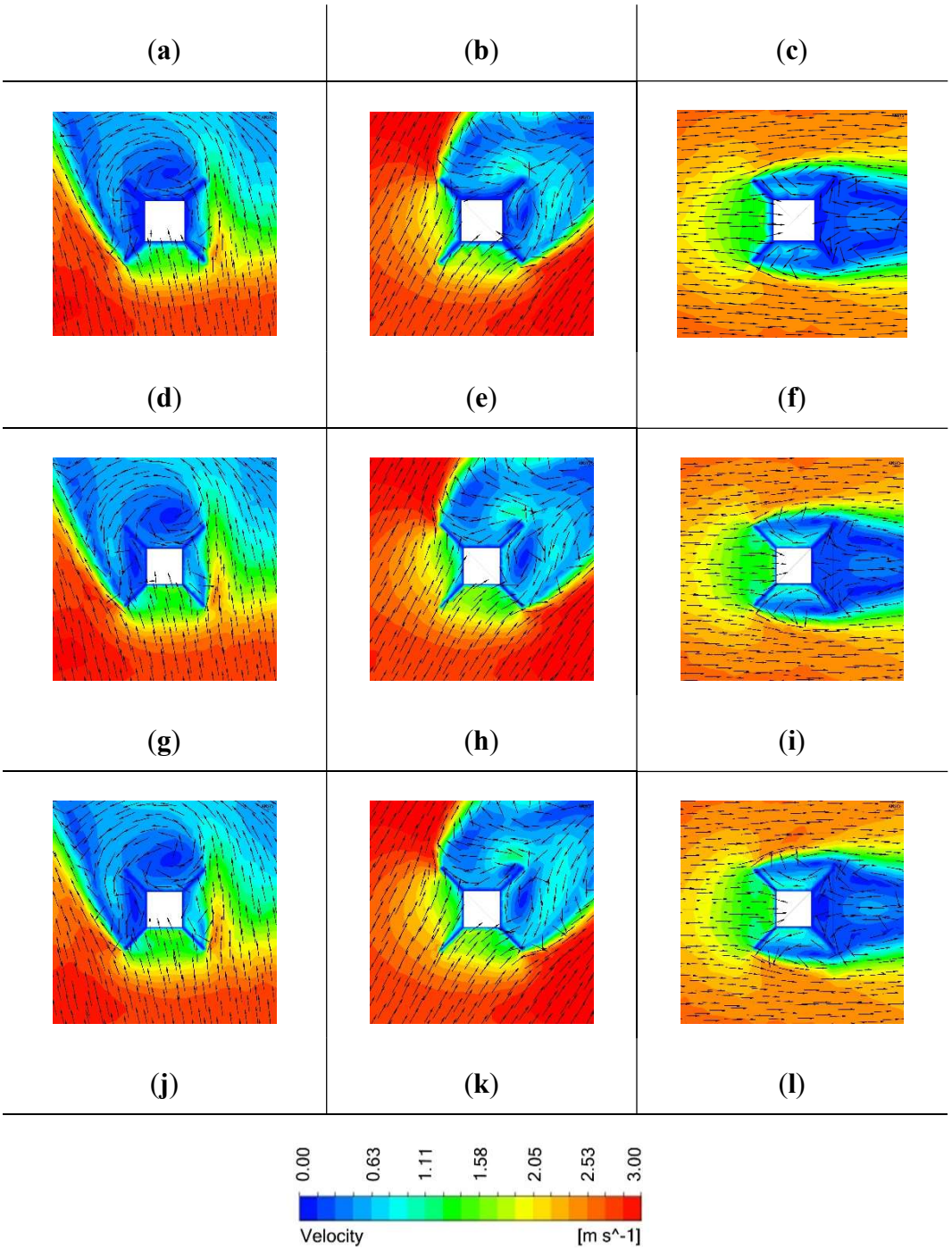

Figure 53. Representation of flow fields around the wind catcher variations by velocity color maps and normalized tangentially projected vector fields on the 1.40 m high horizontal section: (**a-b-c**) 'empty'; (**d-e-f**) 'circle', (**g-h-i**) 'parabola', (**j-k-l**) 'hyperbola' – in the following order: cross (a), diagonal (b) and longitudinal (c) wind direction.

The diagram shows clearly, that there are no significant differences in ACH in the same wind direction cases, only between different wind direction cases is a deviance up to approx. 2 ACH to observe. The best performance values were obtained with the cross direction in all four cases, followed by the 'longitudinal' direction with approx. 1 ACH decrease and the 'diagonal' cases with approx. 2 ACH decrease. The reason behind this phenomenon is that in the parallel, longitudinal case, the roof behind the wind catcher generates frictional losses (Figure 54.),

which deaccelerate the air movement at the outlet chimney's top opening, and thus the ACH becomes less effective. In contrast, higher velocities arise when the currents approach from the orthogonal direction to the building, because there is no obstacle in the proximity of the arriving air. Though in the diagonal cases (as in the cross version as well) the approaching airflow velocity of 3 m/s could be reached, less entering fresh air and ACH evolves in these cases. This is due to the wind incident angle orthogonal to the wind catchers' divider walls, and hence the air rather bypasses the geometry, contrary to the other two situations, where the diagonal walls direct the incoming fresh air to the center of the tower.

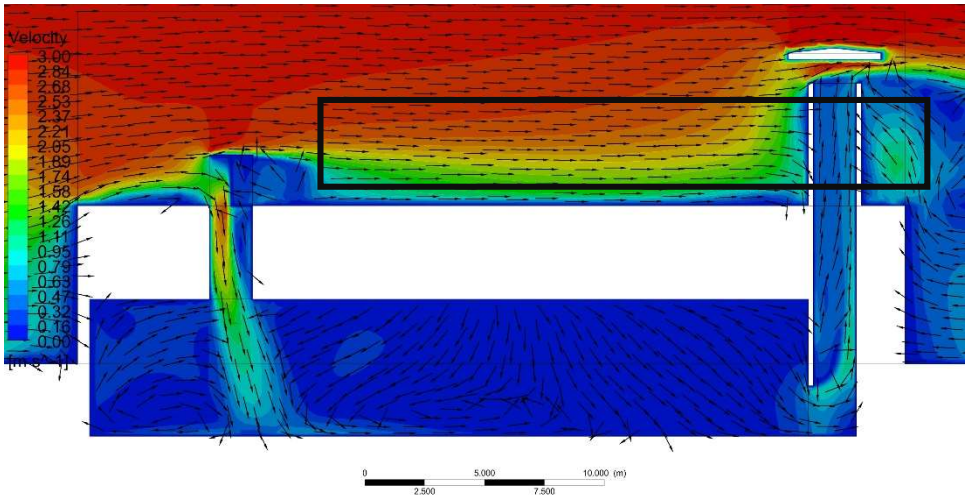

Figure 54. Air velocity color map with normalized tangential vectors on the longitudinal section of the building. The long blue and green area represents the slowed wind by the frictional losses above the roof.

By calculating the average values of the three main sample wind directions, the generic behavior of the omnidirectional inlet can be characterized. This value is in all cases approximately 7.50 h^{-1}. The only shape with poorer mean performance is the version of 'hyperbola', although the deviance is not coming from flow field's change, rather the narrowed cross section area weakens the ventilation rate. Figure 55 (j-k-l) displays distinctly, that the special shape in the chimney shaft helped to decrease the forming of detached vortices on the entering side and in the shaft, thus higher air velocity evolved inside the geometry. Similar to this, Alwetaishi et al. [104] has better air velocity performances in innovative designs of wind catchers with curved towers. However, the narrowed chimney section area was a stronger force for ACH manipulation, therefore a lower value (6.45 h^{-1}) is achieved here.

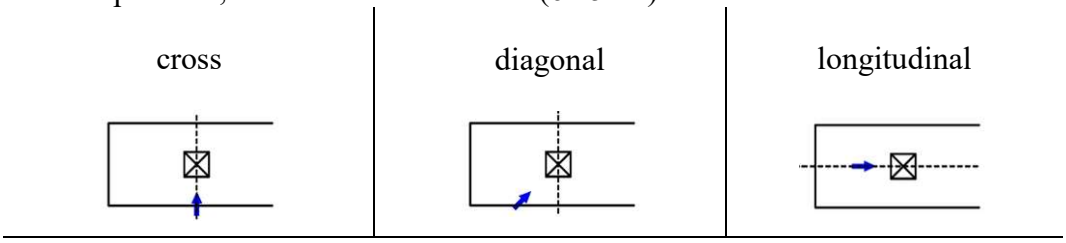

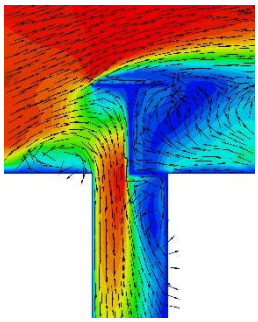	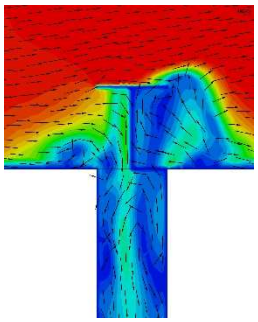	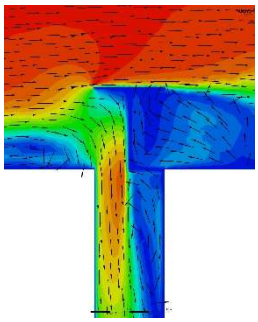
(a)	(b)	(c)
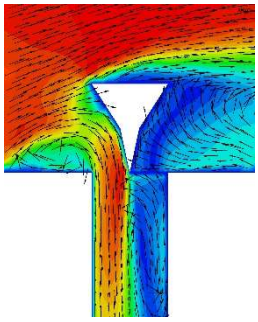	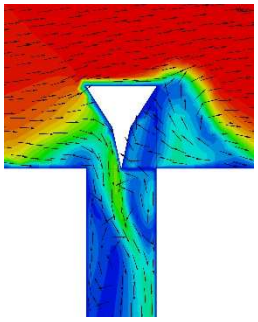	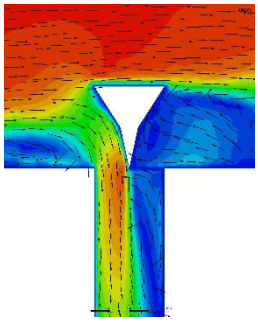
(d)	(e)	(f)
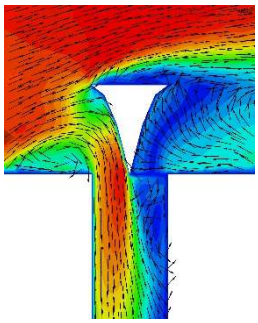	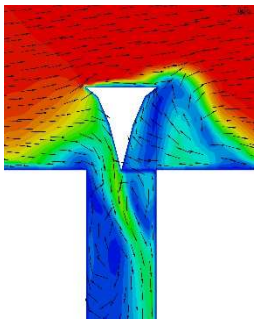	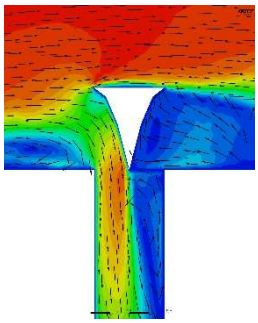
(g)	(h)	(i)
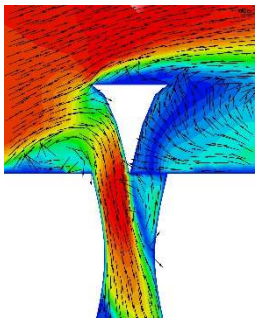	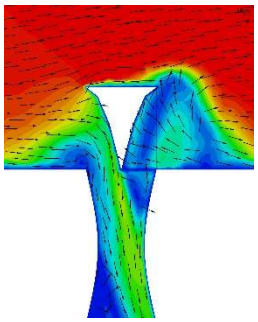	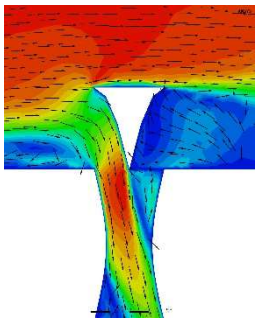
(j)	(k)	(l)

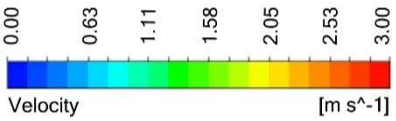

Figure 55. Representation of flow fields around the wind catcher versions by velocity color maps and normalized tangentially projected vector fields on a vertical section: (**a-b-c**) 'empty'; (**d-e-f**) 'circle', (**g-h-i**) 'parabola', (**j-k-l**) 'hyperbola' – in the following order: cross (a), diagonal (b) and longitudinal (c) wind direction

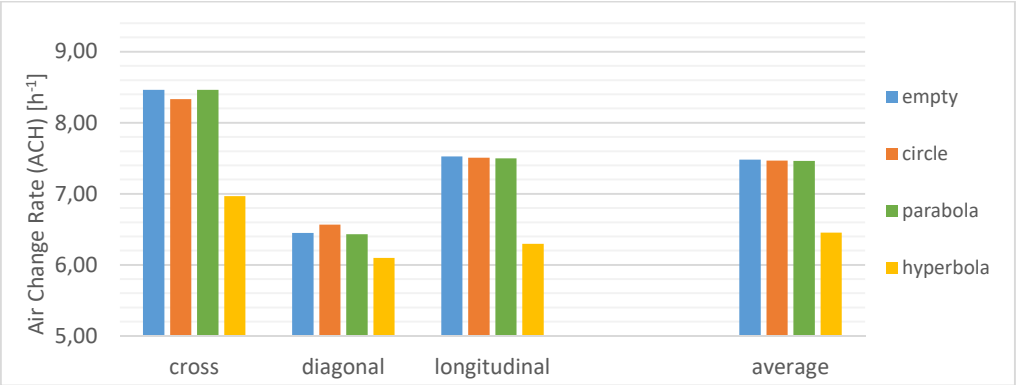

Figure 56. Comparison of the four geometry variations' ventilation performance in ACH [h^{-1}]

5.6.4. Effects of deflectors

In order to increase the 'wind collecting' mechanism of the walls, the diagonal deflectors were extended for further test. Two candidates were selected from the best performing three models, the simplest (and cost-efficient) version 'empty' as well as a curved version ('parabola'). In Figure 57 the walls have been extended in a way, where the inlet's flat roof became 1.00 m wider in all perimeter directions, enlarging the receiving inlet area of the new geometry by 211%. The original size of the diaphragms possessed 1.27 m x 2.10 m with a surface area of 2.67 m^2 in version 'empty' and it became 2.68 m x 2.10 m (surface area 5.64,^{2}) in the new shape.

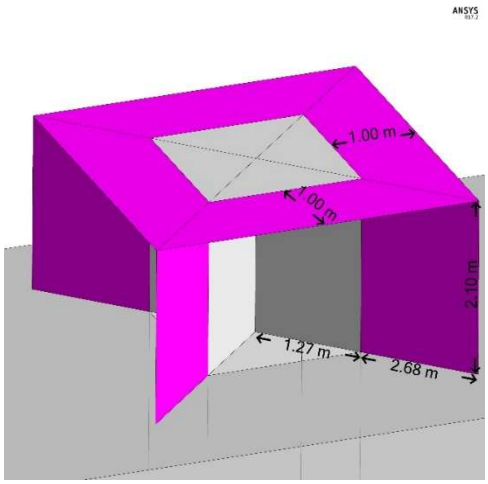

Figure 57. Wind catcher version 'empty + 1 m' (a) and 'parabola + 1 m' (b); dimensions of the enlarged sidewalls (deflectors) of the wind catcher version

In the new cases, unexpected results were obtained (Figure 58): both geometries changed their ventilation behavior with the new deflectors. Thanks to the increased deflector's area, the diagonal cases improved significantly by balancing the disadvantages of the shape: the ACH raised from 6.50 h^{-1} to 7.70 h^{-1}.

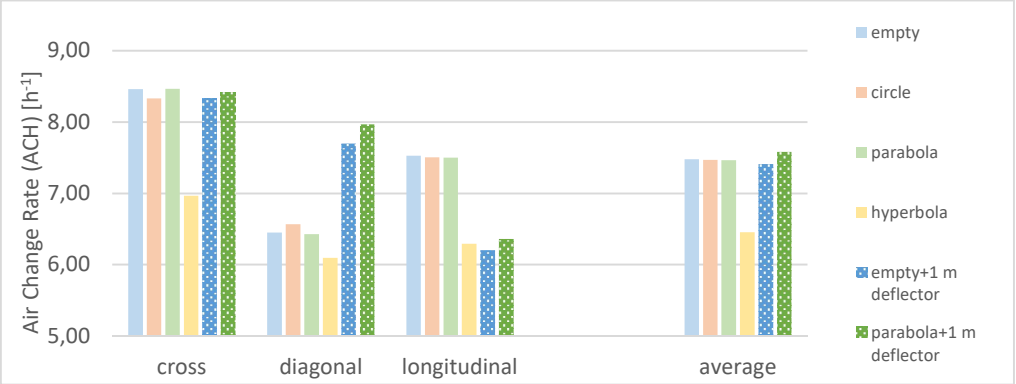

Figure 59. Comparison of geometry variations' performance in ACH [h^{-1}] with added deflectors to 'empty' and 'parabola' versions

While the cross direction's performance did not change appreciably, the longitudinal one features a considerable decrease in ACH from 7.50 h^{-1} to 6.30 h^{-1}. The source of the relapse is presented by Figure 60b and 60d in form of a backflow circulation, immediately in front of the wind catcher's inlet opening. The vortex is generated by the wider deflectors (sidewalls), i.e. the towers opening is not able to sufficiently take all the extra captured airflow. Based on this phenomenon and due to the frictional losses along the roof (see section 3.1) the velocities and thus the ACH is decreased by 16.4 %. The problematic vortices are noticeable in the cross directions as well (Figure 60.a, 60.c) but the faster air velocities can balance out here the restraining effect of the recirculation.

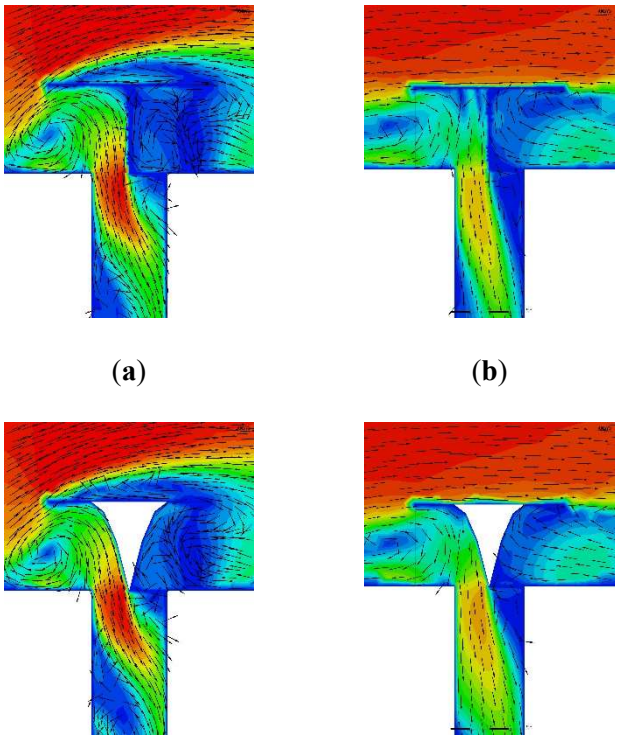

(a) **(b)**

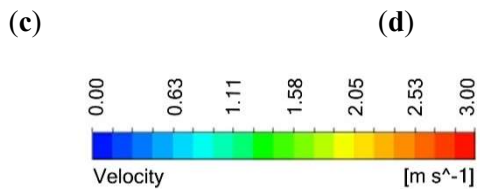

Figure 60. Representation of flow fields around the wind catcher shape variations by velocity color maps and normalized tangentially projected vector fields on the vertical section: 'empty' + 1 m deflector – (**a**) cross and (**b**) longitudinal; 'parabola + 1 m' (**c**) cross and (**d**) longitudinal direction

5.6.5. Modified deflector design

While the performance in the cross direction remained (together with the average ventilation rates – see Figure 59), and the diagonal direction is improved, in longitudinal direction the decreased ACH made further modification on the deflectors necessary. Figure 61 presents the modified topology, where the diagonal sidewalls' bottom part was diminished. The receiving inlet area of the new geometry is reduced b/ 26,46 % and the new surface area of 4.15 m2 in the new shape. The created 'gap' should allow the congested air to bypass the geometry, and lower the chance of arising backflow vortices around the inlet opening.

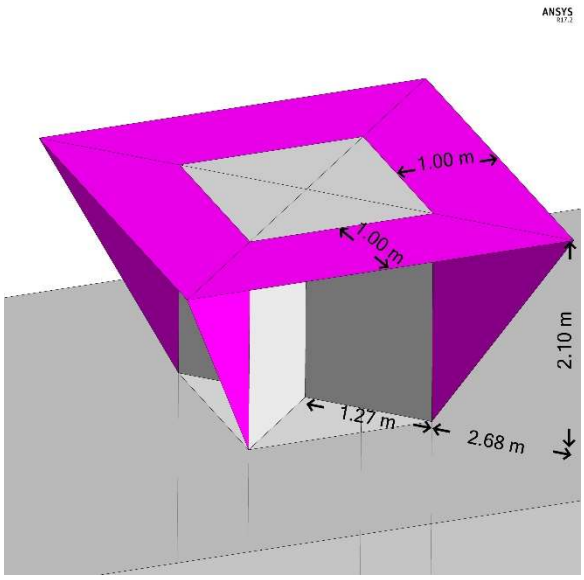

Figure 61. Wind catcher version 'empty +1m'; dimensions of the enlarged sidewalls (deflectors) of the wind catcher version 'empty'

Figure 62 visualize the resulted airflow and Figure 63. displays the obtained ACH performance of the wind catcher development. The accomplished ventilation rates are significantly better compared to the initial topologies, delivering an average advancement of 11.5%. The developed deflectors not only improved the average performance, but they produce in both cross, diagonal and longitudinal directions a visible enhancement of 9.6 %, 22.1 % and 20.2 % to the worst cases, respectively. The average 'parabolic' (8.34 h^{-1} ACH) and 'empty' (8.16 h^{-1} ACH) inlet structure versions' ventilation efficiency was improved by 9.1 % and 11.8 %, respectively. The diagonal scenarios did not bring any change to their previous version, but fundamentally, it is a good outcome, since the improvement in the diagonal direction is already achieved in the previous test. Instead of hindering the evolution of the ACH rates by the smaller deflector

surface, they rather ensured a greater inflow, as the counterproductive recirculating vortices could laterally bypass the structure.

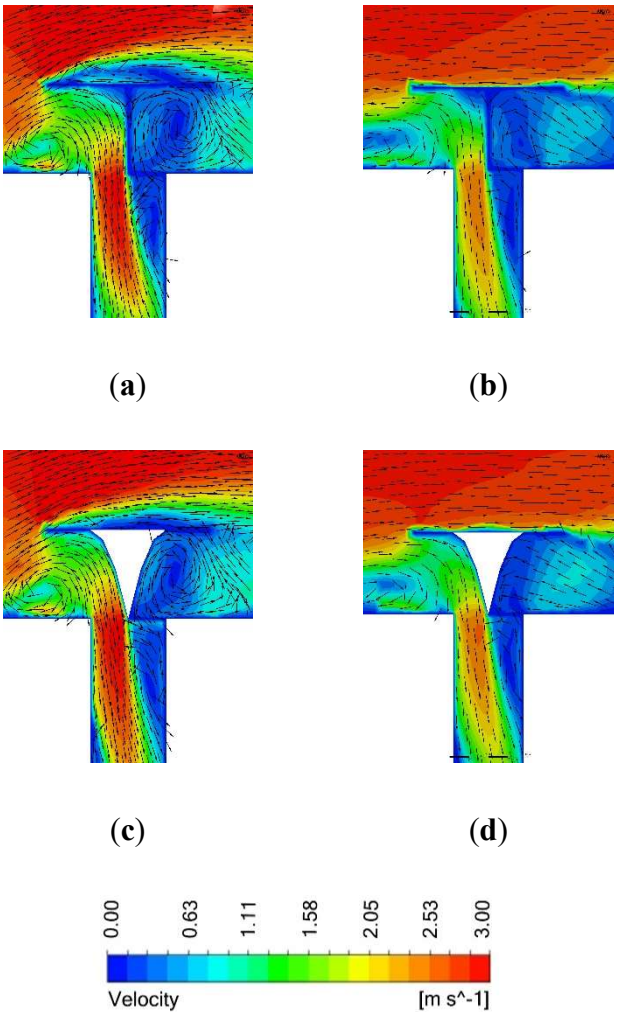

Figure 62. Representation of flow fields around the wind catcher shape variations by velocity color maps and normalized tangentially projected vector fields on the vertical section: 'empty' + modified deflector – (**a**) cross and (**b**) longitudinal; 'parabola + modified deflector' (**c**) cross and (**d**) longitudinal direction.

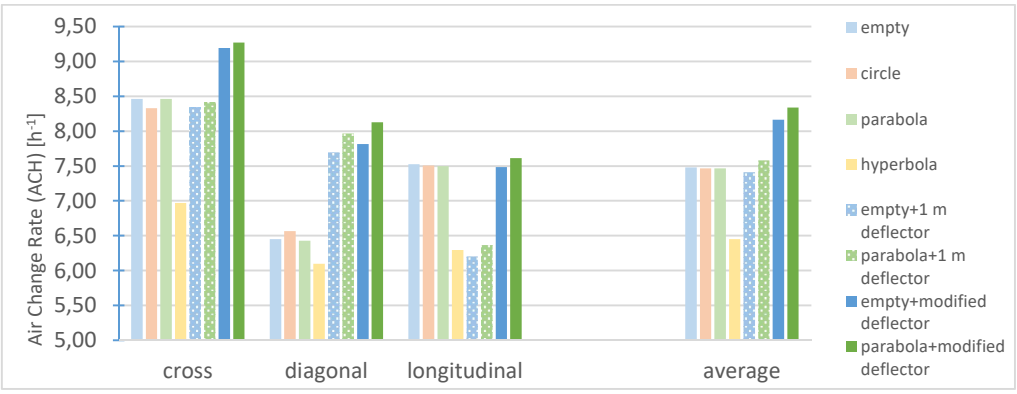

Figure 63. Comparison of geometry variations' performance in ACH [h^{-1}] with the modified deflectors of the 'empty' and 'parabola' versions

The tested tower has smaller dimensions compared to general wind catchers [49,64,105] as well as compared to a previous study of mine [90], where the ventilation chimney cross section was oversized (5.20 x 4.90 m) and hence a counterproductive lateral distribution of the airflow's kinetic energy was developed in the tower. Due to the downsized particular chimneys' cross section area, the lateral vortices are not present in the flow field of the chimneys anymore and hence a more efficient ventilation performance is achieved. (Figure 64.)

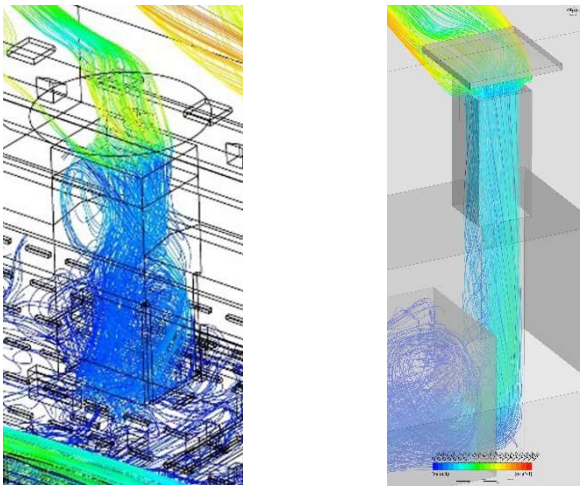

(**a**) (**b**)

Figure 64. Streamline visualization of the stale air's passive extraction via the venture tower: (**a**) My former study showed the possible energy loss inside an oversized wind tower via vortices [90], (**b**) The proposed geometry ratios in this studies avoided the unintentional energy loss, and the stale air has a straight upward movement

The unexpected poor performance from the 'hyperbola' (Figure 49d) version is coming from the reduced cross sectional area of the tower. However, it is easy to identify in the results (Figure 53j, 53k, 53l) that the hyperbola shape decreased the aerodynamically ineffective area in the chimney shaft and in this way higher inner velocities and less detached vortices were generated in the tower. However, the smaller cross section became contra productive, and overwrote the mentioned improvement. Nevertheless, the 'hyperbola bell' should not be devoted after these results, but a more focused study on this promising inner chimney shaft design could be conducted about the synchronization of the hyperbola's parameters and the correct use of this version [106].

In case of wind direction diagonal to the longitudinal axis of the building, the geometries performed generally poorly. The reason behind this phenomenon is the orthogonal position of the deflectors to the coming wind direction, as opposed to the other two situations, where the wind catchers' inner walls collect fresh air with a 45° incident angle on both sides. The high incident impinge angle on the deflectors'' surface lets evolve turbulences, which bypass the inlet structure instead of entering the ventilation opening (Figure 53 b-e-h-k). To avoid this problem, further modifications should be considered, such as multiple (e.g. eight) sectioned tower [49], or more specialized deflector wall shapes as this study's results suggests or even moving (automated) deflectors according to the incoming wind current incident angles (wind direction independency) [11].

In case of the longitudinal direction, the negative behaviors of the passive towers – mentioned by Mohamadabadi's study [60] – could be avoided, due to arranging the chimneys

in greater distance from each other in particular wind direction. The gained ACH values are still the lowest in this direction, however this is solely due to the roof structure caused frictional forces, which are more or less unavoidable in a building situation.

The concept of extended deflector walls of 1 m were intended to capture more incoming fresh air in the wind catcher. It was applied to the 'empty' and 'parabola' shapes, to follow their effect, not just on the general ACH values, but also to see the relations between the alternating geometries. The first test unexpectedly did not modify significantly the averaged performance but the new PACS element behaved differently in the three directions. In the longitudinal situation, the performance dropped, and the visualization of the flow field helped to recognize the generated vortices ahead of the wind catcher's opening. The wider deflectors captured more air at the front of the tower opening, but the inlet opening's area remained the same size, hence a backflow was formed from the congested air, and it has restrained the ventilation by bypassing the wind catcher's deflectors. This results the reduction of incoming fresh air into the inlet tower and hence less ACH performance. In addition, due to roof generated deaccelerating frictions, in this wind direction the ventilation velocities were lower. The recirculation vortices evolved in the cross direction as well, but as it was the case in the first shape test, the cross directed wind could remain faster around the wind catcher. Therefore, the bigger momentum of the incoming air could balance out the negative effect of the vortex, and there was no negative change in the ventilation performance. Under diagonal wind incident angle where specifically the capturing surface was missing in the starting geometries, the deflectors achieved a significant improvement. The obtained results create cohesive experiences about wind catcher geometries with contemporary studies [78,79].

The inclined reduction of the deflectors' shape was proposed to enforce air flow to bypass the wind catcher at its plinth zone (and hence reduce recirculation and ACH reduction), if the resistance from the inlet openings raise critically. The ACH values increased almost 11.5% compared to the initial models. Both cross and longitudinal directions performed better, proving that the forming of restraining vortices were reduced with the proposed geometry.

Limitations

The simulations were solved within an isothermal model, meaning that no energy equations were calculated. The performance of NV is always influenced by the outdoor temperature, occupancies' and solar heat sources and other pressure differences. The consideration of these factors are planned to be carried out in next research step. In the future, it is favorable to examine the role and relation of thermal buoyancy to these wind catcher variations, and other topics of IAQ, such as draught rate, relative humidity or air contaminant distribution.

The target of this study was to find a maximized ACH producing wind catcher topology under strict boundary conditions, and during this optimization process, eventually too high velocities of exiting air from the inlet tower were no considered as a comfort factor. This is due to the fact that in the winery technology hall is a non-continuous occupied space (i.e. during the wine harvesting season, approx. 1.5 month in a year continuous work, otherwise only non-continuous use). During occupied periods, automated dampeners manipulate the incoming airflow rate to ensure comfortable conditions. However, NV solutions need to serve incredibly complex demands with large amount of variables (wind velocity and direction dependent, temperature and humidity dependent as well as anti-draught effect related operation) thus, to map out this complicated synchronized operation of a PACS is a difficult future task.

The generated atmospheric wind profile represented a rural, agricultural (mostly empty) site. Hence, the research cannot give insights about the behavior of the selected topologies in a dense city or other complicated environment with an unstable, more turbulent flow. Additionally, due to the not densely occupied agricultural hall, further investigation in more intensely occupied spaces (office atrium, event hall, sport hall, etc.) would provide useful insights. The modeled

building function gives information about only one segment of buildings (agricultural, industrial) and research in other building typology shows great potential to complete the knowledge on NV systems.

5.6.6. Conclusions of the micro level geometry optimization

Scientific research emphasizes repeatedly the urgent need to reduce the energy consumption in our built environment. The application of NV solutions can result significant energy savings, and in certain climate zones the maintenance is almost possible during the whole year. The available work in the field of PACS geometry optimization shows experiences, according to which NV options have extraordinary complicated aerodynamic properties. Hence, it is inevitable to conduct further research about PACS's topology, to deepen the general, reasonable knowledge about their aerodynamic behavior.

This phase connects organically to my previous work [80], where the direction of the air conduction of the PACS was investigated and a DD system was developed as a multi-directional solution for NV. This study tries to answer to the following questions: Is it possible to enhance the ACH rate of the already developed DD PACS and if yes to what content? How should the inlet structure's shape look like in the previously developed DD PACS, in order to provide as efficient wind capturing as possible? The relation to the previous work [80] was favorable, because within these tests a previous CFD model was adequately compared with the validated CFD model of an in-situ measured, real-world building [90]. Thereby, the experiences in CFD simulation techniques of mine previous studies were applied here. The main implications of this research expand successfully the knowledge in the field, and create a good foundation for further studies about wind catchers:

The shape and size of the building body around the wind catcher can highly influence the flow field around the wind catcher and its air capturing performance. If the in- and outlet structures of the PACS are aligned in line with each other, the cross directed wind - unaffected from the building body - can enter with highest efficiency into the wind catcher structures' inlet. In longitudinal direction the roof surface behind the wind catcher generates frictional losses and notably lower velocities at the exhaust tower's outlet and hence a decrease of the vent-performance. Therefore, weaker ventilation is present under such circumstances in every construction situation. This lower vent-performance can however still provide appropriate or even higher vent-rates (in particular study an ACH of 7.5 h^{-1} was provided, an 846% greater performance as it is required in EN 15215 [62].

The developed small sized wind catchers (smaller than generic, traditional wind catchers [49,64,105]) possess a floor area related PACS ratio of 2.43% and a volumetric PACS ratio of 5.55%. This cross section represents a small-scale inlet structure solution in contrast to a previous measured real-world project [90] with a floor area related PACS ratio of 10% and a volumetric PACS ratio of 30%. A future classification of the diverse historical and contemporary PACSs could rationalize design and development of such ventilation systems.

The topology development confirms that small-scale wind catchers are less responsive to different shape changes regarding their role in the ACH rate distribution of the PACS. The very similar ventilation air flow values (7.50 h^{-1} ACH) of most shapes (three basic geometries) in this study supplement Pearlmutter et al. [106] outcome: while ventilation efficiency rates show similar differences between different inlet geometries, by downscaling the cross section of an inlet chimney, the wind catcher's ventilation performance becomes less sensible to different geometry types in contrast to larger chimney cross-sections.

A V-shaped layout of vertical deflector walls influence positively the air capturing ability of a wind catcher's inlet structure in case of facing the approaching wind direction (in particular study: cross direction). If the incident angle of the coming wind flow to the deflector surfaces

increases, the ventilation rate decreases (particularly with 2 1^{-h} ACH) due to unwanted impinging turbulences.
A wind direction independent, roof integrated ventilation inlet structure is developed for a DD PACS. Through significant upsizing the wind catchers' deflector walls (in this study by 211%) by simultaneously keeping the same inlet opening dimensions, improvements in ventilation rate occur when the wind incident angle to the deflector surfaces are high, i.e. in this study significant increase of ACH is only in certain wind directions delivered (almost 100% vent-increase in diagonal direction). If the capturing surfaces are in a lower incident angle with the coming wind, counterproductive turbulences enforce reduced ACH performance. In order to gain improvements in all directions, the enlarged deflectors' lower part should be trimmed back to the initial inlet opening edge. In that way, significant improvement could be achieved in all wind directions (in this study a mean increase of approx. 1 ACH is achieved).

Finding 4.1

The micro scaled optimization of a Passive Air Conduction System's component, delivers as significant improvements for the ventilation performance, as the macro scaled systematic design of a complete PACS sizing procedure. Based on the obtained results of a complex geometry improvement process, the ventilation rate can be even increased by 25%. Therefore, the micro-optimization is suitable not just newly designed buildings, but it creates a high impact solution for existing buildings' Passive Air Conduction System's refurbishment or equipment as well.

Even with enlarged and optimized capturing deflector walls, the shape independent vent-behavior of wind catcher versions remained. The 'parabola + 1 m' version had only a slightly better mean performance than the 'empty + 1 m' wind catcher versions (2.1%), but the small improvement can possibly not compensate the difficulty of the more complicated construction.

Finding 4.2.

The wind catcher's geometry variations' results in air change rate converge with the downsizing of the ventilating tunnel's cross section area. Therefore, there is a minimum limit for micro scaled optimization of PACS components, where the extra cost in design, money and construction is overstepping the gains of the optimized geometry.

Even if dimensions of a wind catcher are specified by general experiences, and those should positively influence the performance, sometimes unexpected behavior can occur, because aerodynamic systems react in a complex way to design changes. This is in accordance with the conclusions of Varela-Boydo et al. [79] and Zarmehr et al. [66]. To understand fundamentally pressure difference driven PACS, a wide and thorough knowledge is essential, where the parameters are investigated organically.

5.7. New approach – parametric design-optimization

The main objective of the research was to investigate the parametric sensitivity of the geometric dimensions of a building structure suitable for passive ventilation. This is to be understood as the exhaust vents of tower-like structures built on top of industrial halls. So-called 'Venturi' baffles are placed above the tower structures (Figure 54), under which the pressure of the accelerating air mass in the constricted flow cross-section is reduced, creating a depression zone, during which, by opening the exhaust towers, the extraction of the stale air inside can be increased, and this in a completely natural way by means of wind. [43,54]

Figure 54. Practical application of Venturi plates at the production hall of RATI Ltd. in Komló

In this research, I have taken as a basis a typical reinforced concrete hall structure, where a large internal air mass is developed in the cross-section and this typical cross-section does not change significantly in the longitudinal direction (Figure 55). This characteristic of the hall allowed me to perform the CFD simulations of the flow, which can be used to optimally calculate the properties of a ventilation system without the aid of physical models (which are costly and time consuming) [14], using a two-dimensional simplification. This solution saves a lot of computational capacity, which I could use in this case to not only consider two variants in my research, but to evaluate all combinations of certain parameters and their combined effect on the whole system. In this case, I chose three main parameters so that their combinations represented 3x3x3=27 cases in the research.

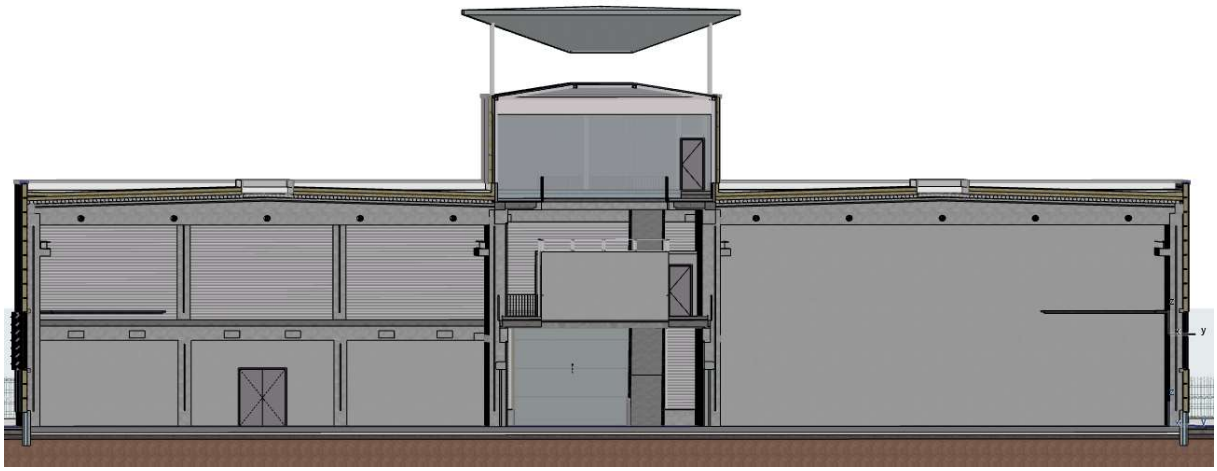

Figure 55. Cross-section of the sample building - right and left with large open hall spaces.

The three main parameters were the height, the width and the angle of the decompression zone (Figure 56). The main significance of the research is that the combination options outlined above show very little variation in terms of design, so they do not change the budget significantly. Thus, with design effort alone, we hypothesize that a significant performance improvement could be achieved, thus increasing the efficiency of natural ventilation and thus reducing the energy consumption of the building - leading to both financial and environmental savings.

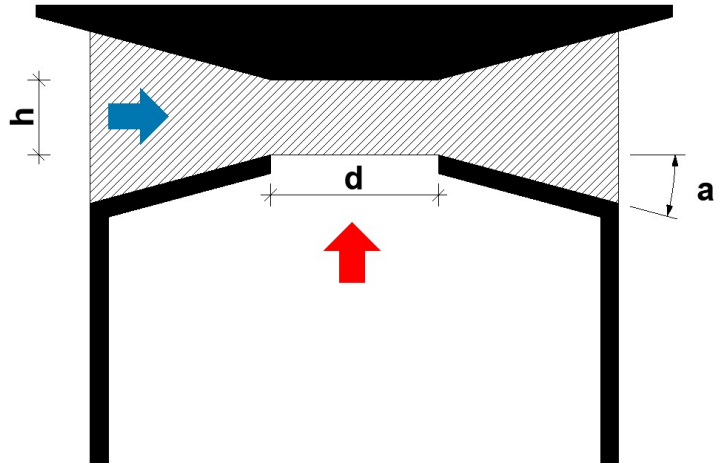

Figure 56 - Visual representation of the decompression zone, where h = the height of the zone, d = the width, a = the angle of contraction. The blue arrow indicates the wind direction, while the red arrow indicates the internal stale air.

5.7.1. The results of the parametric approach of the micro level modifications

The results of the research are scientifically valuable for two reasons. The first reason is that a clearly optimal solution has been found within the boundary conditions of the given parameters, making the method presented here suitable for industrial use. (Figure 57) It can be easily adapted to the optimization of structures under the conditions that arise in a given design task and, by analogy, under the conditions defined by other design criteria.

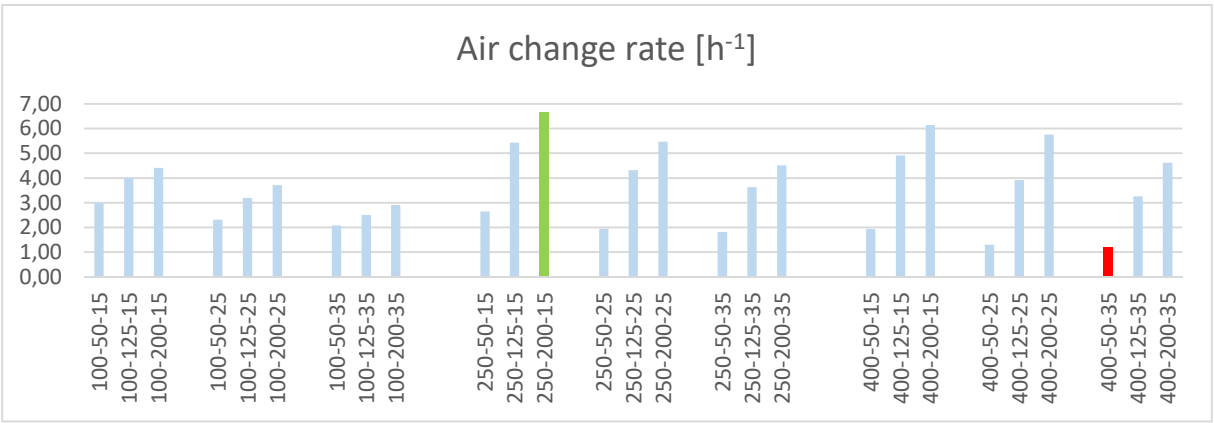

Figure 57 - Comparison of the ventilation capacities of the 27 cases studied using the air exchange rates obtained [h^{-1}]

The second main result of the research is that conclusions can be drawn about the impact of all three parameters on ventilation:

- the width of the zone (100; 250; 400 cm) - where the comparison shows an ideal middle ground, as both extremes performed worse than the mean.
- zone height (50; 125; 200 cm) - where the clear trend is that the higher the compression zone, the more effective the ventilation. However, the present results require that further values are added to the parameter scale to show how long this increase lasts and what optimum can still be achieved.
- the angle of compression of the zone (15; 25; 35°) - where the trend is also clear, namely that performance decreases as the angle increases. It would be equally worthwhile to further extend the range of parameters to determine the optimum.

Finding 5.

The parametric approach of Passive Air Conduction System optimization has great potential in the field of industrial buildings' passive ventilation. Compared to a conventional planning solution, with the generated 3x3x3 parametric matrix the ventilation performance of the determined ‚Venturi' structure's compression zone increased up to 544%. A scientifically thorough generated parametric matrix can point out the most effective version of a Parametric Air Conduction System's geometry in any given boundaries.

The simulations were run in 2D, because even with simple parameters the evaluation process is largely time consuming, and the building characteristics made this 2D approach possible. Future studies need to develop a method to solve the time factor for more complex situations.

The above cases therefore do not yet provide generalizable optimal operating principles, but they do present a generalizable optimization process for specific design cases. Furthermore, clear trends can be identified on the influence of different parameters on the efficiency of the overall structure. This will facilitate the definition of trajectories for similar research in the future.

I see potential for future research in two main directions: one is to investigate the parameters identified here in more depth at finer steps, thus obtaining a more accurate picture of the optimal maxima of a given parameter, and even to include additional parameters in the study (e.g. Another research option is to compare the results with 3D models, since in reality the wind direction can often deviate from the typical or ideal perpendicular incidence angle, so that in other cases different flow patterns can be obtained, either positive or negative.

6. Outlook

Due to the lack of PACS variation assessments in literature, it can be stated that not only the different NV systems need more evaluation, but also the optimization of a chosen method is also difficult, because of the lack of appropriate quantity and quality of results. Therefore, in future studies it would be rewarding to investigate different aspects of individual PACS with a parametric method to obtain the optimum version(s) of all feasible designs. Possible parameters are, for instance, geometrical variations of the inlets and outlets, the 'Venturi'-objects or the inlet chimney crowns—e.g., height, cross-section, shape, number, arrangement, and the relative positions to each other, etc., such as in the work of Nejat et al. [107] about the effect of wing wall parameters on a wind catcher. In the next step of this series of investigation, the wind tower and wind catcher geometries will be tested through a comprehensive parametric method (Figure 58). Sakiyama et al. [108] presented a similar approach for NV evaluation with CFD.

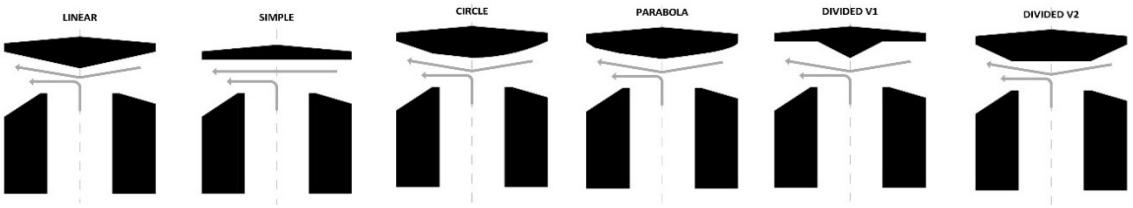

Figure 58. Optional next step of optimization a PACS – multiple geometry scenarios for partial development.

Since a PACS should not only produce as much fresh air as possible but needs to ensure other comfort aspects also, further factors such as humidity and temperature should be considered in future studies as well (see *Limitations* sections). Another interesting investigation scenario would be to combine the used PACS with an evaporative cooling system, representing a financially and technically sustainable solution, as is stated in Soltani et al.'s work [109]. Ghoulem et al. [110] worked on greenhouses, including a downdraught evaporative system, achieving up to 13.3 °C cooling effect in a hot and dry climate. By substantiating the obtained and concluded knowledge, a new guideline should be written from the experiences for architects and NV designers in the future.

In section 6.6. The 'Parabola + modified deflector' version was chosen by the project's contractor, as the most efficient alternative among the tested inlet structure shapes. The airflow velocities will be measured via constant temperature anemometer (CTA). The monitored building is intended to serve as a validation testbed for the CFD simulations as well as to ensure a well-functioning operation of the PACS.

For future research, a challenge will be the complex investigation of geometry parameters, where the dimensions are not separately tested, but their permutations as well. The difficulties come from the numerous generated variations. If only a simple wind catcher is taken for examination, at least four basic parameters are required to calculate (e.g. height, width, tower section separation by deflectors, geometrical shape of the inlet surface, etc.), and for the acceptable fine trends further three to four variations of each parameter should be calculated. It means that a simple series of CFD simulations start with a minimum of $4^4 = 256$ cases, consuming a huge amount of calculation time. Despite of the amount of permutations, to find the financial and energy efficient wind catcher version for a large variety of situations, the mapping of the aerodynamic optimum is indispensable in the future.

Valuable information is missing in the field about the topology's influence on IAQ values. PACSs are intended to improve the indoor comfort of our spaces, therefore, the performance of a wind catcher should not only be measured by volume flow, but other aspects, such as temperature, humidity, draft effect, contaminants, etc. are needed to be considered as well. It is necessary to analyze these variables of the scientifically selected geometries, to locate difficulties and suggest new modifications if needed to avoid local discomfort.
In the base model of this research, the stale air was exhausted by a 'Venturi' tower, with help of a so called Venturi plate that was located on top of the tower. It created a low pressure zone just above the outlet's opening, which helped to extract exhaust air from the interiors. A further investigation could also provide valuable information about the use of the Venturi-effect in PACS, specifically because it is a less recognized tool from NV engineers.
The above-mentioned geometry optimizing future research tasks should generate a generic dataset system of shape dimension parameters for engineers to enable efficient ventilation design.

6.1.1. The promising unified Energy Design Synthesis theory

For future research, a challenge will be the complex investigation of geometry parameters, where the dimensions are not separately tested, but their permutations as well. The difficulties come from the numerous generated variations. If only a simple wind catcher is taken for examination, at least four basic parameters are required to calculate (e.g. height, width, tower section separation by deflectors, geometrical shape of the inlet surface, etc.), and for the acceptable fine trends additional three to four variations of each parameter should be calculated. It means that a simple series of CFD simulations start with a minimum of 4^4 = 256 cases, consuming a huge amount of calculation time. Despite of the number of permutations, to find the cost and energy efficient wind catcher version for a large variety of situations, the mapping of the aerodynamic optimum is indispensable in the future.
The above-mentioned geometry optimizing future research tasks should generate a generic dataset system of shape dimension parameters for engineers to enable efficient ventilation design.
The following text is written by Horváth [16] in his Ph.D. dissertation.

"[…] Today's traditional building design method is not sufficiently focused on energy-optimal performance due to a heuristic experience-based process. The general mindset in conventional building design ignores building geometry as one of the most integrated energy efficiency related variables in the design phase, further, usually only a few number of scenarios are considered, and therefore planning decisions are based on experience. The Energy Design (ED) method is more systematic/regulated and has created a framework for the design process, using more concepts of energy performance, as well as simplified calculations and simulation-based decision making. A new methodology was needed because the standards are not comprehensive and are not sufficient to create comfortable, energy efficient buildings and thus an environmentally conscious and sustainable future. The Energy Design Synthesis (EDS) method is an enhanced version of ED, which aims to provide a comprehensive solution and a guaranteed optimal building development. EDS involves the creation of efficient rules for detecting feasible and possible cases of an objective function by minimizing the amount of sampling and thus minimizing the computational time cost. It identifies the optimal solution(s) according to a predefined set of user preferences for energy and comfort performance. It follows that the Energy Design Synthesis Method will be able to deliver better results than the Energy Design Method, taking into account the above-mentioned aspects. […]"

The presented EDS is the upgraded version of the ED method, where – as it is shown in section 3.1 – non optimal but reliable solutions are designed, but not optimized. The new EDS

offers a huge opportunity for preprocessing in the PACS designing method, because of the huge computational requirements every bit of time and energy saving scan improve the optimization process. The EDS method's key element is the development of a regressive solution finder model, where all mathematical option is taken into account, and not just the 'thumb rule' solutions are chosen by the designer, where the engineer's scientific competency is defining the success. This kind of general thinking without any prejudice can be really useful for complex aerodynamic systems' evaluation. However, the hugest impact of the regressive model is the time saving, because it can calculate all the versions potential with only a few input scenarios dataset, therefore the mentioned 44=256 cases do not need to be simulated manually one by one. This time efficiency is barrier for current simulations.

7. Bibliography

[1] Conclusions adopted by the European Council meeting. EUCO 169/14 On The 2030 Climate and Energy Policy Framework, 2014. http://data.consilium.europa.eu/doc/document/ST-169-2014-INIT/en/pdf.

[2] M. Hamdy, A. Hasan, K. Siren, Applying a multi-objective optimization approach for Design of low-emission cost-effective dwellings, Build. Environ. 46 (2011) 109–123. https://doi.org/10.1016/j.buildenv.2010.07.006.

[3] P.F. Linden, The fluid mechanics of natural ventilation, Annu. Rev. Fluid Mech. 31 (1999) 201–238. https://doi.org/10.1146/annurev.fluid.31.1.201.

[4] Z. Tong, Y. Chen, A. Malkawi, Z. Liu, R.B. Freeman, Energy saving potential of natural ventilation in China: The impact of ambient air pollution, Appl. Energy. 179 (2016) 660–668. https://doi.org/10.1016/j.apenergy.2016.07.019.

[5] G. Chiesa, M. Grosso, D. Pearlmutter, S. Ray, Advances in adaptive comfort modelling and passive/hybrid cooling of buildings, Energy Build. 148 (2017) 211–217. https://doi.org/10.1016/j.enbuild.2017.05.012.

[6] S.D. Ray, N.W. Gong, L.R. Glicksman, J.A. Paradiso, Experimental characterization of full-scale naturally ventilated atrium and validation of CFD simulations, Energy Build. 69 (2014) 285–291. https://doi.org/10.1016/j.enbuild.2013.11.018.

[7] J.M. Holford, G.R. Hunt, Fundamental atrium design for natural ventilation, Build. Environ. 38 (2003) 409–426. https://doi.org/10.1016/S0360-1323(02)00019-7.

[8] B.R. Hughes, C.M. Mak, A study of wind and buoyancy driven flows through commercial wind towers, Energy Build. 43 (2011) 1784–1791. https://doi.org/10.1016/j.enbuild.2011.03.022.

[9] Y. Li, P. Heiselberg, Analysis Methods for Natural and Hybrid Ventilation - a Critical Literature Review and Recent Developments, Int. J. Vent. 1 (2003) 3–20. https://doi.org/10.1080/14733315.2003.11683640.

[10] M. Liddament, J. Axley, P. Heiselberg, Y. Li, T. Stathopoulos, Achieving natural and hybrid ventilation in practice, Int. J. Vent. 5 (2006) 115–130. https://doi.org/10.1080/14733315.2006.11683729.

[11] N. Khan, Y. Su, S.B. Riffat, A review on wind driven ventilation techniques, Energy Build. 40 (2008) 1586–1604. https://doi.org/10.1016/j.enbuild.2008.02.015.

[12] M. Mora-Pérez, G. López-Patiño, P. Amparo López-Jiménez, Quantification of Ventilated Façade Effect Due to Convection in Buildings Buoyancy and Wind Driven Effect, Res. Appl. Mech. Eng. 3 (2014) 1–11. http://www.seipub.org/rame.

[13] N.S. Bunkholt, T. Säwén, M. Stockhaus, T. Kvande, L. Gullbrekken, P. Wahlgren, J. Lohne, Experimental study of thermal buoyancy in the cavity of ventilated roofs, Buildings. 10 (2020) 1–18. https://doi.org/10.3390/buildings10010008.

[14] Q. Chen, Ventilation performance prediction for buildings: A method overview and recent applications, Build. Environ. 44 (2009) 848–858. https://doi.org/10.1016/j.buildenv.2008.05.025.

[15] F. Kuznik, G. Rusaouën, J. Brau, Experimental and numerical study of a full scale ventilated enclosure: Comparison of four two equations closure turbulence models, Build. Environ. 42 (2007) 1043–1053. https://doi.org/10.1016/j.buildenv.2005.11.024.

[16] M. Tapsoba, J. Moureh, D. Flick, Airflow patterns inside slotted obstacles in a ventilated enclosure, Comput. Fluids. 36 (2007) 935–948. https://doi.org/10.1016/j.compfluid.2006.04.002.

[17] P. Rohdin, B. Moshfegh, Numerical predictions of indoor climate in large industrial premises. A comparison between different k-ε models supported by field measurements, Build. Environ. 42 (2007) 3872–3882. https://doi.org/10.1016/j.buildenv.2006.11.005.

[18] L. Zhao, X. Wang, Y. Zhang, G.L. Riskowski, Analysis of airflow in a full-scale room with non-isothermal jet ventilation using PTV techniques, in: ASHRAE Trans., Dallas, 2007: pp. 414–425.

[19] G. Kristóf, B. Papp, Application of GPU-based large eddy simulation in urban dispersion studies, Atmosphere (Basel). 9 (2018). https://doi.org/10.3390/atmos9110442.

[20] H.B. Awbi, Air movement in naturally-ventilated buildings, in: World Renew. Energy Congr., Denver, USA, 1996: pp. 551–556. https://doi.org/10.1016/0960-1481(96)88855-0.

[21] Q. Chen, Z. Zhai, The use of Computational Fluid Dynamics tools for indoor environmental design, in: A.M. Malkawi, G. Augenbroe (Eds.), Adv. Build. Simul., Spon Press, New York, 2003: pp. 119–140. https://doi.org/10.4324/9780203684009.

[22] Y. Tominaga, A. Mochida, R. Yoshie, H. Kataoka, T. Nozu, M. Yoshikawa, T. Shirasawa, AIJ guidelines for practical applications of CFD to pedestrian wind environment around buildings, J. Wind Eng. Ind. Aerodyn. 96 (2008) 1749–1761. https://doi.org/10.1016/j.jweia.2008.02.058.

[23] S.E. Norris, P. Richards, Appropriate boundary conditions for computational wind engineering models using the k-ε turbulence model, in: Fifth Int. Symp. Comput. Wind Eng., Chapel Hill, North Carolina, USA, 2010: pp. 145–153. https://doi.org/10.1016/0167-6105(93)90170-s.

[24] M. Hajdukiewicz, M. Geron, M.M. Keane, Calibrated CFD simulation to evaluate thermal comfort in a highly-glazed naturally ventilated room, Build. Environ. 70 (2013) 73–89. https://doi.org/10.1016/j.buildenv.2013.08.020.

[25] M. Hajdukiewicz, M. Geron, M.M. Keane, Formal calibration methodology for CFD models of naturally ventilated indoor environments, Build. Environ. 59 (2013) 290–302. https://doi.org/10.1017/CBO9781107415324.004.

[26] A.A. Elmualim, Effect of damper and heat source on wind catcher natural ventilation performance, Energy Build. 38 (2006) 939–948. https://doi.org/10.1016/j.enbuild.2005.11.004.

[27] A.N. Eteghad, E.U. Guardiola, S.R.H. Raviz, A.A. Aira, Reinterpretation of Energy Efficiency in Thomas Herzog's Architecture, J. Eng. Archit. 2 (2014). https://doi.org/10.15640/jea.v2n2a8.

[28] P. Paevere, S. Brown, Indoor Environment Quality and Occupant Productivity in the CH2 Building: Post-Occupancy Summary, (2008) 30.

[29] Y.C. Wu, A.S. Yang, L.Y. Tseng, C.L. Liu, Myth of ecological architecture designs: Comparison between design concept and computational analysis results of natural-ventilation for Tjibaou Cultural Center in New Caledonia, Energy Build. 43 (2011) 2788–2797. https://doi.org/10.1016/j.enbuild.2011.06.035.

[30] S. Kato, S. Murakami, T. Takahashi, T. Gyobu, Chained analysis of wind tunnel test and CFD on cross ventilation of large-scale market building, J. Wind Eng. Ind. Aerodyn. 68 (1997) 573–587.

[31] L. Feifer, M. Imperadori, G. Salvalai, A. Brambilla, F. Brunone, Relevant Case Studies: A Benchmark for Future Design, in: Act. House Smart Nearly Zero Energy Build., Springer, 2018: pp. 101–138. https://doi.org/10.1007/978-3-319-90814-4.

[32] G. Bencsik, I.E. Háber, I. Farkas, Preparing climate data and city model for computational fluid dynamics simulation, in: 24th Work. Energy Environ. - B. Abstr., Gödöllő, Hungary, 2018: p. 18.

[33] N.P. Gillett, M. Kirchmeier-Young, A. Ribes, H. Shiogama, G.C. Hegerl, R. Knutti, G. Gastineau, J.G. John, L. Li, L. Nazarenko, N. Rosenbloom, Ø. Seland, T. Wu, S. Yukimoto, T. Ziehn, Constraining human contributions to observed warming since the pre-industrial period, Nat. Clim. Chang. 11 (2021) 207–212. https://doi.org/10.1038/s41558-020-00965-9.

[34] A Roadmap for moving to a competitive low carbon economy in 2050, European Union, 2011.

[35] R. Schmalensee, T.M. Stoker, R.A. Judson, World carbon dioxide emissions: 1950-2050, Rev. Econ. Stat. 80 (1998) 15–27. https://doi.org/10.1162/003465398557294.

[36] O. Akashi, Y. Hijioka, T. Masui, T. Hanaoka, M. Kainuma, GHG emission scenarios in Asia and the world: The key technologies for significant reduction, Energy Econ. 34 (2012) S346–S358. https://doi.org/10.1016/j.eneco.2012.04.011.

[37] Office of Pollution Prevention and Toxins, U.S EPA: Cost of Illness Handbook, 2007. http://nepis.epa.gov/Exe/ZyPDF.cgi/901A0E00.PDF?Dockey=901A0E00.PDF.

[38] M. Coelho, F. Baptista, V. Fitas Da Cruz, Comparison of four natural ventilation systems in a Mediterranean greenhouse, Acta Hortic. 719 (2006) 157–164. https://doi.org/10.17660/ActaHortic.2006.719.15.

[39] N. Tomasello, F. Valenti, G. Cascone, S.M.C. Porto, Development of a CFD model to simulate natural ventilation in a semi-open free-stall barn for dairy cows, Buildings. 9 (2019). https://doi.org/10.3390/buildings9080183.

[40] Š. Nosek, Z. Kluková, M. Jakubcová, Q. Yi, D. Janke, P. Demeyer, Z. Jaňour, The impact of atmospheric boundary layer, opening configuration and presence of animals on the ventilation of a cattle barn, J. Wind Eng. Ind. Aerodyn. 201 (2020). https://doi.org/10.1016/j.jweia.2020.104185.

[41] L. Rong, D. Liu, E.F. Pedersen, G. Zhang, The effect of wind speed and direction and surrounding maize on hybrid ventilation in a dairy cow building in Denmark, Energy Build. 86 (2014) 25–34. https://doi.org/10.1016/j.enbuild.2014.10.016.

[42] N. Tanasić, G. Jankes, H. Skistad, Cfd analysis and airflow measurements to approach large industrial halls energy efficiency: A case study of a cardboard mill hall, Energy Build. 43 (2011) 1200–1206. https://doi.org/10.1016/j.enbuild.2010.12.034.

[43] I. Kistelegdi, B. Baranyai, Windkanaluntersuchungen zwecks Quantifizierung und Validierung der Wirkung von Windinduktion und thermischen Auftriebskräften auf die natürliche Lüftung eines industriellen Innovationszentrums, Bauphysik. 34 (2012) 229–237. https://doi.org/10.1002/bapi.201200029.

[44] I. Cañas, F.R. Mazarrón, The effect of traditional wind vents called zarceras on the hygrothermal behaviour of underground wine cellars in Spain, Build. Environ. 44 (2009) 1818–1826. https://doi.org/10.1016/j.buildenv.2008.12.006.

[45] F.R. Mazarrón, C. Porras-Amores, J. Cid-Falceto, I. Cañas-Guerrero, Natural ventilation in underground wine cellars, in: Int. Conf. Agric. Eng., 2012: pp. 1–5.

[46] F.R. Mazarrón, C. Porras-Amores, I. Cañas-Guerrero, Annual evolution of the natural ventilation in an underground construction: Influence of the access tunnel and the ventilation chimney, Tunn. Undergr. Sp. Technol. 49 (2015) 188–198. https://doi.org/10.1016/j.tust.2015.04.015.

[47] M.N. Bahadori, Passive Cooling Systems in Iranian Architecture, Sci. Am. 238 (1978) 144–154. https://doi.org/10.1038/scientificamerican0278-144.

[48] O. Saadatian, L.C. Haw, K. Sopian, M.Y. Sulaiman, Review of windcatcher technologies, Renew. Sustain. Energy Rev. 16 (2012) 1477–1495. https://doi.org/10.1016/j.rser.2011.11.037.

[49] B.R. Hughes, J.K. Calautit, S.A. Ghani, The development of commercial wind towers for natural ventilation: A review, Appl. Energy. 92 (2012) 606–627. https://doi.org/10.1016/j.apenergy.2011.11.066.

[50] S. Omrani, V. Garcia-Hansen, B. Capra, R. Drogemuller, Natural ventilation in multi-storey buildings: Design process and review of evaluation tools, Build. Environ. 116 (2017) 182–194. https://doi.org/10.1016/j.buildenv.2017.02.012.

[51] F. Jomehzadeh, P. Nejat, J. Kaiser, M. Badruddin, M. Yusof, S. Ahmad, B. Richard, M. Noor, W. Muhammad, A review on windcatcher for passive cooling and natural ventilation in buildings , Part

1: Indoor air quality and thermal comfort assessment, Renew. Sustain. Energy Rev. 70 (2017) 736–756. https://doi.org/10.1016/j.rser.2016.11.254.

[52] A. Takayama, K. Asano, S. Shuchi, K. Hasegawa, Study on reusing abandoned chimneys as solar chimneys to induce breeze in residential areas, in: PLEA2009 - 26th Conf. Passiv. Low Energy Archit., Quebec City, Canada, 2009.

[53] C.H. Lim, Omidreza Saadatian, K. Sopian, M. Yusof Sulaiman, S. Mat, E. Salleh, K.C. Ng, Design configurations analysis of wind-induced natural ventilation tower in hot humid climate using computational fluid dynamics, Int. J. Low-Carbon Technol. 10 (2015) 332–346. https://doi.org/10.1093/ijlct/ctt039.

[54] T. van Hooff, B. Blocken, L. Aanen, B. Bronsema, A venturi-shaped roof for wind-induced natural ventilation of buildings: Wind tunnel and CFD evaluation of different design configurations, Build. Environ. 46 (2011) 1797–1807. https://doi.org/10.1016/j.buildenv.2011.02.009.

[55] A.A. Badran, Performance of cool towers under various climates in Jordan, Energy Build. 35 (2003) 1031–1035. https://doi.org/10.1016/S0378-7788(03)00067-7.

[56] M. Sadeghi, R. De Dear, B. Samali, G. Wood, Optimization of Wind Tower Cooling Performance: A Wind Tunnel Study of Indoor Air Movement and Thermal Comfort, in: Procedia Eng., Elsevier Ltd, 2016: pp. 611–620. https://doi.org/10.1016/j.proeng.2017.04.220.

[57] J. Saif, A. Wright, S. Khattak, K. Elfadli, Keeping cool in the desert: Using wind catchers for improved thermal comfort and indoor air quality at half the energy, Buildings. 11 (2021). https://doi.org/10.3390/buildings11030100.

[58] M.N. Bahadori, A.R. Pakzad, Performance evaluation of new designs of wind towers, in: Am. Soc. Mech. Eng. Fluids Eng. Div., Montreal, Quebec, Canada, 2002: pp. 1015–1022. https://doi.org/10.1115/FEDSM2002-31247.

[59] Z. Hedayat, B. Belmans, M.H. Ayatollahi, I. Wouters, F. Descamps, Performance assessment of ancient wind catchers - an experimental and analytical study, in: Energy Procedia, Elsevier B.V., 2015: pp. 2578–2583. https://doi.org/10.1016/j.egypro.2015.11.292.

[60] H.D. Mohamadabadi, A.A. Dehghan, A.H. Ghanbaran, A. Movahedi, A.D. Mohamadabadi, Numerical and experimental performance analysis of a four-sided wind tower adjoining parlor and courtyard at different wind incident angles, Energy Build. 172 (2018) 525–536. https://doi.org/10.1016/j.enbuild.2018.05.006.

[61] K.L. Peterman, M. Weber, eds., ASHRAE Standard 62.1-2019 - Ventilation for acceptable indoor air quality, American Society of Heating, Refrigerating and Air-Conditioning Engineers Bookstore, Atlanta, GA, 2019. https://www.ashrae.org/technical-resources/bookstore/standards-62-1-62-2.

[62] EN 15251 - Indoor environmental input parameters for design and assessment of energy performance of buildings addressing indoor air quality, thermal environment, lighting and acoustics, European Union, 2006. http://www.sysecol2.ethz.ch/OptiControl/LiteratureOC/CEN_06_prEN_15251_FinalDraft.pdf.

[63] Hungarian Ministry for Innovation and Technology, Az épületek energetikai jellemzőinek meghatározásáról, Hungary, 2021. https://net.jogtar.hu/jogszabaly?docid=a0600007.tnm.

[64] A.R. Dehghani-Sanij, M. Soltani, K. Raahemifar, A new design of wind tower for passive ventilation in buildings to reduce energy consumption in windy regions, Renew. Sustain. Energy Rev. 42 (2015) 182–195. https://doi.org/10.1016/j.rser.2014.10.018.

[65] A. Heidari, S. Sahebzadeh, Z. Dalvand, Natural ventilation in vernacular architecture of Sistan, Iran; Classification and CFD study of compound rooms, Sustainability. 9 (2017). https://doi.org/10.3390/su9061048.

[66] A. Zarmehr, J.T.K. Jr, C. Florida, Modeling and Simulation of Parametric Wind-Catcher Designs for Natural Ventilation in Sustainable Building Skin Architecture, in: Adv. Build. Ski. 2018, Bern, Switzerland, 2018.

[67] J.K. Calautit, B.R. Hughes, D.S. Nasir, Climatic analysis of a passive cooling technology for the built environment in hot countries, Appl. Energy. 186 (2017) 321–335. https://doi.org/10.1016/j.apenergy.2016.05.096.

[68] J.K. Calautit, B.R. Hughes, D. O'Connor, S.S. Shahzad, Numerical and experimental analysis of a multi-directional wind tower integrated with vertically-arranged heat transfer devices (VHTD), Appl. Energy. 185 (2016) 1120–1135. https://doi.org/10.1016/j.apenergy.2016.02.025.

[69] N.L. Long, S.D. Pless, P.A. Torcellini, R. Judkoff, Evaluation of the low-energy design process and energy performance of the Zion National Park Visitor Center, ASHRAE Trans. 112 PART 1 (2006) 321–340.

[70] A. Balabel, M. Alwetaishi, W.A. El-Askary, H. Fawzy, Numerical study on natural ventilation characteristics of a partial-cylinder opening for one-sided-windcatcher of variable air-feeding orientations in taif, saudi arabia, Sustain. 13 (2021). https://doi.org/10.3390/su132011310.

[71] A.P. Haghighi, S.H. Pakdel, A. Jafari, A study of a wind catcher assisted adsorption cooling channel for natural cooling of a 2-storey building, Energy. 102 (2016) 118–138. https://doi.org/10.1016/j.energy.2016.02.033.

[72] L.W. Chew, N. Nazarian, L. Norford, Pedestrian-level urban wind flow enhancement with wind catchers, Atmosphere (Basel). 8 (2017) 1–22. https://doi.org/10.3390/atmos8090159.

[73] M. Alwetaishi, Use of Underground Constructions Enhanced with Evaporative, (2021).

[74] M. Afshin, A. Sohankar, M.D. Manshadi, M.K. Esfeh, An experimental study on the evaluation of natural ventilation performance of a two-sided wind-catcher for various wind angles, Renew. Energy. 85 (2016) 1068–1078. https://doi.org/10.1016/j.renene.2015.07.036.

[75] N. Benkari, I. Fazil, A. Husain, Design and performance comparison of two patterns of wind-catcher for a semi-enclosed courtyard, Int. J. Mech. Eng. Robot. Res. 6 (2017) 396–400. https://doi.org/10.18178/ijmerr.6.5.396-400.

[76] H. Ansar, A.K. Arumugham-Achari, J. Johnson, Parametric Study on the Effect of a Domestic Wind Catcher-Solar Chimney System for Arid Regions, Int. Res. J. Adv. Eng. Sci. 2 (2017) 316–322.

[77] Sarjito, T.W.B. Riyadi, A parametric study of wind catcher model in a typical system of evaporative cooling tower using CFD, Appl. Mech. Mater. 660 (2014) 659–663. https://doi.org/10.4028/www.scientific.net/AMM.660.659.

[78] M. Alsailani, H. Montazeri, A. Rezaeiha, Towards optimal aerodynamic design of wind catchers: Impact of geometrical characteristics, Renew. Energy. 168 (2021) 1344–1363. https://doi.org/10.1016/j.renene.2020.12.053.

[79] C.A. Varela-Boydo, S.L. Moya, Inlet extensions for wind towers to improve natural ventilation in buildings, Sustain. Cities Soc. 53 (2020) 101933. https://doi.org/10.1016/j.scs.2019.101933.

[80] Á.L. Katona, I.E. Háber, I. Kistelegdi, Comparison of downdraught and up draft passive air conduction systems (PACS) in awinery building, Buildings. 11 (2021). https://doi.org/10.3390/buildings11060259.

[81] H.E. Beck, N.E. Zimmermann, T.R. McVicar, N. Vergopolan, A. Berg, E.F. Wood, Present and future köppen-geiger climate classification maps at 1-km resolution, Sci. Data. 5 (2018) 1–12. https://doi.org/10.1038/sdata.2018.214.

[82] I. Kistelegdi, C.H. Radha, B. Balint, Decision-making Tool for Energy and Thermal Comfort Optimization in Residential Building Refurbishment Using Passive Strategies, Zanco J. Pure Appl. Sci. 31 (2019). https://doi.org/10.21271/zjpas.31.s3.41.

[83] G. Habtay, I. Farkas, P. Control, Mathematical Modelling of a cylindrical chimney effect in solar dryer, Hungarian Agric. Eng. 36 (2019) 69–74. https://doi.org/10.17676/HAE.2019.36.69.

[84] D.W. Bechert, M. Bruse, W. Hage, R. Meyer, Fluid mechanics of biological surfaces and their technological application, Naturwissenschaften. 87 (2000) 157–171. https://doi.org/10.1007/s001140050696.

[85] H. Zsiborács, N.H. Baranyai, A. Vincze, L. Zentkó, Z. Birkner, K. Máté, G. Pintér, Intermittent renewable energy sources: The role of energy storage in the European power system of 2040, Electron. 8 (2019). https://doi.org/10.3390/electronics8070729.

[86] T. Mikeska, J. Fan, S. Svendsen, Full scale measurements and CFD investigations of a wall radiant cooling system integrated in thin concrete walls, Energy Build. 139 (2017) 242–253. https://doi.org/10.1016/j.enbuild.2017.01.033.

[87] C.S. Yuan, The effect of building shape modification on wind pressure differences for cross-ventilation of a low-rise building, Int. J. Vent. 6 (2007) 167–176. https://doi.org/10.1080/14733315.2007.11683775.

[88] J. Remund, Accuracy of Meteonorm, Manual. (2015) 273. www.meteotest.ch.

[89] R.J. de Dear, G.S. Brager, Developing an adaptive model of thermal comfort and preference, ASHRAE Trans. 104 (1998) 145–167.

[90] Á.L. Katona, H. Xuan, S. Elhadad, I. Kistelegdi, I. Háber, High-resolution CFD and in-situ monitoring based validation of an industrial passive air conduction system (PACS), Energies. 13 (2020). https://doi.org/10.3390/en13123157.

[91] Y. Chen, Z. Tong, A. Malkawi, Investigating natural ventilation potentials across the globe: Regional and climatic variations, Build. Environ. 122 (2017) 386–396. https://doi.org/10.1016/j.buildenv.2017.06.026.

[92] A. Hosseinzadeh, A. Keshmiri, Computational simulation of wind microclimate in complex urban models and mitigation using trees, Buildings. 11 (2021) 1–19. https://doi.org/10.3390/buildings11030112.

[93] H. Huang, R. Ooka, H. Chen, S. Kato, Optimum design for smoke-control system in buildings considering robustness using CFD and Genetic Algorithms, Build. Environ. 44 (2009) 2218–2227. https://doi.org/10.1016/j.buildenv.2009.02.002.

[94] M.F. Mohamed, S. King, M. Behnia, D. Prasad, Coupled outdoor and indoor airflow prediction for buildings using Computational Fluid Dynamics (CFD), Buildings. 3 (2013) 399–421. https://doi.org/10.3390/buildings3020399.

[95] I.B. Celik, U. Ghia, P.J. Roache, C.J. Freitas, H. Coleman, P.E. Raad, Procedure for estimation and reporting of uncertainty due to discretization in CFD applications, J. Fluids Eng. Trans. ASME. 130 (2008). https://doi.org/10.1115/1.2960953.

[96] M. Balogh, A. Parente, C. Benocci, RANS simulation of ABL flow over complex terrains applying an Enhanced k-ε model and wall function formulation: Implementation and comparison for fluent and OpenFOAM, J. Wind Eng. Ind. Aerodyn. 104–106 (2012) 360–368. https://doi.org/10.1016/j.jweia.2012.02.023.

[97] M. Balogh, A. Parente, Realistic boundary conditions for the simulation of atmospheric boundary layer flows using an improved k-ε model, J. Wind Eng. Ind. Aerodyn. 144 (2015) 183–190. https://doi.org/10.1016/j.jweia.2015.01.010.

[98] B. Ford, E. Errell, Component Design and Controls, in: B. Ford, R. Schlano-Phan, E. Francis (Eds.), Archit. Eng. Downdraught Cool. A Des. Source B., 1st ed., PHDC Press, 2010: pp. 168–189.

[99] I. Kistelegdi, I. Háber, Gebäudeaerodynamische Untersuchungen einer Plusenergie-Produktionsstätte mit passiven Lüftungstürmen in Sikonda (Südungarn), Bauphysik. 34 (2012) 107–120. https://doi.org/10.1002/bapi.201200016.

[100] R. Ramponi, B. Blocken, CFD simulation of cross-ventilation for a generic isolated building: Impact of computational parameters, Build. Environ. 53 (2012) 34–48. https://doi.org/10.1016/j.buildenv.2012.01.004.

[101] L. Peng, P. V. Nielsen, X. Wang, S. Sadrizadeh, L. Liu, Y. Li, Possible user-dependent CFD predictions of transitional flow in building ventilation, Build. Environ. 99 (2016) 130–141. https://doi.org/10.1016/j.buildenv.2016.01.014.

[102] J.I. Perén, T. van Hooff, B.C.C. Leite, B. Blocken, CFD analysis of cross-ventilation of a generic isolated building with asymmetric opening positions: Impact of roof angle and opening location, Build. Environ. 85 (2015) 263–276. https://doi.org/10.1016/j.buildenv.2014.12.007.

[103] S.H. Hosseini, E. Shokry, A.J. Ahmadian Hosseini, G. Ahmadi, J.K. Calautit, Evaluation of airflow and thermal comfort in buildings ventilated with wind catchers: Simulation of conditions in Yazd City, Iran, Energy Sustain. Dev. 35 (2016) 7–24. https://doi.org/10.1016/j.esd.2016.09.005.

[104] M. Alwetaishi, M. Gadi, New and innovative wind catcher designs to improve indoor air quality in buildings, Energy Built Environ. 2 (2021) 337–344. https://doi.org/10.1016/j.enbenv.2020.06.009.

[105] D. Pearlmutter, E. Erell, Y. Etzion, I.A. Meir, H. Di, Refining the use of evaporation in an experimental down-draft cool tower, Energy Build. 23 (1996) 191–197. https://doi.org/10.1016/0378-7788(95)00944-2.

[106] D. Pearlmutter, E. Erell, Y. Etzion, A multi-stage down-draft evaporative cool tower for semi-enclosed spaces : Experiments with a water spraying system, Sol. Energy. 82 (2008) 430–440. https://doi.org/10.1016/j.solener.2007.12.003.

[107] P. Nejat, F. Jomehzadeh, H.M. Hussen, J.K. Calautit, M.Z. Abd Majid, Application of wind as a renewable energy source for passive cooling through windcatchers integrated with wing walls, Energies. 11 (2018). https://doi.org/10.3390/en11102536.

[108] N.R.M. Sakiyama, J. Frick, T. Bejat, H. Garrecht, Using CFD to Evaluate Natural Ventilation through a 3D Parametric Modeling Approach, Energies. 14 (2021). https://doi.org/10.3390/en14082197.

[109] M. Soltani, A. Dehghani-Sanij, A. Sayadnia, F.M. Kashkooli, K. Gharali, S. Mahbaz, M.B. Dusseault, Investigation of airflow patterns in a new design of wind tower with awetted surface, Energies. 11 (2018) 1–23. https://doi.org/10.3390/en11051100.

[110] M. Ghoulem, K. El Moueddeb, E. Nehdi, F. Zhong, J. Calautit, Design of a passive downdraught evaporative cooling windcatcher (PDEC-WC) system for greenhouses in hot climates, Energies. 13 (2020). https://doi.org/10.3390/en13112934.

Appendix A – CFD meshing validation

The fine grid convergence-index was calculated by the guidelines of Celik et al. [95]. In their work they presented a step by step method for evaluation of the reliability of CFD simulations' finite grid. The following steps and calculations were proceeded.

Step 1

$$h = \left[\frac{1}{N}\sum_{i=1}^{N}(\Delta V_i)\right]^{1/3} \tag{A1}$$

where *h* is the representative cell size of the generated grid. Detailed nomenclature is in the end of the section.

Step 2

The refinement factor is described by the following, and the value should be at least 1.3 based on experiments.

$$r = \frac{h_{coarse}}{h_{fine}} \tag{A2}$$

Step 3

Apparent order *p* is calculated as follows:

$$p = \frac{1}{\ln(r_{21})}\left|\ln\left|\frac{\varepsilon_{32}}{\varepsilon_{21}}\right| + q(p)\right| \tag{A3}$$

where $q(p) = 0$ because r_{21} and r_{32} is identical, as it is clarified by Celik. And where

$$\varepsilon_{21} = \dot{V}_2 - \dot{V}_1 \text{ and } \varepsilon_{32} = \dot{V}_3 - \dot{V}_2 \tag{A4}$$

Step 4

Extrapolated value was calculated:

$$\dot{V}_{ext}^{21} = \frac{\left(r_{21}^{p}\dot{V}_1 - \dot{V}_2\right)}{r_{21}^{p} - 1} \tag{A5}$$

Step 5

Following error estimates were calculated with the apparent order *p*

approximate relative error

$$e_a^{21} = \left|\frac{\dot{V}_1 - \dot{V}_2}{\dot{V}_1}\right| \tag{A6}$$

extrapolated relative error

$$e_{ext}^{21} = \left|\frac{\dot{V}_{ext}^{21} - \dot{V}_1}{\dot{V}_{ext}^{21}}\right| \tag{A7}$$

fine-grid convergence index

$$GCI_{fine}^{21} = \left|\frac{1.25e_a^{21}}{r_{21}^{p} - 1}\right| \tag{A8}$$

Table A1 presents the results obtained during the estimation of the uncertainty of the generated grids.

Variable	Grid 3 (coarse)	Grid 2 (medium)	Grid 1 (fine)
N—number of elements	353,622	776,196	1,696,657
V—volume of the mesh [m^3]	847,027	847,027	847,027
$\dot{V}$—volume flow rate [m^3/s]	1.86	1.79	1.78
h—representative cell size [m]	1.338	1.030	0.793
	Grid 3 Related to Grid 2		**Grid 2 Related to Grid 1**
r—refinement factor		1.3	
p—apparent order		6.58	
$\dot{V}_{ext}$—extrapolated value		1.79	
e_a—approximate relative error	3.80%		0.71%
e_{ext}—extrapolated relative error	0.83%		0.16%
GCI_{fine}—fine-grid convergence index	1.04%		0.19%

Appendix B – Graphical data about the results of the complex new PACS geometry development

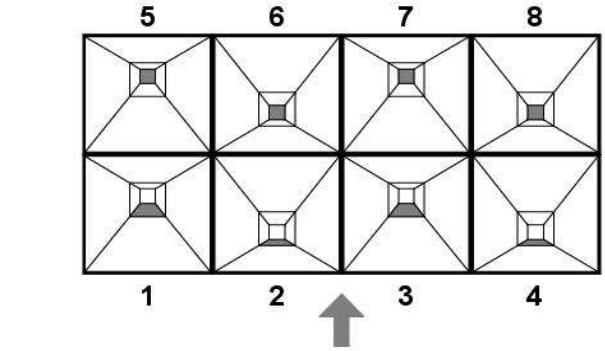

Binary code – 11110000-O

-33 246	-37 526	-34 074	-32 717
46 508	23 216	46 620	23 170

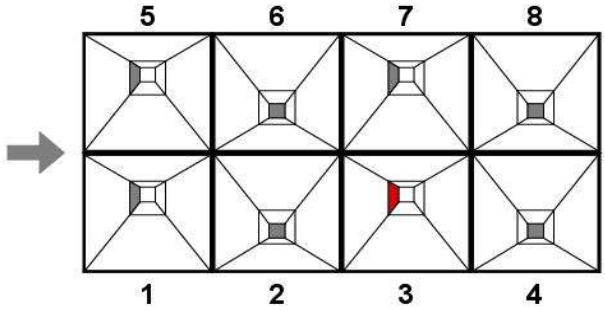

Binary code – 10101010-P1

71 388	-24 804	40 788	-38 412
72 504	-35 892	-56 700	-29 016

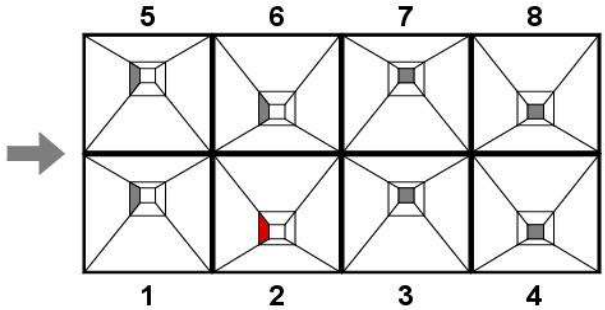

Binary code – 11001100-P1

73 899	36 530	-27 357	-35 735
74 619	-61 747	-36 830	-23 496

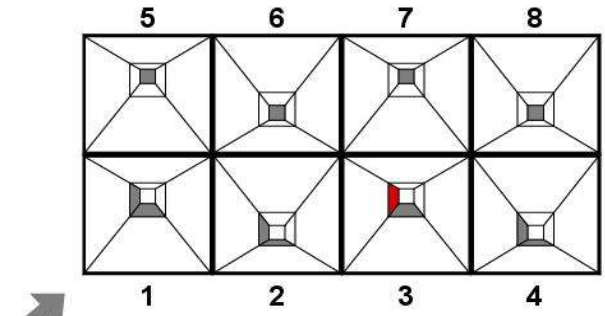

Binary code – 11110000-D1

-16 372	-45 340	-46 934	-44 059
79 276	46 366	-8 826	43 033

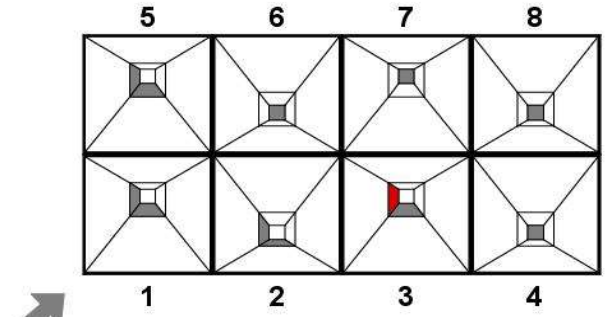

Binary code – 11101000-D1

46 485	-47 160	-49 039	-45 110
79 843	37 303	-2 931	-21 239

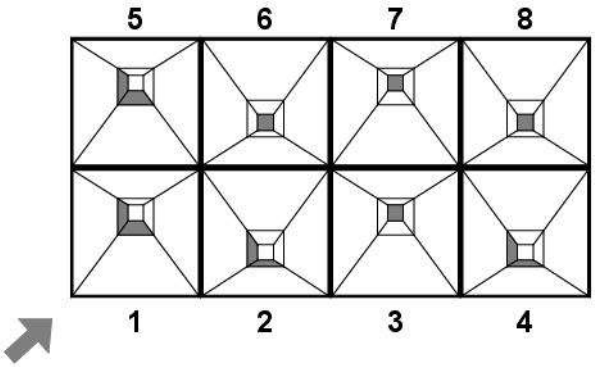

Binary code – 11011000-D1

38 784	-48 493	-49 626	-47 379
73 945	31 465	-26 159	27 443

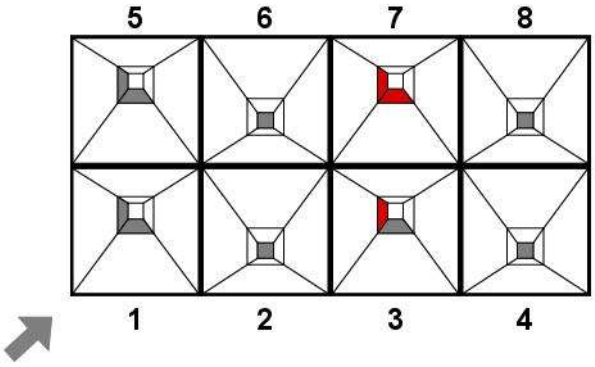

Binary code – 10101010-D1

102 759	-35 513	-185 316	-41 144
125 373	-11 784	59 124	-13 372

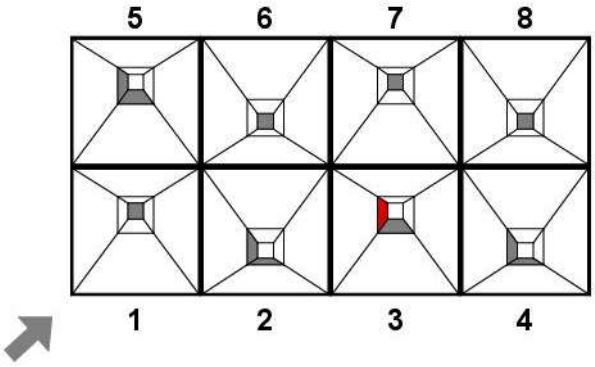

Binary code – 01111000-D1

71 434	-43 817	-46 964	-44 253
-10 844	45 341	-12 429	41 331

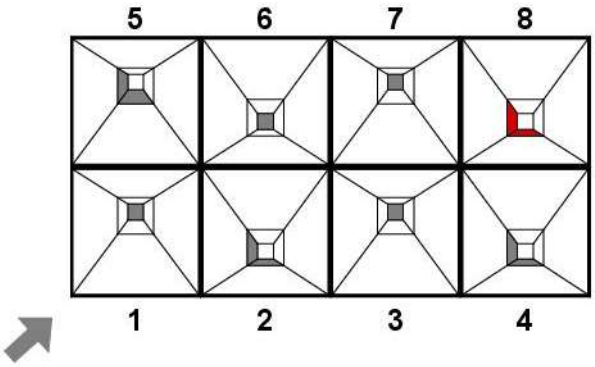

Binary code – 01011001-D1

105 669	-36 935	-41 005	-133 083
-7 163	63 958	-14 586	62 945

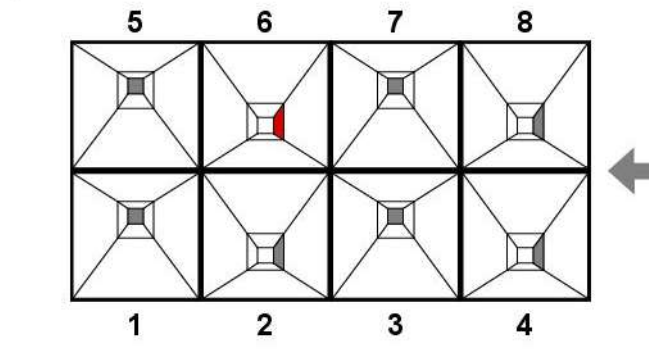

Binary code – 01010101-P2

-29 390	-59 505	-36 643	71 149
-34 993	43 678	-24 866	70 513

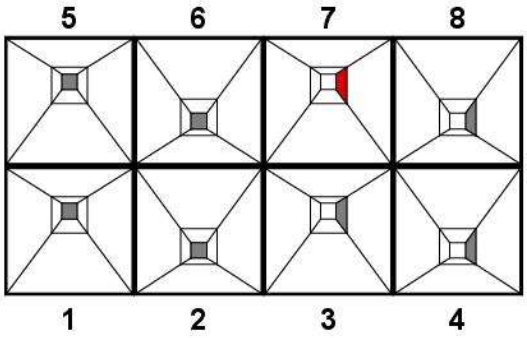

Binary code – 00110011-P2

-25 931	-32 215	-76 807	79 415
-34 206	-23 077	34 050	78 775

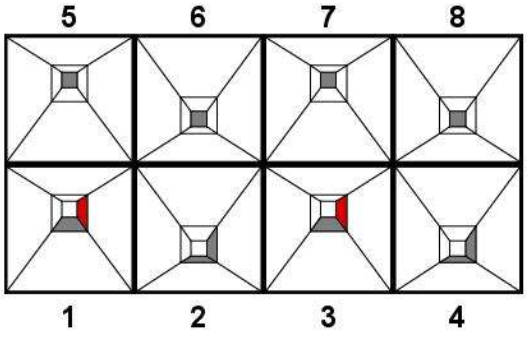

Binary code – 11110000-D2

-43 538	-43 744	-44 490	-19 815
10 729	48 003	26 564	66 356

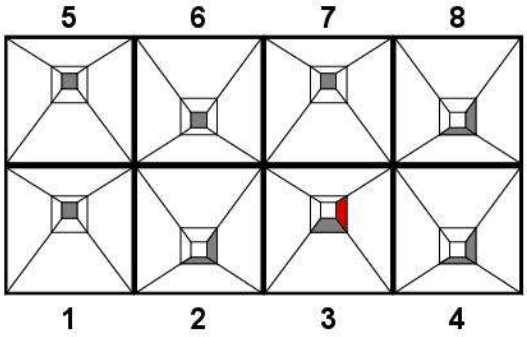

Binary code – 01110001-D2

-44 118	-44 921	-45 774	41 124
-25 218	41 032	16 498	61 351

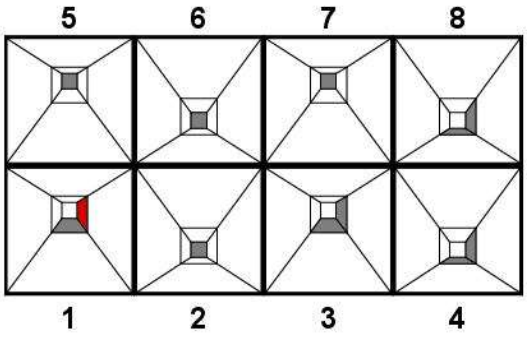

Binary code – 10110001-D2

-44 188	-45 332	-44 716	41 856
7 848	44 173	-21 884	62 167

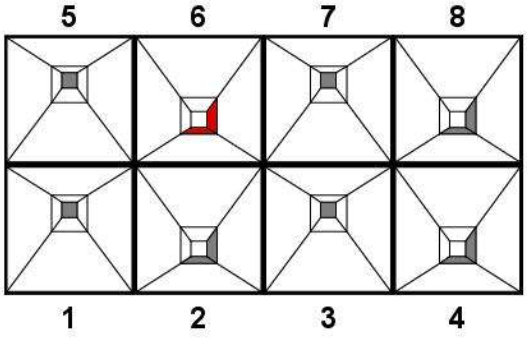

Binary code – 01010101-D2

-38 454	-130 485	-33 709	68 099
-17 448	75 233	-14 129	87 351

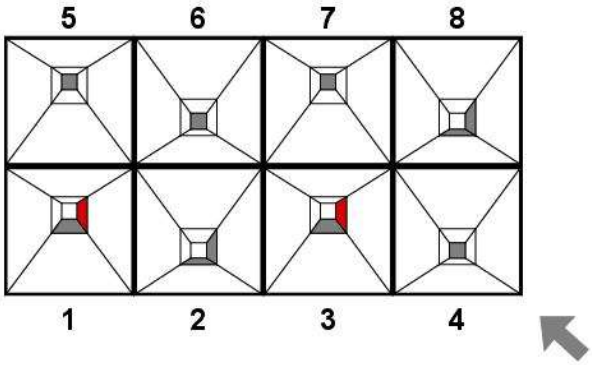

Binary code – 11100001-D2

-42 577	-41 808	-45 228	49 020
15 125	49 766	28 671	-12 994

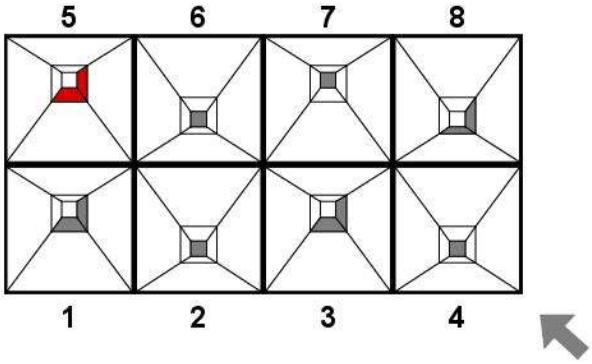

Binary code – 10101001-D2

-168 646	-29 801	-31 443	84 249
69 303	-10 144	93 945	-7 447

Figure AB2: Airflow and ACH performance of the input and output towers, in parallel, perpendicular and diagonal wind direction to basic module units' towers connecting axis. Red = unplanned, reverse outflow in one of two input chimneys, yellow = outflow in all (one or two) input chimneys; And binary code means that 1 is inlet 0 is outlet of each towers, ranked by their Nos.

Appendix C – Graphical data for parametric micro level geometry optimization

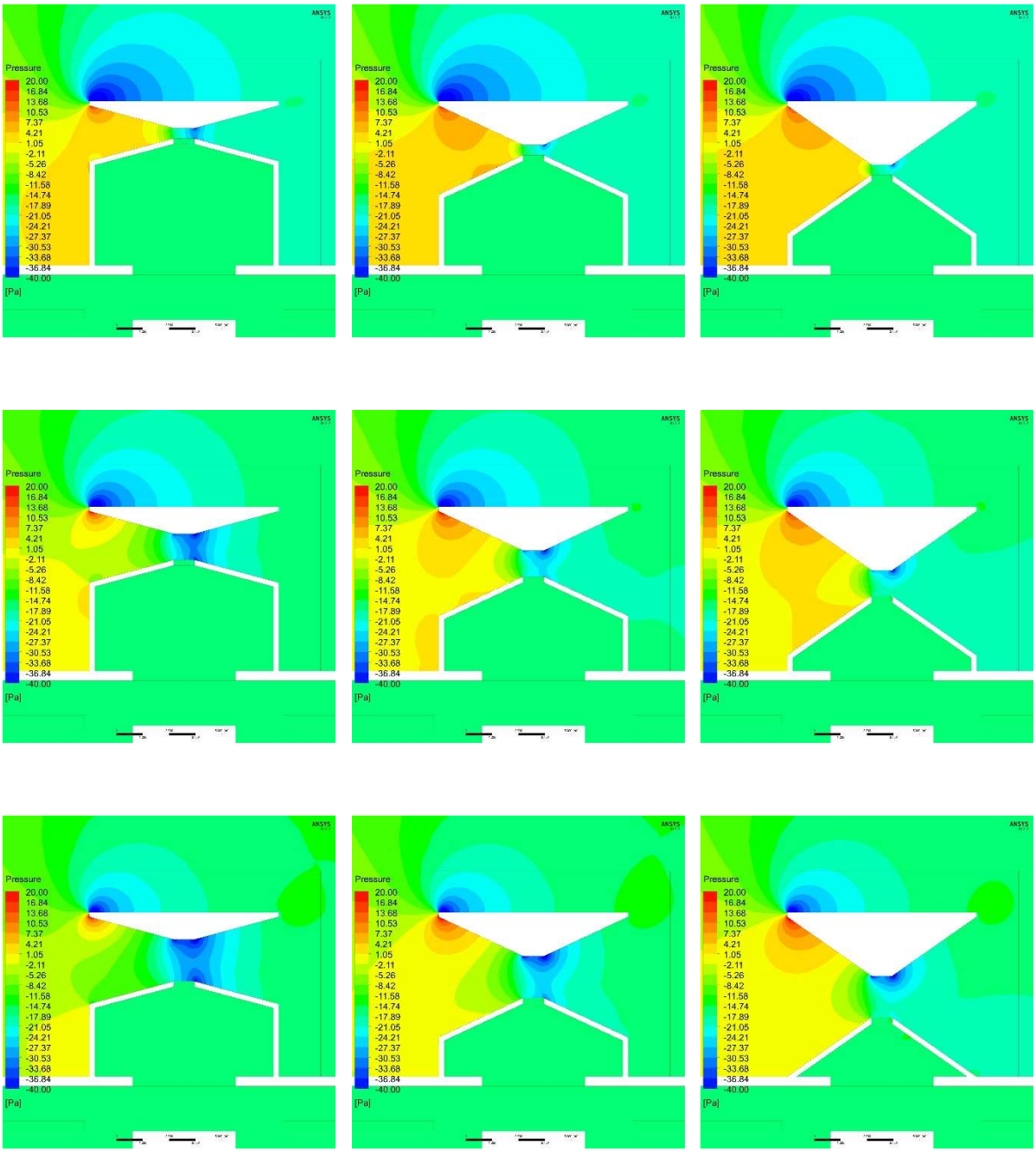

Figure AC1 - Pressure versus spectral analysis of 100 cm wide compression zone combinations [Pa]

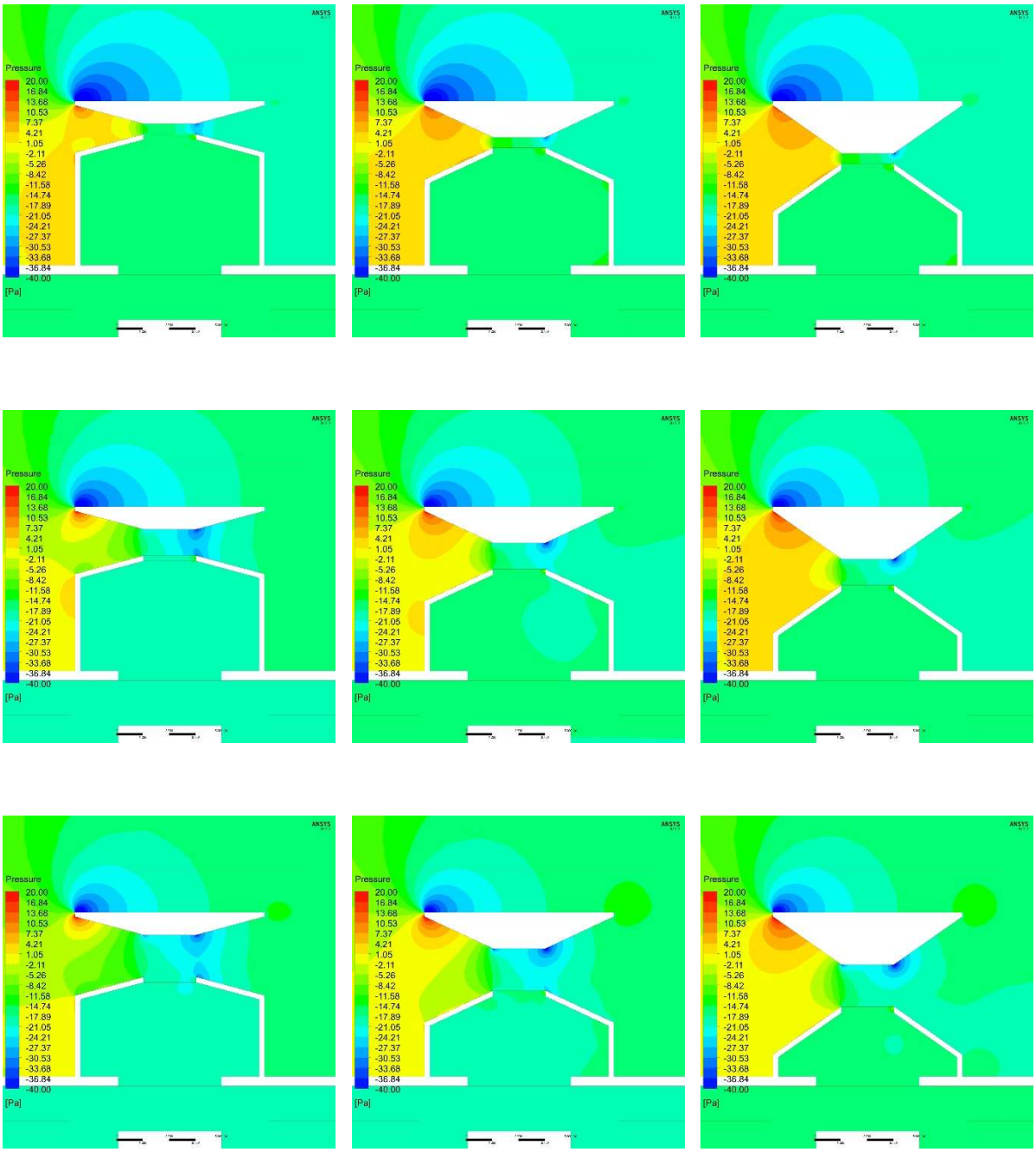

Figure AC2 - Pressure ratios for 250 cm wide compression zone combinations by spectral analysis [Pa]

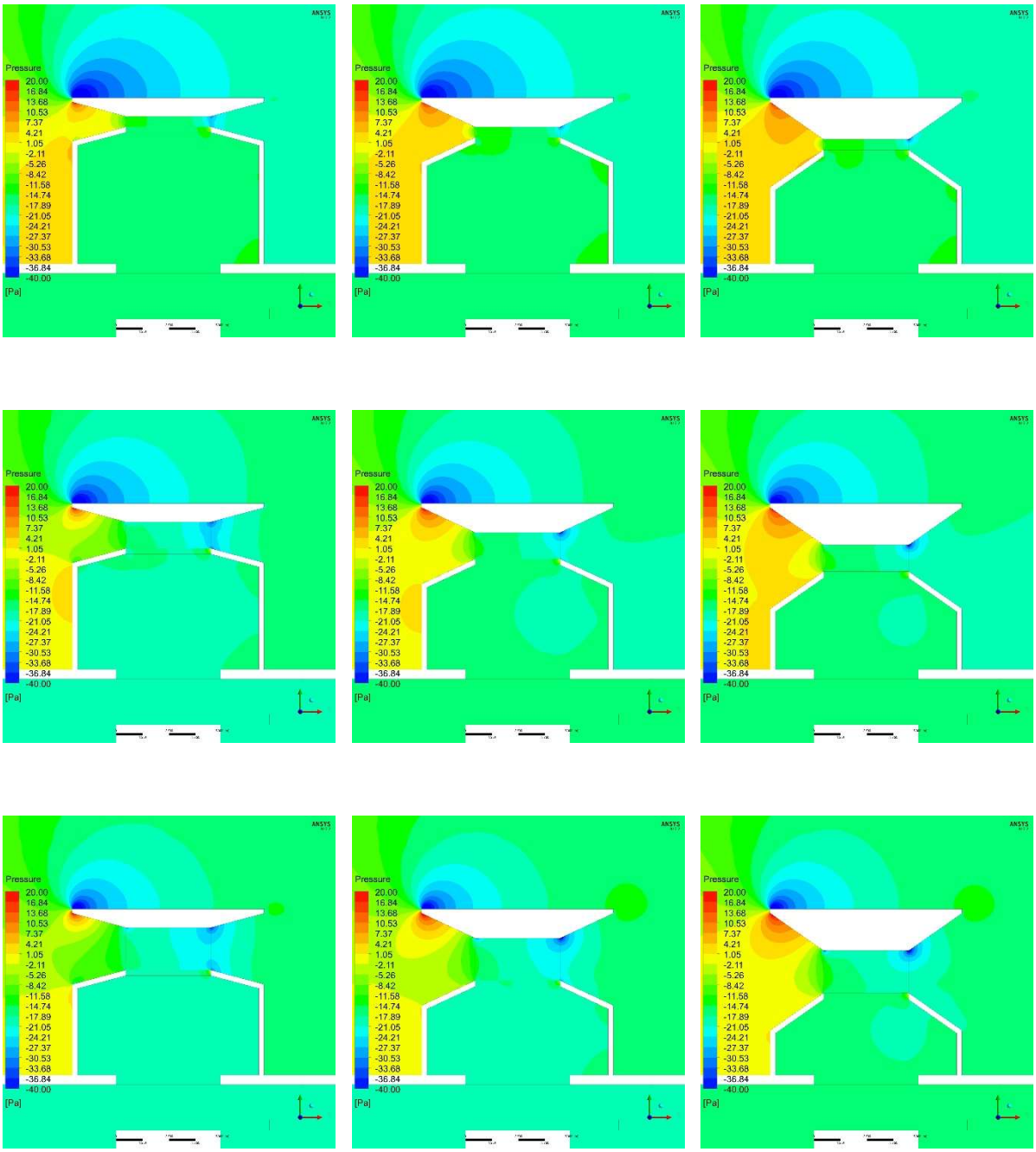

Figure AC3 - Pressure ratios for 400 cm wide compression zone combinations by spectral analysis [Pa]